MODULATING NEURONAL AGING:

INSIGHTS FROM INSULIN SIGNALING GENES AND ALASKAN NUTRACEUTICALS

By

Courtney Scerbak

RECOMMENDED:

Elena Vayndorf, Ph.D.

Monica Driscoll, Ph.D.

Kriya Dunlap, Ph.D.

Michael Harris, Ph.D.

Andrej Podlutsky, Ph.D.

Barbara Taylor, Ph.D.
Advisory Committee Chair

Diane Wagner, Ph.D.
Chair, Department of Biology and Wildlife

APPROVED:

Paul Layer, Ph.D.
Dean, College of Natural Science and Mathematics

John Eichelberger, Ph.D.
Dean of the Graduate School

8 April 2016
Date

MODULATING NEURONAL AGING:

INSIGHTS FROM INSULIN SIGNALING GENES AND ALASKAN NUTRACEUTICALS

A

DISSERTATION

Presented to the Faculty

of the University of Alaska Fairbanks

in Partial Fulfillment of the Requirements

for the Degree of

DOCTOR OF PHILOSOPHY

By

Courtney Scerbak, B.S.

Fairbanks, Alaska

May 2016

Abstract

While aging impacts most, if not all, living organisms, the molecular mechanisms behind this phenomenon are not completely understood. Here, I aimed to further describe the intricate relationship between genetics and diet in aging, focusing on touch receptor neuron aging processes in the model nematode, *Caenorhabditis elegans*. I specifically tested the hypotheses that (1) age-related touch receptor neuron morphological changes are associated with whole organism health, (2) intrinsic (i.e. genetic) and extrinsic (i.e. nutritional) factors can influence these morphological changes, and (3) specific cellular signaling processes underlie these morphological changes. To this end, this dissertation has three components: (1) the impact of insulin signaling disruption on neuron morphology and protein aggregation in a model of Huntington's Disease; (2) establishment of Alaskan nutraceutical treatments that extend lifespan and offset age-related decline in neuron and whole organism health; and (3) description of mechanisms driving Alaskan nutraceutical treatment effects using RNA sequencing to target subsequent experiments. In all three of these components, I measured markers of whole organism health (e.g. lifespan, motility, endogenous reactive oxygen species) and markers of touch receptor neuron health (e.g. neuron morphology, mechanosensation). Together, this dissertation demonstrated that lifespan-extending interventions (e.g. decreased insulin signaling, Alaskan nutraceutical treatments) improved mechanosensation and, interestingly, differentially modulated development of age-related neuron morphological changes. That beneficial treatments increased the occurrence of posterior neuron process branching and/or decreased the occurrence of several anterior cell soma morphologies (e.g. soma outgrowths) suggests that some morphologies are representative of successful defense of the cell against age-related deterioration, while others are markers of cellular dysfunction. These results support the idea that multiple cellular signaling pathways are involved in aging of touch receptor neurons, and thus, there are multiple mechanisms for promoting health with age at the cellular level.

Dedication

I would like to dedicate this dissertation to my parents, whose unwavering support allowed me to pursue my education at University of Alaska Fairbanks, and to my husband, who never let me forget what is most important in life – family and my sanity.

Table of Contents

Page

Signature Page i
Title Page iii
Abstract v
Dedication vii
Table of Contents ix
List of Figures xiii
List of Tables xv
Acknowledgements xvii
Chapter 1: General Introduction 1
1.1 Biology of aging 1
1.2 Brain and neuron aging 3
1.3 Genetic determinants of aging 5
1.4 Nutritional aging interventions 7
1.5 References cited 10
Chapter 2: A Dual Role of the Insulin Signaling Pathway in the Aging of Healthy and Proteotoxically Stressed Mechanosensory Neurons 17
2.1 Abstract 17
2.2 Introduction 18
2.3 Materials and methods 21
2.3.1 Strains 21
2.3.2 Worm maintenance 21
2.3.3 RNA interference treatments 21
2.3.4 Lifespan analysis 22
2.3.5 Mechanosensory response assay 22
2.3.6 Neuron morphology imaging 23
2.3.7 Protein aggregate quantification and data analysis 23
2.4 Results 24
2.4.1 Neuron and systemic RNAi knockdown of insulin signaling proteins alters polyQ0 and polyQ128 *C. elegans* lifespan 24
2.4.2 Decreased insulin signaling through RNAi knockdown influences healthy mechanosensory neuron morphology and function 26

2.4.3 Touch response, mechanosensory neuron morphology, and protein aggregate accumulation are affected by insulin signaling in a model strain of Huntington's disease pathogenesis 28
2.4.4 RNAi knockdown of *daf-2* returns polyQ128 mechanosensory neuron morphology to healthy levels 30
2.5 Discussion 30
2.5.1 Summary of findings 30
2.5.2 Extending understanding of the influence of insulin signaling on healthy aging mechanosensory neurons 31
2.5.2.1 *daf-2* insulin receptor 31
2.5.2.2 age-1 PI3 kinase and other insulin signaling molecules 32
2.5.2.3 *daf-16* 33
2.5.3 Distinctive outcomes of *daf-2* RNAi in the proteotoxically stressed Huntington's disease model strain 33
2.5.3.1 *daf-2* 33
2.5.3.2 *age-1* PI3 kinase and other insulin signaling molecules 34
2.5.3.3 *daf-16* 35
2.5.4 *daf-2* RNAi uniquely changes distribution of polyQ128 aggregate load 35
2.5.5 Neurons aging under extreme aggregate challenge exhibit differences from natural aging 36
2.6 Acknowledgements 38
2.7 References cited 51
Chapter 3: Differential Mechanosensory Neuron Aging Trajectories and Lifespan Extension Following Medicinal Alaskan Berry and Fungal Treatments in *Caenorhabditis elegans* 57
3.1 Abstract 57
3.2 Introduction 58
3.3 Materials and methods 61
3.3.1 *C. elegans* strains and maintenance 61
3.3.2 Berry and fungus extract preparation 61
3.3.3 Biochemical quantification of extracts 62
3.3.4 Berry and fungus treatment administration 62
3.3.5 Lifespan analysis 63
3.3.6 Motility measurement 63
3.3.7 Reactive oxygen species quantification 64
3.3.8 Fecundity measurement 64
3.3.9 Mechanosensory neuron aging assay 65
3.3.10 *hsp16-2*::GFP gene expression assay 66

3.4 Results 66
3.4.1 Standardization of Alaskan plant and fungus extracts 66
3.4.2 Alaskan berry and fungus treatments extend *C. elegans* lifespan 67
3.4.3 Alaskan berry and fungus treatments improve healthspan 68
3.4.4 Alaskan berry and fungus treatments differentially alter mechanosensory neuron aging 70
3.5 Discussion 73
3.6 Acknowledgements 79
3.7 References cited 96
Chapter 4: Neuronal Aging in *Caenorhabditis elegans* is Modulated via Distinct Cellular Signaling and Genetic Mechanisms: Insights from Alaskan Berry and Fungal Treatments 103
4.1 Abstract 103
4.2 Introduction 104
4.3 Materials and methods 106
4.3.1 *C. elegans* strains and maintenance 106
4.3.2 Berry and fungus extract preparation and treatment administration 106
4.3.3 Transcription factor activation assays 107
4.3.4 RNA extraction and sample preparation 108
4.3.5 RNA sequencing and analysis 108
4.3.6 RNA interference treatment 109
4.3.7 Touch receptor neuron morphology and touch response analysis 110
4.4 Results 111
4.4.1 Alaskan lowbush cranberry activates DAF-16/FOXO late in life 111
4.4.2 Alaskan lowbush cranberry modulates DAF-16 to extend lifespan and influences touch receptor neuron aging 112
4.4.3 Alaskan blueberry and chaga treatments differentially impact the transcriptome . 114
4.4.4 Cytoskeleton- and metabolism-mediating candidate genes impact aging touch receptor neuron morphology and function 116
4.5 Discussion 119
4.6 Acknowledgements 125
4.7 References cited 142
Chapter 5: General Conclusions 149
5.1 Summary of findings 149
5.2 Proteostasis in aging neurons 150
5.3 Nutritional impacts on insulin signaling and DAF-16/FOXO activity 152
5.4 Aging phenotypes of anterior versus posterior touch receptor neurons 153

5.5 Environmental factors in medicinal food efficacy 155
5.6 Final conclusions 155
5.7 References cited 156

List of Figures

Page

Figure 2.1 The insulin signaling pathway in *Caenorhabditis elegans*. 39

Figure 2.2 PolyQ0 and polyQ128 exhibit basal differences in mechanosensory neuron morphology and function without altered lifespan. 40

Figure 2.3 Neuronal and systemic insulin signaling mediates lifespan of both healthy (polyQ0) and proteotoxically stressed (polyQ128) animals. 41

Figure 2.4 *daf-2* RNAi mediates mechanosensory neuron morphology and function in polyQ0 animals. 43

Figure 2.5 The insulin signaling pathway mediates mechanosensory neuron morphology and function in polyQ128 animals. 45

Supplemental Figure 2.1 polyQ0 and polyQ128 neurons are sensitive to RNAi treatments. 46

Supplemental Figure 2.2 Insulin signaling mediates poly128 aggregate area. 47

Figure 3.1 Alaskan berry and fungus treatments extend wildtype *C. elegans* lifespan. 80

Figure 3.2 Lifespan-extending Alaskan berry and fungus treatments improve wildtype *C. elegans* motility late in life. 81

Figure 3.3 Lifespan-extending Alaskan berry and fungus treatments improve wildtype *C. elegans* gentle touch response late in life. 82

Figure 3.4 Lifespan-extending Alaskan berry and fungus treatments change endogenous reactive oxygen species (ROS) levels in young wildtype *C. elegans*. 83

Figure 3.5 Alaskan blueberry treatments alter the accumulation of aberrations in aging anterior touch receptor neurons. 85

Figure 3.6 Alaskan lowbush cranberry treatments increase occurrence of process branching in aging posterior touch receptor neurons. 86

Figure 3.7 Alaskan chaga treatments impact aging anterior and posterior touch receptor neurons. 88

Figure 3.8 Schematic summary of results. 89

Supplemental Figure 3.1 Crowberry treatment does not affect wildtype *C. elegans* lifespan. 90

Supplemental Figure 3.2 Blueberry and lowbush cranberry treatments increase wildtype *C. elegans* lifespan even with UV killed bacterial food source. 91

Supplementary Figure 3.3 Lifespan-extending Alaskan berry and fungus treatments alter wildtype *C. elegans* daily progeny production, but not total progeny produced. 92

Figure 4.1 Alaskan lowbush cranberry activates DAF-16/FOXO nuclear translocation later in life. 126

Figure 4.2 Alaskan lowbush cranberry requires DAF-16 for lifespan extension and posterior neuron branching events late in life. 127

Figure 4.3 Gene expression is differentially regulated following treatment with Alaskan blueberry and chaga extracts. 128

Figure 4.4 Transcriptome comparison between blueberry and chaga treatment yields more effects. 129

Figure 4.5 The impacts of Alaskan blueberry-mediated candidate gene on aging neuron morphology. 130

Figure 4.6 The impacts of Alaskan chaga-mediated candidate gene on aging neuron morphology. 131

Figure 4.7 The impacts of candidate neuron morphology modulators on aging neuron morphology. 132

Figure 4.8 Summary of touch receptor neuron aging modulators detected with Alaskan nutraceutical treatment. 133

Supplemental Figure 4.1 DAF-16 and HSF-1 nuclear translocation are not induced after 48h treatment with Alaskan berry or fungus. 134

Supplemental Figure 4.2 GFP RNAi treatment blocks GFP expression..... 135

List of Tables

Page

Table 2.1 Effect of RNAi treatment on polyQ0 and polyQ128 motility. 48

Table 2.2 Effects of RNAi treatment targeting insulin signaling on polyQ0 and polyQ128 animals' mean lifespan. 49

Table 2.3 RNAi treatments targeting the insulin signaling pathway differentially effect polyQ128 specific mechanosensory neuron aberrations. 50

Table 3.1 Biochemical quantification of crude extracts..... 93

Table 3.2 Alaskan berry and fungus treatments extend wildtype *C. elegans* lifespan..... 94

Table 3.3 Alaskan berry and fungus treatments do not alter total progeny produced by wildtype *C. elegans*..... 95

Table 4.1 Alaskan lowbush cranberry treatments cause DAF-16::GFP nuclear foci formation later in life. 136

Table 4.2 The effect of Alaskan berry and fungus treatments on *daf-16(mgdf50)* mutant lifespan. 137

Table 4.3 Summary of alignments from RNA library. 138

Table 4.4 Candidate touch receptor neuron morphology regulators selected for follow-up. 139

Table 4.5 Known interactions of the aging *C. elegans* touch receptor neuron aging modulators detected with Alaskan nutraceutical treatment with the cytoskeleton, axon transport, and developmental processes. 140

Supplemental Table 4.1 Comparison of control versus blueberry treatment transcriptomes. .. 141

Supplemental Table 4.2 Comparison of control versus chaga treatment transcriptomes. 141

Supplemental Table 4.3 Comparison of blueberry versus chaga treatment transcriptomes. ... 141

Supplemental Table 4.4 Selection of candidate touch receptor neuron morphology regulators. 141

Acknowledgements

I would like to thank the past and present members of the Taylor/Harris laboratory, the members of my graduate committee, and all of my coauthors for helping to make this dissertation possible. For Chapter 2, thank you to: Elena Vayndorf for training me in *C. elegans* laboratory techniques, troubleshooting experimental design, initiating the collaborations to make this research possible, selecting and training me on data analysis techniques, and participating in in-depth methods and results discussions; Alex Parker and Christian Neri for providing essential *C. elegans* strains and editing the manuscript; Monica Driscoll for assisting in establishing methods in our laboratory at UAF essential to this research, participating in in-depth methods and results discussions, detailed writing and editing assistance, and funding for the project; Barbara Taylor for participating in in-depth methods and results discussions, detailed writing and editing assistance, and funding for the project. For Chapters 3 and 4, thank you to: Elena Vayndorf for helping to plan appropriate experiments and participating in in-depth discussions about methods, data analysis, and results; Alicia Hernandez for assistance in data collection and analysis; Colin McGill for advising and assisting in Alaskan berry and fungus extractions; and Barbara Taylor for participating in in-depth methods and results discussions, detailed writing and editing assistance, and funding for the project.

I'd also like to thank the funding sources that supported me through my graduate studies: Alaska IDeA Network of Biomedical Research Excellence (INBRE), UAF Biomedical Learning and Student Training (BLaST), UAF Institute of Arctic Biology (IAB), and Arctic Institute of North America (AINA).

Chapter 1

General Introduction

1.1 Biology of aging

Aging is a ubiquitous process affecting the health of increasing numbers of individuals throughout the world. Because aging impacts everyone, many of the physiological effects of aging are well known; including decreased sensory perception (e.g. hearing, smell, sight) and sarcopenia (i.e. loss of muscle tissue). At the cellular and molecular level, aging is characterized by genomic instability, proteostasis dysregulation, telomere shortening, epigenetic modifications, mitochondrial dysfunction, cellular senescence, and poor intercellular communication (reviewed in Lopez-Otin, 2013). Additionally, increased age is correlated with increased risk for development of chronic diseases (e.g. cardiovascular or neurodegenerative disease, cancer) and acute, life-threatening diseases (e.g. pneumonia). Thus, development of strategies to improve tissue, system, and organismal aging is an increasing public health priority.

As opposed to being a random process, aging is now known to be subject to highly regulated, evolutionarily-conserved processes (Kenyon, 2005). However, the exact molecular mechanisms that underlie the aging process (e.g. pre-programmed timetable vs. accumulation of too much damage) are not fully described and are often hotly disputed. Early beliefs and theories argued that aging was due to wear on the body and mind from the challenges of life, much like erosion. August Weismann (1834-1914) is one of the first theorists credited with using evolutionary biology concepts to predict a cellular aging theory (Gavrilov and Gavrilova, 2002). Weismann's "theory of programmed cell death" posited that the number of replication cycles of a cell is limited, and after that limit is reached, the cell dies.

More theories of aging were proposed in the 1950's, based on evolutionary and molecular biological concepts. One such theory that has stood the test of time is the "mutation accumulation theory of aging," proposed by Peter Medawar (1915-1987). This theory states that genes controlling aging reveal their phenotypes too late in life to be selected upon via evolution (i.e. after reproductive senescence), which results in passive accumulation of negative, aging-related phenotypes over evolutionary time (Medawar, 1946). The "antagonistic pleiotropy theory of aging" proposed by George Williams (1926-2010) is an alternative theory of aging that also has modern day supporters. This theory predicts that pleiotrophy, the phenomenon where a gene may be involved in more than one phenotype, is at the center of the aging process (Williams, 1957). Williams hypothesized that the same genes that result in negative aging phenotypes late in life exhibit beneficial phenotypes early in life, when they are subject to natural selection and, thus, propagated in a population. The "disposable soma theory of aging," proposed by Thomas Kirkwood (1951-) builds on antagonistic pleiotropy by stating that organisms strategically allocate resources to allow for successful reproduction, leaving fewer resources to maintain somatic cells throughout life.

Modern theories of aging build off of the interrelated historical theories and generally fall into two categories: damage/error accumulation and programmed aging/cell death (reviewed in Jin, 2010). One well-known damage accumulation theory of aging is the "free radical theory of aging", proposed by Denham Herman (1916-2014). This theory is built on the knowledge that cellular nucleic acids, proteins, and lipids accumulate damage over time from exogenous and endogenous free radicals (i.e. molecules with an unpaired electron), such as reactive oxygen species (e.g. hydrogen peroxide), and predicts that this accumulation of damage underlies the aging process. Programmed cell death theories posit that cellular processes in the nervous, endocrine, and immune systems continue the biological timetable begun during growth and development through aging and death. These modern theories are indirectly supported by experimental data, but no single theory has emerged as the definitive theory of aging. The more

we discover about molecular biology and the mechanisms behind longevity-promoting interventions, the more theories arise, some novel and some further explicating historical theories. However, the molecular, cellular, systemic, and evolutionary aspects of aging are indeed interrelated; thus, multiple theories (as we define them today) are likely necessary to describe the aging process (reviewed in Weinert and Timiras, 2003).

1.2 Brain and neuron aging

Maintaining nervous system integrity with age is critical to maintaining overall health, as the nervous system is the central regulator of internal and external information. Many physical and functional changes in the nervous system and brain are associated with the natural, non-diseased aging process. For example, decreased cerebral cortex volume has historically been associated with increased age. Importantly, this loss in volume is not due to neuronal death (reviewed in Yankner et al., 2008). Rather, the overall volume decreases due to changes in neuron and dendritic morphology (Freeman et al., 2008) and a loss of white matter (i.e. myelination and glial cells; Bartzokis et al., 2003). In other brain regions, such as the hippocampus, dentritic branching increases with age (Buell and Coleman, 1979). Additionally, these morphological changes are correlated with poor interregional brain communication and cognitive performance (reviewed in Bishop et al., 2010). While numerous research groups have made observations of age-related physical and functional changes in the human brain, the molecular mechanisms driving these changes are unknown.

Neurodegenerative diseases result in additional brain phenotypes that are distinct from the natural, healthy aging process. Many neurodegenerative disorders are caused by genetic mutations and the toxic aggregation of proteins within neurons. For example, one neurodegenerative disease, Huntington's disease, is caused by a polyglutamine-expansion mutation in the huntingtin gene leading to impairments in movement, cognitive function, and psychological disorders. Huntington's disease progression results in extensive atrophy and cell

death in the striatal putamen and caudate brain regions and the cerebral cortex, the extent of which is correlated with the level of polygluatmine expansion (Halliday et al., 1998). The striatal medium spiny neurons that do not die during disease progression exhibit drastic morphological changes both in moderate-grade (e.g. recurved dendrites, increased number and size of dendritic spines) and severe-grade (e.g. dendritic spine loss, shortened and swollen dendrites) Huntington's disease (Ferrante et al., 1991). Both neurodegenerative disease and healthy aging phenotypes are characterized by drastic changes in the nervous system. Thus, uncovering the molecular mechanisms behind these nervous system changes is a pertinent approach to providing recommendations and therapies to improve the health of aging individuals.

Caenorhabditis elegans is a powerful *in vivo* model system for aging. These nematodes contain important neuronal components found in humans (i.e. neurotransmitters, ligand receptors, ion channels), are easy to genetically manipulate, and have a short wildtype lifespan (~3 weeks). Importantly, *C. elegans* experience age-related deterioration of different tissue types similar to humans (e.g. muscle deterioration; Herndon et al., 2002). Also similar to humans, the *C. elegans* nervous system exhibits physical and functional changes with age. *C. elegans* neurons do not die nor disintegrate in old age (Herndon et al., 2002). Instead, specific classes of neurons (e.g. touch receptor and GABAergic motor neurons) exhibit altered phenotypes with age (Toth et al., 2012; Pan et al., 2011; Tank et al., 2011). Interestingly, these aging neurons develop additional outgrowths from their axons and cell somas (rather than a loss of outgrowths) in conjunction with decreased synaptic integrity, function (i.e. touch response), and locomotion (Toth et al., 2012). Other molecular changes occur within aging *C. elegans* neurons as well. For example, mitochondrial density and trafficking within neurons decreases with age (Morsci et al., 2016). Also, decreased sensory perception, neurotransmission, and intercellular communication of chemosensory neurons (i.e. food detection) occur with age (Leinwand et al., 2015). The similarities between human and *C. elegans* neuron aging is striking and supports the use of these nematodes as experimental

models to further our understanding of human nervous system aging and to develop novel therapies for neurodegenerative disease.

1.3 Genetic determinants of aging

Genetic mutations that increase lifespan are also proposed to postpone age-related declines in motor and cognitive function. Amazingly, the longer long-lived individuals live, the lower the proportion of time they spend in poor health, disabled, and with chronic disease. One study found that 17% of centenarians (age 100-104) "survive" with at least one chronic disease, 53% "delay" onset of chronic disease, and 30% "escape" chronic disease altogether in their lifespan (Anderson et al., 2012). Compare this to 12%, 32%, and 56% of semisupercentenarians (age 105-109) and 8%, 23%, and 69% of supercentenarians (age 110+), respectively, for "surviving," "delaying", and "escaping" chronic disease in their lifetime (Anderson et al., 2012). These statistics indicate that increasing population lifespan has the potential to improve healthspan and quality of life, a very desirable outcome.

To examine the role of genetics in the aging process in living humans, very long-lived people (i.e. centenarians) and long-term, aging adult cohorts are studied to identify variations in allele frequency and gene expression that correlate with long life. Many genes and signaling pathways have arisen as potential determinants of longevity using these methods (reviewed in Newman and Murabito, 2013). However, only two such genes have been repeatedly described in multiple studies: apolipoprotein E (APOE; cholesterol transport and brain injury repair) and forkhead transcription factor (FOXO3A; insulin signaling). Genome-wide association meta-analyses found that variations in APOE strongly associated and FOXO3A modestly associated with survival to more than 90 years old (Deelen et al., 2014; Beekman et al., 2013). Specific APOE alleles are associated with Alzheimer's and cardiovascular disease risk, while others are associated with longevity, suggesting that a critical balance of APOE function must be maintained for improved healthspan (reviewed in Shadyab and LaCroix, 2015). In Ashkenazi

Jewish centenarians, one common allele and two common regulatory units of APOE are expressed at a significantly lower level while one APOE allele is expressed at a significantly higher level when compared to control populations without a family history of longevity (Ryu et al., 2016). Additionally, males and females from diverse ethnic groups (and multiple research study groups) with more than one copy of the minor FOXO3A allele are consistently more likely to live to centenarian status (reviewed in Newman and Murabito, 2013). It will be interesting to see whether these genes remain relevant as new cohorts of aging individuals survive changing health challenges in their lifetimes (e.g. historical pre-antibiotic medical care versus the modern-day obesity epidemic; Newman and Murabito, 2013). Since specific gene allele frequencies are associated with human longevity, molecular studies exploring the specific role of these genes in the aging process are warranted.

The use of model organisms, including *C. elegans*, to study the genetic and molecular basis of aging is a burgeoning field with many results complementary to human genome studies, including FOXO3A findings (Kenyon, 2005). The longevity-associated insulin signaling pathway is highly conserved across multicellular organisms and is a key signaling pathway involved in metabolic responses to nutrient availability (Broughton and Partridge, 2009)[1]. A mutation in the *C. elegans* insulin receptor (DAF-2/IGFR) conferring decreased function was the first genetic mutation discovered to double the lifespan of an organism (Kenyon, 1993). These long-lived mutants also exhibit improved response to stress (Kenyon, 1993) and various improved molecular aging phenotypes (e.g. mitochondrial patterns, Morsci et al., 2016), demonstrating that lifespan extension in model organisms may also improve healthspan. Conversely, mutations in the *C. elegans* FOXO3A homolog (DAF-16/FOXO) confer decreased lifespan, demonstrating the negative regulation of DAF-16/FOXO (i.e. excluded from the nucleus) in response to insulin availability (Ogg et al., 1997). Genetically modifying insulin

[1] *C. elegans* cholesterol transport occurs via endocytosis rather than APOE mechanisms, which is sufficiently different from humans to negate the utility of *C. elegans* as a model for this process.

signaling in neurons (e.g. DAF-2/IGFR or DAF-16/FOXO mutations) also impacts the development of age-related morphological and functional changes in *C. elegans* mechanosensory and GABAergic neurons (Toth et al., 2012; Pan et al., 2011; Tank et al., 2011). Thus, in part because of its role in regulating lifespan and healthspan, the insulin signaling pathway has been heavily studied as a modulator of proteotoxicity and neurodegeneration (reviewed in Cohen and Dillin, 2008), again linking processes that increase and improve lifespan with those that drive disease development.

1.4 Nutritional aging interventions

Modifying diet, specifically consuming fruits, vegetables, nuts, and specific spices (e.g. tumeric, which contains curcumin), is proposed to be a practical method to lower age-related cognitive decline (Joseph et al., 2009). From Ancient Egypt (Ebers Papyrus from c. 1550 BC) to the modern-day extreme Alaskan environment (Garabaldi, 1999; Kari, 1995), people have both attempted to and successfully used plants and fungi as medicines. Historically, cultures developed pharmacopeia through instincts (e.g. smell, taste) and/or the Doctrine of Signatures (i.e. the shape of a plant represents the part of the body whose ailment it can treat). Today, we know that medicinal value is often determined, at least in part, by the plant or fungi's molecular biology. Secondary metabolites, or compounds not directly involved in growth, development, and reproduction, are often credited with conferring medicinal properties to plant and fungal foods. This class of compounds includes the following: alkaloids (e.g. caffeine), terpenes (e.g. provide aroma and flavor of hops), glyosides (e.g. found in liquorice), and polyphenols (e.g. tannins, anthocyanins). The function of secondary metabolites is to increase the survival of the plant or fungus by defending against environmental stressors, herbivory, infection, and/or competition (i.e. allelopathy). Interestingly, these inherently bioactive secondary metabolites can confer stress resistance and even improved aging trajectories to the animals that consume them. This phenomenon, an inter-species hormesis principle coined "xenohormesis" (Hooper, et

al., 2010; Howitz and Sinclair, 2008) is thought to be due to the adaptive response of the animal to the consumed stress response compounds in an effort to increase its own survival to the perceived environmental stressors. Xenohormesis is founded on the idea that the health benefits from secondary metabolite consumption "result not from responses to mild cellular damage or from their antioxidant properties, but rather from the evolutionarily adaptive modulation of the enzymes and receptors of stress-response pathways in mammals" (pg 389, Howitz and Sinclair, 2008).

Epidemiological studies consistently show that dietary patterns rich in plant food sources are correlated with increased lifespan, decreased incidence of age-related diseases, or both (reviewed in Fleming et al., 2013). For example, the Mediterranean diet, rich in fruits, vegetables, whole grains, fish, and legumes, is frequently heralded for its association with increased lifespan and decreased incidence of chronic disease when compared to modern, "Western" diet patterns high in sugar, processed foods, and red meat (reviewed in Jong et al., 2014). Other place-based, traditional diet patterns appear to reduce the risk of developing age-related disorders. Even transitioning away from the Alaska Native traditional diet rich in meat and fat (90% from fish and game meat fat compared to <3% plant matter; Bersamin et al., 2007) to "Western" high-sugar diet patterns increases the risk of cardiovascular disease (Loring and Gerlach, 2009; Ebbesson et al., 2005). This observation may be due to the promotion of fatty acid profiles associated with cardiovascular health benefits over Western diets by Alaska Native diets (i.e. higher eicosapentanoic and docosahexaenoic fatty acids in red blood cells; Bersamin et al., 2008). These epidemiological data highlight the important role of nutrition in longevity and maintaining health throughout the lifespan.

There are numerous, specific examples of the interactions of plant compounds with cellular signaling pathways of plant consumers. For example, quercetin, a flavonol extracted from fruits, such as apples, interacts beneficially with insulin signaling to improve wildtype *C. elegans* health and decrease cellular oxidative damage (Youl et al., 2010). Extracts from

roseroot, coffee, and curcumin specifically alter *C. elegans* DAF-16/FOXO transcription factor activity in models of healthy aging (Wiegant et al., 2009), Alzheimer's disease (Dostal et al., 2010), and various neurodegenerative diseases (Monroy et al., 2013), respectively. Even in human cell culture and mammalian model systems, nutraceutical and bioactive molecule treatments are a promising direction for improving health, aging, and neurodegeneration (reviewed in Seidl et al., 2014). Berries in particular have been heavily studied for their impact on brain signaling and neurodegeneration (Miller and Shukitt-Hale, 2012; Shukitt-Hale, 2012; Spencer, 2008). For example, blueberry supplementation not only increases wildtype *C. elegans* lifespan (Wilson et al., 2006) but also improves memory in aging rats (Joseph et al., 1999), children (Whyte et al., 2015), and older adults (Krikorian et al., 2010). The specific molecular mechanisms behind plant compound regulation of longevity, health, and improved nervous system function may provide insights into the molecular mechanisms of the aging process itself.

Through this work, we aimed to further describe the intricate relationship between genetics and diet in the aging process, focusing on neuronal aging processes. We tested the hypothesis that the conserved, aging-related insulin signaling pathway regulates touch receptor neuron aging in diseased (i.e. Huntington's disease) and nutrition supplementation models (i.e. Alaskan berry and fungal extract treatments) and discovered novel genetic modifiers of touch receptor neuron aging. Alaskan traditional knowledge holds that a diverse array of local plants and fungi benefit health and wellness (Garabaldi, 1999; Kari, 1995). Alaskan plant and fungus species have adapted to the region's extreme environment, in part by producing a wide variety of secondary metabolites (Elks et al., 2013). As such, Alaskan berry species consistently contain higher levels of antioxidant and anti-inflammatory compounds than commercially grown species as well as those in lower temperate and tropical regions (Dinstel et al., 2013; Grace et al., 2013). By studying the *in vivo* biological effects of ingesting Alaskan nutraceuticals (i.e. interactions with cellular signaling pathways, such as insulin signaling), which are produced by

plants and fungi adapted to a more stressful environment than other, more well-studied nutraceuticals, we have a unique opportunity to study the biology of aging and identify novel anti-aging and neurodegeneration therapies.

1.5 References cited

Anderson, S.L., Sebastiani, P., Dworkis, D.A., Feldman, L., and Perls, T.T. (2012). Health span approximates life span among many supercentenarians: Compression of morbidity at the approximate limit of life span. *J Gerontol A Biol Sci Med Sci* 4, 395-405.

Bartzokis, G., Cummings, J.L., Sultzer, D., Henderson, V.W., Nuechterlein, K.H., and Mintz, J. (2003). White matter structural integrity in healthy aging adults and patients with Alzheimer disease: a magnetic resonance imaging study. *Arch Neurol* 60, 393-398.

Beekman, M., Blanche, H., Perola, M., Hervonen, A., Bezrukov, V., Sikora, E., Flachsbart, F., Christiansen, L., De Craen, A.J.M., Kirkwood, T.B.L., Rea, I.A., Poulain, M., Robine, J.M., Valensin, S., Stazi, M.A., Passarino, G., Deiana, L., Gonos, E.S., Paternoster, L., Sørensen, T.I.A., Tan, Q., Helmer, Q., van den Akker, E.B., Deelen, J., Martella, F., Cordell, H.J., Ayers, K.L., Vaupel, J.W., Teornwall, O., Johnson, T.E., Schreiber, S., Lathrop, M., Skytthe A., Westendorp, R.G.J., Christensen, K., Gampe, J., Nebel, A., Houwing-Duistermaat, J.J., Slagboom, P.E., and Franceschi, C. (2013). Genome-wide linkage analysis for human longevity: Genetics of healthy aging study. *Aging Cell* 12, 184-193.

Bersamin, A., Zidenberg-Cherr, S., Stern, J., and Luick, B. (2007). Nutrient intakes are associated with adherence to a traditional diet among Yup`ik Eskimos living in remote Alaska Native communities: the CANHR Study. *International J Circumpolar Health 66*.

Bersamin, A., Luick, B.R., King, I.B., Stern, J.S., and Zindenberg-Cherr, S. (2008). Westernizing diets influence fat intake, red lood cell fatty acid composition, and health in remote Alaskan Native communities in the Center for Alaska Native Health Study. *J American Dietetic Assoc* 35, 266-273.

Bishop, N.A., Lu, T., and Yankner, B.A. (2010). Neural mechanisms of ageing and cognitive decline. *Nature* 464, 529-535.

Broughton, S and L Partridge. (2009). Insulin/IGF-like signaling, the central nervous system and aging. *Biochem J* 418, 1-12.

Buell S.J. and Coleman, P.D. (1979). Dendritic growth in the aged human brain and failure of growth in senile dementia. *Science* 206, 854-896.

Cohen, E., and Dillin, A. (2008). The insulin paradox: aging, proteotoxicity and neurodegeneration. *Nat Rev Neurosci* 9, 759–67.

Deelen, J., Beekman, M., Uh, H.W., Broer, L., Ayers, K.L., Tan, Q., Kamatani, Y., Bennet, A.M., Tamm, R., Trompet, S., Guõbjartsson, D.F., Flachsbart, F., Rose, G.,Viktorin, A., Fischer, K., Nygaard, M., Cordell, H.J., Crocco, P., van den Akker, E.B., Böhringer, S., Helmer, Q., Nelson, C.P., Saunders, G.I., Alver, M., Andersen-Ranberg, K., Breen, M.E., van der Breggen, R., Caliebe, A., Capri, M., Cevenini, E.,Collerton, J.C., Dato, S., Davies, K., Ford, I., Gampe, J., Garagnani, P., de Geus, E.J., Harrowo, J., van Heemst, D., Heijmans, B.T., Heinsen, F.A., Hottenga, J.J.,Hofman, A., Jeune, B., Jonsson, P.V., Lathrop, M., Lechner, D., Martin-Ruiz, C.,McNerlan, S.E., Mihailov, E., Montesanto, A., Mooijaart, S.P., Murphy, A., Nohr, E.A., Patemoster, L., Postmus, I., Rivadeneira, F., Ross, O.A., Salvioli, S., Sattar, N.,Schreiber, S., Stefansson, H., Stott, D.J., Tiemeier, H., Uitterlinden, A.G., Westen-dorp, R.G., Willemsen, G., Samani, N.J., Galan, P., Sørensen, T.I., Boomsma, D.I.,Jukema, J.W., Rea, I.M., Passarino, G., de Graen, A.J., Christensen, K., Nebel, A., Stefánsson, K., Metspalu, A., Magnusson, P., Blanché, H., Christiansen, L., Kirkwood,T.B., van Duijn, C.M., Franceschi, C., Houwing-Duistermaat,

J.J., and Slagboom, P.E., (2014). Genome-wide association meta-analysis of human longevity identifies a novel locus conferring survival beyond 90 years of age. *Hum Mol Genet* 23, 4420–4432.

Dinstel, R.R., Cascio, J., and Koukel, S. (2013). The antioxidant level of Alaska's wild berries: high, higher and highest. *Nutrition* 1, 1–7.

Dostal, V., Roberts, C.M., and Link, C.D. (2010). Genetic mechanisms of coffee extract protection in a Caenorhabditis elegans model of β-amyloid peptide toxicity. *Genetics* 186(3), 857–66.

Ebbesson, S., Adler, A., Risica, P., Ebbesson, L., Yeh, J.L., Go, O., Doolittle, W., Ehlert, G., Swenson, M., and Robbins, D. (2005). Cardiovascular disease and risk factors in three Alaskan Eskimo populations: the Alaska-Siberia project. *International J Circumpolar Health* 64, 365–386.

Elks, C.M., Francis, J., Stull, A.J., Cefalu, W.T., Shukitt-Hale, B., and Ingram, D.K. (2013). "Overview of the health properties of blueberries," in *Bioactives in fruit: Health benefits and functional foods*, eds. M. Skinner and D. Hunter (John Wiley & Sons), 251–271.

Ferrante, R.J., Kowall, N.W., and Richardson, E.P. Jr. (1991). Proliferative and degerative changes in striatal spiny neurons in Huntington's disease: A combined study using the section-Golgi method and calbindin D28k immunocytochemistry. *J Neurosci* 11(12), 3877-3887.

Fleming, J.A., Holigan, S., and Kris-Etherton, P.M. (2013). Dietary patterns that decrease cardiovascular disease and increase longevity. *J Clin Exp Cardiolog* S6: 006.

Freeman, S.H., Kandel, R., Cruz, L., Rozkalne, A., Newell, K., Frosch M.P., Hedley-Whyte, E.T., Locascio, J.J., Lippsitz, L., and Hyman, B.T. (2008). Preservation of neuronal number despite age-related cortical brain atrophy in elderly subjects without Alzheimer Disease. *J Neuropathol Exp Neurol* 67(12), 1205-1212.

Garabaldi, A. (1999). *Medicinal flora of the Alaska Natives.* Anchorage, Alaska: Environment and Natural Resources Institute, Alaska Natural Heritage Program.

Gavrilov, L.A. and Gavrilova, N.S. (2002). Evolutionary theories of aging and longevity. *Sci World J* 2, 339-356.

Grace, M.H., Esposito, D., Dunlap, K.L., and Lila, M.A. (2013). Comparative Analysis of Phenolic Content and Profile, Antioxidant Capacity, and Anti-inflammatory Bioactivity in Wild Alaskan and Commercial Vaccinium Berries. *J Agric Food Chem* 62, 4007–4017.

Halliday, G.M., McRitchie, D.A., Macdonald, V., Double, K.L., Trent, R.J., and McCusker E. (1998). Regional specificity of brain atrophy in Huntington's disease. *Exp Neurol* 154(2), 663-672.

Herndon, L., Schmeissner, P., Dudaronek, J., Brown, P., Listner, K., Sakano, Y., Paupard, M., Hall, D., and Driscoll, M. (2002). Stochastic and genetic factors influence tissue-specific decline in ageing *C. elegans*. *Nature* 419, 808–814.

Hooper, P.L., Hooper, P.L., Tytell, M., and Vigh, L. (2010). Xenohormesis: Health benefits from an eon of plant stress response evolution. *Cell Stress Chaperones* 15, 761-770.

Howitz, K. and Sinclair, D.A. (2003). Xenohormesis: Sensing the chemical cues of other species. *Cell* 133, 387-391.

Jin, K. (2010). Modern biological theories of aging. *Aging Dis* 1(2), 72-74.

Joseph, J.A., Shukitt-Hale, B., and Denisova, N.A. (1999). Reversals of age-related declines in neuronal signal transduction, cognitive, and motor behavioral deficits with blueberry, spinach, or strawberry dietary supplementation. *J Neurosci* 19(18), 8114-8121.

Joseph, J., Cole, G., Head, E., and Ingram, D. (2009). Nutrition, Brain Aging, and Neurodegeneration. *J Neurosci 29*, 12795–12801.

Kari, P.R. (1995). *Tanaina plantlore, Dena'ina k'et'una*. 4th ed. Fairbanks, Alaska : Alaska Native Language Center, Alaska Natural History.

Kenyon, C.J. (1993). A *C. elegans* mutant that lives twice as long as wild type. *Nature* 366, 461–464.

Kenyon, C. (2005). The plasticity of aging: insights from long-lived mutants. *Cell* 120, 449–60.

Krikorian, R., Shidler, M., Nash, T., Kalt, W., Vinqvist-Tymchuk, M., Shukitt-Hale, B., and Joseph, J. (2010). Blueberry supplementation improves memory in older adults. *J Agric Food Chem 58*, 3996–4000.

Jong, J.C.K., Mathers, J.C., and Franco, O.H. (2014). Nutrition and health aging: the key ingredients. *Pro Nutrition Soc* 73, 249-259.

Leinwand, S.G., Yang, C.J., Bazopoulou, D., Chronis, N., Srinivasan, J., and Chalasani, S.H. (2015). Circuit mechanisms encoding odors and driving aging-associated behavioral declines in *Caenorhabditis elegans. Elife* 4:e10181.

Lopez-Otin, C., Blasco, M.A., Partridge, L., Serrano, M., and Kroemer, G. (2013). The hallmarks of aging. *Cell* 153, 1194-1217.

Loring, P. and Gerlach, S.C. (2009). Food, culture, and human health in Alaska: an integrative health approach to food security. *Env Science & Policy* 12, 466–478.

Medawar, P.B. (1946). Old age and natural death. *Modern Q* 1, 30–56.

Miller, M., and Shukitt-Hale, B. (2012). Berry fruit enhances beneficial signaling in the brain. *J Agric Food Chem* 60, 5709–5715.

Monroy, A., Lithgow, G. J., and Alavez, S. (2013). Curcumin and neurodegenerative diseases. *BioFactors*, 39(1), 122–32.

Morsci, N.S., Hall, D.H., Driscoll, M., and Sheng, Z.H. (2016). Age-related phasic patterns of mitochondria in adult *Caenorhabditis elegans* neurons. *J Neurosci* 36(4), 1373-1385.

Newman, A.B. and Murabito, J.M. (2013). The epidemiology of longevity and exceptional survival. *Epidemiology Rev* 35, 181-197.

Ogg, S., Paradis, S., Gottlieb, S., Patterson, G.I., Lee, L., Tissenbaum, H.A., and Ruvkun, G. (1997). The Fork head transcription factor DAF-16 transduces insulin-like metabolic and longevity signals in *C. elegans*. *Nature* 389, 994–9.

Pan, C.L., Peng, C.Y., Chen, C.H., and McIntire, S. (2011). Genetic analysis of age-dependent defects of the *Caenorhabditis elegans* touch receptor neurons. *PNAS* 108, 9274–9279.

Ryu, S., Atzmon, G., Barzilai, N., Raghavachari, N., and Suh, Y. (2016). Genetic landscape of *APOE* in human longevity revealed by high-throughput sequencing. *Mech Age Devel* 155, 7-9.

Seidl, S. E., Santiago, J. A, Bilyk, H., and Potashkin, J. A. (2014). The emerging role of nutrition in Parkinson's disease. *Front Aging Neurosci* 36, 1-14.

Shadyab, A.H. and LaCroix, A.Z. (2015). Genetic factors associated with longevity: a review of recent findings. *Aging Res Review* 19, 1-7.

Shukitt-Hale, B. (2012). Blueberries and neuronal aging. *Gerontology 58*, 518–523.

Spencer, J. (2008). Food for thought: the role of dietary flavonoids in enhancing human memory, learning and neuro-cognitive performance. *Proc Nutrition Soc 67*, 238–252.

Tank, E., Rodgers, K., and Kenyon, C. (2011). Spontaneous age-related neurite branching in *Caenorhabditis elegans*. *J Neurosci* 3, 9279 - 9288.

Toth, M., Melentijevic, I., Shah, L., Bhatia, A., Lu, K., Talwar, A., Naji, H., Ibanez-Ventoso, C., Ghose, P., Jevince, A., Xue, J., Herndon, L.A., Bhanot, G. Rongo, C., Hall, D.H., and Driscoll, M. (2012). Neurite sprouting and synapse deterioration in the aging *Caenorhabditis elegans* nervous system. *J Neurosci* 32, 8778–8790.

Weinet, B.T., Timiras, P.S. (2003). Invited review: Theories of aging. *J Applied Phys* 95(4), 1706-1716.

Whyte, A., Schafer, G., and Williams, C. (2015). Cognitive effects following acute wild blueberry supplementation in 7- to 10-year-old children. *European J Nutrition*, *ePub ahead of print.*

Wiegant, F.C., Surinova, S., Ytsma, E., Langelaar-Makkinje, M., Wikman, G., and Post, J. (2009). Plant adaptogens increase lifespan and stress resistance in *C. elegans*. *Biogerontology*, 10(1), 27–42.

Williams, G.C. (1957). Pleiotropy, natural selection and the evolution of senescence. *Evolution* 11, 398–411.

Wilson, M., Shukitt-Hale, B., Kalt, W., Ingram, D.K., Joseph, J., and Wolkow, C. (2006). Blueberry polyphenols increase lifespan and thermotolerance in *Caenorhabditis elegans*. *Aging Cell* 5, 59–68.

Yankner, B., Lu, T., and Loerch, P. (2008). The aging brain. *Ann Rev Pathology 3*, 41–66.

Youl, E., Bardy, G., Magous, R., Cros, G., Sejalon, F., Virsolvy, A., Richard, S., Quignard, J.F., Gross, R., Petit, P., Bataille, D., and Oiry, C. (2010). Quercetin potentiates insulin secretion and protects INS-1 pancreatic β-cells against oxidative damage via the ERK1/2 pathway. *Br J Pharmacol* 161, 799–814.

Chapter 2

A Dual Role of the Insulin Signaling Pathway in the Aging of Healthy and Proteotoxically Stressed Mechanosensory Neurons[1]

2.1 Abstract

Insulin signaling is central to cellular metabolism and organismal aging. However, the role of insulin signaling in natural and proteotoxically stressed aging neurons has yet to be fully described. We studied aging of *Caenorbaditis elegans* mechanosensory neurons expressing a neurotoxic expanded polyglutamine transgene (polyQ128), or lacking this proteotoxicity stressor (polyQ0), under conditions in which the insulin signaling pathway was disrupted by RNA interference (RNAi). We describe specific changes in lifespan, mechanosensory neuron morphologies, and mechanosensory function following RNAi treatment targeting the insulin signaling pathway. Overall, we confirmed that transcription factor DAF-16 is neuroprotective in the proteotoxically stressed model, though not strikingly in the naturally aging model. Decreased insulin signaling through *daf-2* RNAi improved mechanosensory function in both models and decreased protein aggregation load in polyQ128, yet showed opposing effects on accumulation of neuronal aberrations in both strains. Decreased DAF-2 signaling slightly enhanced mechanosensation while greatly enhancing branching of the mechanosensory neuron axons and dendrites in polyQ0 animals, suggesting that branching is an adaptive response in natural aging. These effects in polyQ0 did not appear to involve DAF-16, suggesting the existence of a non-canonical DAF-2 pathway for the modulation of morphological adaptation. However, in polyQ128 animals, decreased *daf-2* signaling significantly enhanced mechanosensation while decreasing neuronal aberrations. Unlike other interventions that reduce the strength of insulin

[1] Published as Scerbak, C., Vayndorf, E., Parker, A., Neri, C., Driscoll, M., and Taylor, B. (2014). Insulin signaling in the aging of healthy and proteotoxically stressed mechanosensory neurons. Frontiers in Genetics *5*. doi: 10.3389/fgene.2014.00212

signaling, *daf-2* RNAi dramatically redistributed large polyQ128 aggregates to the cell body, away from neuronal processes. Our results suggest that insulin signaling strength can differentially affect specific neurons aging naturally or under proteotoxic stress.

2.2 Introduction

The insulin/insulin-like growth factor (IGF) signaling pathway is involved in longevity and stress response across species (Broughton and Partridge, 2009). Signaling through this evolutionarily conserved pathway can promote longevity through increased expression of cellular stress and metabolism genes, including those encoding stress-response, chaperone, and antioxidant proteins (Kenyon, 1993; Cohen et al., 2009; Hsu et al., 2003; Taguchi et al., 2007). The progression of neurodegenerative disorders, such as Huntington's, Alzheimer's, and Parkinson's diseases, has been linked to insulin signaling in both invertebrate and mammalian model systems (Dillin and Cohen, 2011). In addition, decreased insulin signaling has protective effects against neurodegenerative-associated proteotoxicity across species (Killick et al., 2009; Freude et al., 2009).

The *Caenorhabditis elegans* insulin signaling pathway is regulated by insulin-like signaling ligands, INS-1 through INS-39,that modulate the activity of the DAF-2 tyrosine kinase receptor (Figure 2.1). DAF-2 is orthologous to the mammalian insulin/IGF receptor. This receptor activates a protein kinase signaling pathway, which, through phosphorylation of downstream transcription factor DAF-16 by AKT protein kinase, regulates functions similar to receptor kinases in the insulin signaling pathway in humans. Under high signaling conditions, DAF-16 is phosphorylated to prevent nuclear entry and hence transcription. Under low signaling conditions, DAF-16 is free from inhibitory phosphorylation and can regulate the expression of many different genes contributing to metabolism and physiological defense and homeostasis responses (Mukhopadhyay et al., 2006). This insulin signaling pathway has many branch points, including AKT, and there is some variation in the identities of proteins involved in nematodes, flies, and mice, three organisms in which the role of insulin signaling in aging has been

investigated. Nevertheless, this central, conserved insulin signaling pathway is critical for appropriate cellular metabolism and maintenance of overall organismal health.

Various mutations in genes modulating the *C. elegans* insulin signaling pathway have been shown to directly regulate lifespan. For example, *daf-2* insulin receptor mutants live twice as long as wildtype animals (Kenyon, 1993), *age-1* PI3K mutants live longer than wildtype animals (Friedman and Johnson, 1988), and the lack of the *daf-16* FOXO transcription factor gene shortens lifespan (Oh et al., 2006). Longevity effects can result from limiting insulin signaling in only the neurons or intestinal cells (Libina et al., 2003). In mammals, the effect of reduced insulin signaling on overall health and lifespan is complex, but combined evidence from many studies points to the potential of insulin signaling reduction to extend lifespan (Taguchi and White, 2008). In mice, reduced neuronal or whole animal expression of IRS2, a kinase activated by the insulin receptor, increases lifespan (Taguchi et al., 2007). In humans, various studies have detected an association between longevity and single nucleotide polymorphisms in genes involved in insulin signaling, including the DAF-16-related transcription factor inhibited by insulin signaling (FOXO3A), the insulin receptor (IGF1R), and a central protein kinase (AKT-1) (Newman and Murabito, 2013). Excellent reviews comparing insulin signaling in various model systems have been published (Taguchi and White, 2008; Broughton and Partridge, 2009; Neri, 2012).

C. elegans exhibit many important neuronal components found in humans, including, but not limited to, neurotransmitters, ligand receptors, and ion channels; thus, these animals are a powerful model for studying neuronal aging and neurodegeneration *in vivo*. Neurodegenerative disorders, such as Huntington's, Alzheimer's, and Parkinson's diseases, result in the progressive loss of structure and function of neurons with age. Of these protein aggregation-associated neurodegenerative diseases, Huntington's disease is caused by the expansion of CAG trinucleotide repeats in the huntingtin gene, which results in an expansion of the length of polyglutamine residues at the N-terminus of the huntingtin protein. Expanded polyglutamine

repeats in mutated huntingtin lead to neuronal protein aggregation, impairments in movement and cognitive function, and psychological disorders. Multiple Huntington's disease model strains of *C. elegans* have been developed (Faber et al., 1999; Morley et al., 2002; Parker et al., 2001, 2005). In the model strain used in this study, touch receptor neuron-specific expression of a transgene encoding the first 57 amino acids of human huntingtin with 128 polyglutamine repeats impairs function, without neuronal death (Parker et al., 2001, 2005). Thus, this model may feature conserved events associated with dysfunction that typify early disease stages in humans.

Aging is the primary risk factor for multiple neurodegenerative diseases, yet the intersection of natural neuronal aging and neurodegenerative states is not well understood. As a consequence of sensing and responding to the environment, the nervous system is known to play a role in physiological aging (Alcedo et al., 2013). In normal, healthy aging, *C. elegans* mechanosensory and other neuron classes develop morphological aberrations, including new outgrowths from the soma, novel process branching, and dendritic restructuring (Pan et al., 2011; Tank et al., 2011; Toth et al., 2012). Neuronal insulin signaling appears to be involved in this natural aging process; the link between normal aging and decline under disease conditions is relatively unexplored. To address this relationship, we studied and compared morphological features of aging mechanosensory neurons with and without a neurotoxic expanded polyglutamine transgene, under conditions in which genes of the canonical insulin signaling pathway were disrupted by neuron-targeted RNA interference (RNAi). Our findings suggest that insulin signaling strength can differentially affect specific neurons aging naturally or under conditions of disrupted proteostasis. Under conditions of polyglutamine expansion stress, insulin receptor DAF-2 appears to act through DAF-16/FOXO. However, under conditions of normal aging, DAF-2 activates a non-canonical pathway that acts independently to induce neuroprotection.

2.3 Materials and methods

2.3.1 Strains

The *C. elegans* Huntington's disease model strain used was derived from two previously engineered strains. Strain ID1 (*igIs1 [P_{mec-7}yfp, P_{mec-3}htt57Q128::cfp, lin-15(+)]*) (polyQ128) contains the first 57 amino acids of human huntingtin fused to CFP-labeled expanded polyglutamine tract (Q128) expressed in the 6 mechanosensory neurons as well as in PVD and FLP neurons (Parker et al., 2001). These polyQ128 animals show functional deficiencies in touch response and accumulation of huntingtin protein aggregate in mechanosensory neurons, without cell death (Parker et al., 2001). Strain TU3270 (*uIs57 [$P_{unc-119}$SID-1, $P_{unc-119}$yfp, P_{mec-6}mec-6]*) overexpresses the transmembrane channel SID-1 pan-neuronally, allowing the dsRNA from RNAi treatment to enter all neurons (Calixto et al., 2010). TU3270 and ID1 were crossed to generate a polyQ128-expressing strain with neurons susceptible to RNAi (ID121). We also crossed a healthy transgenic model, ZB154 (*zdIs5* [P_{mec-4}GFP]), to TU3270 to render neurons susceptible to RNAi treatment (ZB123; "polyQ0").

2.3.2 Worm maintenance

Standard methods were used for strain maintenance, bacterial culturing, and animal manipulation (Brenner, 1974). Stock animals were cultured at room temperature (about 22ºC) on nematode growth media (NGM) agar plates seeded with live bacteria (*E. coli* strain OP50-1).

2.3.3 RNA interference treatments

We prepared RNAi plates using 4X concentrated live HT115 *E. coli* bacteria from the Ahringer Library induced at room temperature for 2 days on agar plates. For each batch of RNAi experiments, we performed a control experiment comparing the amount of nerve ring fluorescence knockdown following GFP treatment to empty vector (L4440) in age-matched animals to confirm neuronal RNAi sensitivity of the strain used (Supplemental Figure 2.1). Only

experiments that showed a significant (unpaired *t*-test, $p<0.05$) knockdown of GFP were used for further RNAi studies. We performed RNAi treatments at 25ºC protected from light with age-synchronous populations created using timed egg lay. To perform each egg lay, adult worms laid eggs on each of the described RNAi treatment plates for 4 hours. Animals in all RNAi experiments were transferred by hand each day of adulthood to fresh RNAi plates. We performed and analyzed RNAi experiments "blinded" to the intervention so that the experimenter was not aware of the genetic identity of the RNAi treatment given to each population of animals. We repeated each experiment at least 3 times. We selected day 5 of adulthood as a time point for analysis in the following experiments based on Toth et al. (2012), who reported a significant difference in mechanosensory neuron morphology between day 1 and day 5 of adulthood.

2.3.4 Lifespan analysis

Following the production of age-synchronous populations, we transferred approximately 50 animals from each RNAi treatment group everyday of adulthood to fresh, seeded RNAi treatment small plates and checked for survival by visual observation or gentle prodding with a platinum wire. Animals with protruding intestines, those that bore live young, or that crawled off the plates were censored. Survival experiments always included all 6 RNAi treatment groups (L4440 empty vector, *daf-2, age-1, daf-18, akt-1, daf-16*) at once for, usually, one strain at a time, and were repeated at least twice. We used Kaplan-Meier log-rank survival statistics to analyze differences in mean survival between RNAi treatment groups and $p<0.05$ was noted as significant.

2.3.5 Mechanosensory response assay

We generated synchronous populations as described above, maintained cultures at 25ºC, and transferred each day of adulthood to fresh RNAi treatment plates. On day 5 of adulthood we scored individuals for motility class. Individuals were grouped into 3 classes: A

class indicates normal, voluntary sinusoidal movement, B class indicates locomotion following gentle prodding, and C class indicates inability to locomote. We then tested individuals for their ability to respond to touch by gently touching alternatively on the anterior and posterior end with an eyelash pick, 5 times each (Figure 2.2B). Animals responded either by moving (or attempting to move) in the opposite direction of the touch or by showing no movement. We scored animals (0-5) based on the number of positive responses to touch out of 5 touches at the anterior and 5 touches at the posterior. We also recorded the mobility of each animal. We then imaged the mechanosensory neurons of the tested individuals as described below.

2.3.6 Neuron morphology imaging

Following the mechanosensory response assay on day 5 of adulthood, we mounted animals between 2 cover slips using 2µL of 36% w/v Pluronic™ solution dissolved in water and imaged using the 20X objective of an Axiovert S100 inverted fluorescent microscope. Using constant microscope settings, we collected images of the 6 mechanosensory neurons of each individual and their associated huntingtin protein aggregates, if present, using FITC and CFP filters, respectively. We discarded animals after imaging, so data presented is cross-sectional rather than longitudinal. We repeated mechanosensory response assays and neuron morphology imaging for each strain and RNAi treatment group at least 3 times. We examined the images of 6 mechanosensory neurons of each individual for morphological aberrations, namely cell body outgrowths, cell body guidance errors, and process branching (Toth et al., 2012).

2.3.7 Protein aggregate quantification and data analysis

For polyQ128 experiments, we analyzed huntingtin aggregates (fused with CFP) with ImageJ, using a custom macroinstruction that includes quantification of the total area of aggregates seen in each cell. For comparisons of mechanosensory response and neuron morphology between empty vector control polyQ0 and polyQ128 strains, we used a Mann-

Whitney U comparison. For the mechanosensory response assays, neuron morphology imaging, and protein aggregate counts following RNAi treatments, we used a generalized linear model with a log link function (Poisson regression) and Wald tests for significance of treatment effects. For total aggregate area measurements, we used a one-way ANOVA with Tukey's pairwise comparisons. SPSS (Version 20) statistical software was used to perform, the analyses. A *p*-value of less than 0.05 was considered statistically significant. Values presented in the text represent mean ± standard error.

2.4 Results

2.4.1 Neuron and systemic RNAi knockdown of insulin signaling proteins alters polyQ0 and polyQ128 *C. elegans* lifespan

To initiate analysis of the influence of key insulin signaling pathway genes on normal aging and polyQ128-induced neuronal deficits in mid-adult life, we constructed *C. elegans* strains by genetic crosses with fluorescent mechanosensory (or touch) neuron reporters that express the *sid-1* double stranded (ds) RNA transporter pan-neuronally. This *sid-1* compensates for the lack of a neuronal dsRNA transporter, enabling genes expressed in neurons to be targeted by RNAi (Calixto et al., 2010). Moreover, *sid-1* overexpression in neurons can diminish nonneuronal RNAi effects, such that the *sid-1(+)* neurons act as a sink for double stranded RNA (Calixto et al., 2010). We studied one strain that was free of proteotoxic stress (polyQ0), and one that expresses the first 57 amino acids of human huntingtin protein with expanded polyglutamines fluorescently labeled with CFP (polyQ128) (Parker et al., 2001). In these strains, we can measure neuronal function via mechanosensory touch response assays, visualize neuron morphology structures, and directly observe polyQ128 aggregates. We first confirmed that polyQ0 and Huntington's disease model (polyQ128) strain neurons were sensitive to RNAi treatment by feeding as detected by GFP knockdown in the nerve ring (Supplemental Figure 2.1). Indeed, GFP knockdown was efficient in both strains, supporting that

our intended studies on insulin signaling pathway genes could effectively target mechanosensory neurons.

Interestingly, healthy polyQ0 and proteotoxically stressed polyQ128 empty vector (L4440) treated animals exhibited similar, not significantly different, mean lifespan (Figure 2.2A). Thus, increased polyglutamine load in mechanosensory neurons does not confer decreased lifespan, consistent with previous work showing mechanosensory neurons are dispensable for viability and lifespan (Chalfie et al., 1985). However, empty vector treated control polyQ128 animals do exhibit signs of abnormal function as measured by motility, touch response, and accumulation of mechanosensory neuronal aberrations (Table 2.1, Figure 2.2C and 2.2D), agreeing with previous work (Parker et al., 2001). Specifically, polyQ128 posterior touch response is significantly decreased (Mann-Whitney U, $p<0.01$) and neuronal aberrations are increased at the whole worm (Mann-Whitney U, $p<0.01$), anterior cells (Mann-Whitney U, $p<0.01$), and posterior cells level (Mann-Whitney U, $p=0.04$) when compared to age-matched polyQ0 individuals. This suggests that increased polyglutamine load in the mechanosensory neurons negatively affects the function and healthspan of polyQ128 animals.

Because several previously published mutant and RNAi experiments did not utilize *sid-1* enhanced neuronal RNAi targeting, and thus would not have assayed neuronal knockdown effects, we also confirmed RNAi effects on longevity under the conditions we used for our studies. We found that knockdown of insulin signaling pathway genes in neurons and other tissues altered healthy polyQ0 life as previously reported, with *daf-2*, *age-1*, and *akt-1* RNAi interventions lengthening lifespan, and *daf-16* RNAi shortening it (Figure 2.3A and Table 2.2). Insulin signaling pathway interventions in the polyQ128 strain (*daf-2, age-1*) similarly increased mean lifespan, while *daf-16* RNAi treatment decreased mean lifespan (Figure 2.3B and Table 2.2). In the 3 biological replicates of *akt-1* RNAi in polyQ128 animals, lifespan impact was variable.

To further address whether there might be differences in general viability between polyQ0 and polyQ128 strains, we compared percent change in mean lifespan between polyQ0 and polyQ128 animals for each RNAi treatment group. We found no significant differences in relative percent change between healthy transgenic and polyQ128 animals for the same RNAi treatment (t-tests, $p>0.05$), except for *daf-16* RNAi, which approached significance in the polyQ128 background (Figure 2.3C; $p=0.07$). We also measured endogenous reactive oxygen species (ROS) as detected by the membrane permeable 2', 7'-Dichlorofluorescin diacetate (DCF-DA, Sigma) following RNAi treatments and found that RNAi treatment targeted at insulin signaling pathway proteins from embryo did not consistently significantly affect young adult (day 1) endogenous ROS levels in both healthy transgenic and polyQ128 strains (data not shown). However, *daf-16* RNAi treatment through mid-life in polyQ128 worms significantly increased endogenous ROS levels across all biological replicates.

We conclude that RNAi interventions in our polyQ0 and polyQ128 strains are efficacious and exert similar general influences on aging biology in polyQ0 and polyQ128 strains. Disruption of a small set of sensory neurons by the proteotoxic stress of polyQ128 is not sufficient to grossly impair whole animal function, although there are some functional impairment and increased morphological aberrations. However, we note that in middle-aged adults, *daf-16* RNAi is associated with elevated ROS levels and decreased mid-life viability specifically in the polyQ128 strain, raising the possibility that the combination of small scale neuronal proteostasis disruption can influence entire organism decline when DAF-16-dependent defenses are impaired.

2.4.2 Decreased insulin signaling through RNAi knockdown influences healthy mechanosensory neuron morphology and function

Previous studies on morphological aging of mechanosensory neurons indicated that manipulation of the insulin signaling pathway can change accumulation of neuronal aberrations

(Pan et al., 2011; Tank et al., 2011; Toth et al., 2012). These studies differed in details of methods and outcomes, and did not address *akt-1* or *daf-18* activities. Moreover, these studies left open the question of how morphological features relate to function. To address these gaps and discrepancies, we measured neuron morphology and touch response as a surrogate for mechanosensory function when components of the insulin signaling pathway were knocked down in polyQ0 animals. We performed touch response tests (Figure 2.4A) and then imaged mechanosensory neurons of characterized animals for changes in morphology (Figure 2.4B and 2.4C) at mid-life (day 5 of adulthood; described in detail in Materials and Methods). Total neuronal aberrations include all morphological aberrations observed in an individual or cell type, including soma outgrowths, abnormal cell somas, process branching, and process punctae (Figure 2.4B).

Our analysis of touch sensory function revealed that both anterior and posterior touch responses in *daf-2* RNAi were better than empty vector at day 5 of adult life (Figure 2.4A; Wald test, $p<0.01$ for anterior and posterior scores). *daf-16* RNAi preferentially decreased posterior touch ($p<0.01$), revealing an interesting difference between anterior and posterior mechanosensory neurons. We found that RNAi knockdown of *age-1*, *daf-18*, and *akt-1* did not alter touch responses as compared to empty vector.

A striking result from our analysis of morphological aberrations at day 5 of adulthood is that *daf-2* RNAi increased the occurrence of total neuronal aberrations as compared to control (from 3.2±0.23 to 4.7±0.26 per individual) in both anterior and posterior neurons (Fig. 4C). We found that this increase was driven exclusively by process branching, which was the only specific neuronal aberration observed to change with *daf-2* RNAi (Fig. 4D; from 12.8±3.40% to 32.7±3.80% in anterior cells and 14.5±3.20% to 39.4±3.70% in posterior cells). *age-1* RNAi also increased total aberrations (from 3.2±0.23 to 4.4±0.23 per individual) (Fig. 4C) and novel branching in anterior neurons (Fig. 4D; from 12.8±3.40% to 25.3±3.40% in anterior cells and 14.5±3.20% to 26.7±3.30% in posterior cells), whereas *daf-18*, *akt-1*, and *daf-16* interventions

did not induce statistically significant changes in overall aberrations or in the hyper-branching phenotype. Our findings suggest that *daf-2* disruption, and lowered insulin signaling could differentially effect different morphologies, and raise the question as to whether branching might be an indication of a neuroprotective response (see Discussion).

2.4.3 Touch response, mechanosensory neuron morphology, and protein aggregate accumulation are affected by insulin signaling in a model strain of Huntington's disease pathogenesis

We next examined functionality and morphological aberrations in the polyQ128 strain in which mechanosensory neurons are exposed to a chronic proteotoxic stress that promotes early dysfunction (Parker et al., 2001). As previously noted, empty vector treated polyQ128 animals exhibit increased aberrant neuron morphology and decreased touch response compared to age-matched, empty vector treated wildtype animals (Figure 2.3C and 2.3D).

We tested touch response in polyQ128 animals subjected to RNAi for insulin signaling pathway components (Figure 2.5A). *daf-2* RNAi had a neuroprotective effect on both anterior (Wald test, $p<0.001$) and posterior touch sensitivity (Wald test, $p<0.001$). Interestingly, however, all other RNAi knockdown interventions (*age-1*, *daf-18*, *akt-1* and *daf-16*) had generally deleterious effects on touch sensitivity in the polyQ128 background, with a particularly significant change in posterior touch response in polyQ128 animals compared with empty vector (L4440).

We then examined neuron morphology in the polyQ128 strain following RNAi of the insulin signaling pathway genes (Figure 2.5B). We found that numbers of aberrations in the polyQ128 strain were reduced upon *daf-2* RNAi when compared to empty vector (from 4.78±0.21 to 2.94±0.15 per individual, Wald test, $p<0.001$). In contrast, *age-1* RNAi, modestly increased aberrations (from 4.3±0.2 to 5.4±0.1 per individual), as did *akt-1* and *daf-16* interventions in anterior mechanosensory neurons. Thus for polyQ128-expressing neurons,

morphological aberrations generally inversely correlate with function: low abnormality abundance corresponds to enhanced mechanosensory function.

In polyQ128 animals, the huntingtin:polyQ128 protein is fused with CFP and can be visualized as aggregates in our strain (Figure 2.5C). We therefore also examined the number and size of fluorescent aggregates in mechanosensory neurons following RNAi knockdown of insulin signaling components (Figure 2.5D). Under conditions of *daf-2* RNAi we found that mean numbers of aggregates were lowered compared to wildtype (Wald test, $p<0.01$ for whole individuals, anterior cells, and posterior cells). Mean aggregate area was unchanged for *daf-2* RNAi (Supplemental Figure 2.2), suggesting that less aggregated protein persists in mid-life mechanosensory neurons when DAF-2 signals are reduced. Conversely, we found modest increases in aggregate number and size for *age-1, akt-1*, and *daf-16* knockdown (Figure 2.5D and Supplemental Figure 2.2). Importantly, Parker et al. (2005) showed no difference in huntingtin expression of the polyQ128 animals in *age-1* and *daf-16* genetic mutants. This suggests that our findings of altered protein aggregation in the polyQ128 strain is likely not due to changed huntingtin expression, but rather is more likely attributed to cellular responses of the expanded polyglutamine protein (Figure 2.5).

Interestingly, we noted a striking difference in the localization of polyQ128 protein aggregates in posterior and anterior cells for *daf-2* RNAi (Figure 2.5E and 2.5F). In *daf-2* RNAi treated animals, 80-90% of the detected aggregates localized in the cell body of anterior and posterior cells whereas other insulin signaling pathway knockdowns were associated with a majority (50-60%) of aggregates localized within the process of these cells, similar to empty vector controls. We also note that aggregates were never observed in outgrowths without also being present in the cell body. This dramatic difference of aggregate localization in *daf-2* RNAi animals suggests that subcellular distribution of protein aggregates is regulated by a DAF-2 non-canonical pathway.

2.4.4 RNAi knockdown of *daf-2* returns polyQ128 mechanosensory neuron morphology to healthy levels

At the whole worm and anterior and posterior cell levels, *daf-2* RNAi knockdown in the neurons of polyQ128 worms lowers the occurrence of total neuronal aberrations to levels observed in polyQ0 empty vector treated animals (Wald test, $p<0.01$). However, *daf-2* RNAi polyQ128 touch response is still significantly lower than polyQ0 empty vector treated animals (Wald test, $p<0.01$).

2.5 Discussion

2.5.1 Summary of findings

To begin to address the relationship between natural and proteotoxically challenged neuronal aging in a physiological context, we took advantage of high resolution *in vivo* analyses of *C. elegans* mechanosensory neuron morphology and function. We compared mid-life morphological and functional features of mechanosensory neurons that aged without, or with, the proteotoxic stressor polyQ128, under RNAi conditions that mimic systemic, including neurons, low or high activation of the insulin signaling pathway. Our data suggest that insulin signaling plays complex roles in neuronal maintenance in both healthy (polyQ0) and degenerate (polyQ128) neurons, with distinct outcomes on individual neurons notable even among the similar group of 6 mechanosensory neurons. Our data on individual neurons highlight remarkable neuronal diversity of responses to cellular signaling. Comparison of how the insulin signaling pathway impacts natural and proteotoxic-associated decline reveals some interesting differences in these two processes.

We conclude that RNAi down-regulation of the *daf-2* insulin receptor plays a role in morphological aging of mechanosensory neurons in both normally aging (polyQ0) and proteotoxically stressed (polyQ128) animals. Anterior and posterior neurons can be differentially affected by altered neuronal insulin signaling (Table 2.3). Importantly, our data suggest that

decreased insulin signaling in normally aging systems (polyQ0) actually enhances some process aberrations in middle aged adults, with a focused impact on formation of ectopic branches on axons and dendrites. That *daf-2* mechanosensory function is improved raises the possibility that the structural aberrations (branching) we observe actually reflect consequences of a defensive response that enhances or protects neuronal health during aging (Figure 2.4). *age-1* may contribute partially to this process in polyQ0 animals, but evidence for the involvement of other pathway components is not compelling in our study. We also find that *daf-2* RNAi knockdown has distinctive impact on the proteotoxically stressed polyQ128 mechanosensory neurons: morphological aberrations are lower; and aggregates are fewer in number and smaller in size, with a striking subcellular restriction of aggregates to the cell body, as compared to empty vector controls. Somewhat surprisingly, other insulin signaling pathway disruptions have relatively modest impact on cell function, aggregate morphology, and aggregate distribution in polyQ128 animals; we found that *age-1* RNAi, which extends overall lifespan, did not confer dramatic changes in mechanosensory neurons, and often correlated with *daf-16* RNAi in inducing modest effects. Our data raise the possibility that, under conditions of extreme proteotoxic stress, neurons utilize a non-canonical *daf-2* pathway to enhance neuroprotection.

2.5.2 Extending understanding of the influence of insulin signaling on healthy aging mechanosensory neurons

2.5.2.1 *daf-2* insulin receptor

Mechanosensory neuron morphology changes with age in wildtype animals (Tank et al., 2011; Toth et al., 2012; Pan et al., 2011). Overall, genetic mutants and systemic RNAi treatments have suggested that *daf-2* mutants maintain youthful, aberration-free phenotypes longer than wildtype animals. Toth et al. (2012) distinguished among specific abnormality classes to measure decreases in cell body outgrowths and wavy process phenotypes, with a

trend toward delaying branching in posterior mechanosensory neurons. Tank et al. (2011) showed that 10 day old *daf-2(e1370)* mutants had decreased process branching. Using a neuron-targeted *daf-2* RNAi approach, we measured an increase in neuronal aberrations at day 5 of adulthood, the vast majority of which are novel branches (Figure 2.4D and 2.4E). Because we find increased aberrations in *daf-2* RNAi coincident with a period of enhanced function (Figure 2.4A), we raise the question of whether mid-life branching might be a manifestation of a normal neuronal defense mechanism that actually improves sensory capacity, although this issue remains to be resolved with single animal functional imaging. This finding is also significant in that it suggests that all changes in morphology seen with age or treatments are not the same mechanistically and that some phenotypes, such as process branching, may be protective to neurons. Differences from other studies (Toth et al., 2012; Tank et al., 2011; Pan et al., 2011) could arise from differences in methods for reducing *daf-2* expression (with RNAi knockdown being distinct from modulation of specific amino acid resides in receptor reduction-of-function mutants) and different timing of scoring during adult life.

2.5.2.2 *age-1* PI3 kinase and other insulin signaling molecules

We found that *age-1* RNAi modestly increased branching of mechanosensory neuron processes at day 5 of adult life, but did not alter touch sensitivity. The latter observation establishes that morphological phenotype and function are not always linked. *akt-1*, *daf-18*, and *daf-16* RNAi interventions did not alter the trajectory of age-related morphological change in otherwise healthy neurons. The role of *age-1, akt-1*, and *daf-18* in morphological aging of the mechanosensory neurons has not been previously reported. Overall, *age-1* knockdown can have an effect on mechanosensory neuron morphological aging (Figure 2.4D and 2.4E) but impact on function is not large at mid-life. Other pathways that run in parallel may be important in mid-adult life (Tank et al., 2011).

2.5.2.3 *daf-16*

For natural aging of mechanosensory neurons, we find that *daf-16* RNAi exerts a small but statistically significant effect on day 5 adult posterior touch response, but not on aberrations. Tank et al. (2011) also came to the conclusion that aberrations for day 10 branching in a *daf-16* deletion mutant were similar to wildtype; whereas Pan et al. (2011) and Toth et al. (2012) noted a small increase in aberrations in *daf-16* mutants at days 9 and 10 (note the latter study, like ours, found no change at adult day 5). Still, time course studies do not support a profound impact of *daf-16* disruption on morphological aging of the mechanosensory neurons. *daf-16* appears to be needed for *daf-2(rf)*-mediated suppression of excess branching, though cell autonomy of this activity is disputed (Pan et al., 2011; Tank et al., 2011).

Overall, although compelling data support that insulin signaling a factor in natural aging of mechanosensory neurons, with reduced signaling correlating with reduced function, other pathways likely influence the process as well (Tank et al., 2011).

2.5.3 Distinctive outcomes of *daf-2* RNAi in the proteotoxically stressed Huntington's disease model strain

2.5.3.1 *daf-2*

In middle-aged polyQ128 animals, we found that daf-2 RNAi improved mechanosensory function, limited the number of morphological aberrations, and decreased overall aggregate number and size, compared to empty vector controls (Figure 2.5). Thus, reduced insulin receptor signaling through DAF-2 confers neuroprotection that is associated with diminished polyQ128 aggregate load in this model. Our data are consistent with studies in other disease models (Cohen et al., 2010) implicating daf-2 in enhanced proteostasis during toxic protein challenge.

2.5.3.2 *age-1* PI3 kinase and other insulin signaling molecules

We found that *age-1* RNAi modestly impairs touch sensitivity at a time point at which the mean number of aberrations and of aggregates are elevated relative to empty vector controls (Figure 2.4). Unexpectedly, *akt-1* and *daf-16* RNAi, which should have opposing impacts on the signal transduction pathway, induce similar outcomes in these proteotoxically challenged mechanosensory neurons. Because *age-1* RNAi (and sometimes *akt-1* (Hertweck et al., 2004)) extend lifespan (Table 2.2), dysfunction is not the anticipated outcome of such interventions. We emphasize two points here: first, our data raise the possibility that the most commonly outlined downstream pathway for DAF-2 signaling may not be the operative signaling pathway for the mechanosensory neuron proteotoxicity pathway; and second, as it has previously been noted that other healthspan phenotypes differentially affected by *daf-2* vs *age*-1 mutations. For example, in *age-1* mutants the biphasic profile for rate of increase in lipofuscin/age pigments during adulthood shows a temporal shift (delay in onset without change in time course), whereas for *daf-2* mutants the rate of lipofuscin accumulation remains low across adulthood (Gerstbrein et al., 2005). In other words, *daf-2* is more effective in preventing long term elevation in age pigment accumulation, while *age-1* delays onset of accumulation. This anomaly is a precedent for differential health outcomes following closely related insulin signaling pathway interventions.

In previous work, Morley et al. (2002) found that *C. elegans* expressing polyQ82 in body wall muscle show slower development of aggregates and motility defects with *age-1* RNAi and *age-1* mutants. While those authors showed the opposite effect of *age-1* RNAi on polyQ accumulation and toxicity compared to our study using a different cell type, they stressed the importance of threshold stresses in their interpretation. We note that our model carries an elevated polyglutamine load (polyQ128) as compared to polyQ82. In humans, longer polyglutamine expansion in huntingtin is well known to result in earlier onset of Huntington's disease and lower life expectancy.

2.5.3.3 *daf-16*

As expected, we observed *daf-16* RNAi confers diminished mechanosensory function together with increased anterior aberration and increased number and size of aggregates. Our results are consistent with previous studies showing that *daf-16* deficiency is associated with exacerbated polyQ128 proteotoxicity in young adult mechanosensory neurons (Parker et al., 2005, 2012; Lejeune et al., 2012) and with enhanced proteotoxicity in a polyQ82 model (Morley et al., 2002) and an Alzheimer's disease model (Cohen et al., 2009).

Overall, changes in anterior and posterior cell function, morphology, and protein aggregation load and localization (Figures 2.4 and 2.5) correlate with whole animal observations (Figure 2.3) in both polyQ0 and polyQ128 strains. However, with polyQ128 *daf-16* RNAi we observed decreased anterior and posterior mechanosensory function (Figure 2.5A) and increased protein aggregate area and number in whole animal and both cell types (Figure 2.5D and Supplemental Figure 2.2), while only anterior mechanosensory neurons (ALML or ALMR) increased significantly in total neuronal aberrations (Figure 2.5B). This maintenance of neuron morphology with worsened function and protein aggregation suggests other mechanisms can mediate these endpoints.

2.5.4 *daf-2* RNAi uniquely changes distribution of polyQ128 aggregate load

A striking observation of *daf-2* RNAi animals is a profound difference in the distribution of polyQ128 aggregates (Figure 2.5E and 2.5F). *daf-2* RNAi is the only intervention we tested that induces localization of CFP-labeled polyQ128 aggregates nearly exclusively to the neuron cell body. Most aggregates we concentrated in only a few dots, which resembled perinuclear lysosomes. Although this subcellular domain restriction remains to be definitively identified, our observations suggest that for both anterior and posterior mechanosensory neurons, *daf-2* may exert neuroprotection by sequestering aggregates to prevent them from interfering with other cellular functions. The lower aggregate size suggests that enhanced degradation may occur

when DAF-2 signaling is low. Our data also suggest that DAF-2 signaling could influence axonal transport of aggregate proteins or their retention in the cell body. Since we did not observe the cell body restricted pattern of *age-1* RNAi, a non-canonical downstream signaling pathway might be responsible for the observed effect.

2.5.5 Neurons aging under extreme aggregate challenge exhibit differences from natural aging

It is striking that the *daf-2* RNAi polyQ128 neuronal aberration level is below that of polyQ128 empty vector controls (Figure 2.5B), and similar to that of polyQ0 empty vector controls (Figure 2.4C), while polyQ0 *daf-2* RNAi increases aberrations. Together with stresses induced by polyQ128, low insulin signaling (*daf-2* and *age-1* RNAi treatment) is associated both with protection from and an increase in morphological restructuring. Without extreme proteotoxic challenge at mid-life (as in polyQ0), however, neuronal aberrations are more apparent when insulin signaling is low. One possibility to explain these differences between *daf-2* RNAi in the naturally aging (polyQ0) and proteotoxically stressed (polyQ128) models is that hormetic consequences induced by polyQ128 are involved in suppression of aberrations. Alternatively, the aberrations in polyQ0 may be a manifestation of cellular maintenance that cannot be executed in the face of extreme polyQ128 challenge. An interesting question is whether additional neuron classes in the polyQ128 animals are affected by the expression of polyQ aggregates in the mechanosensory neurons or whether these effects are cell autonomous.

A second striking difference between natural aging and aging under extreme proteotoxic stress resides in *daf-16* RNAi treatment effects. In polyQ0 animals, *daf-16* RNAi impairs posterior touch sensation, but does not markedly alter neuron morphology (only affecting anterior touch sensitivity). In contrast, in polyQ128 animals, *daf-16* RNAi results in both impaired touch response and increased neuronal aberrations. Also, *daf-16* RNAi in polyQ128, aggregate load increases and lifespan decreases proportionally more than in polyQ0. This suggests that

polyQ128 expression in mechanosensory neurons induces stress signaling to other body tissues to disrupt the overall health of the animal.

A potential mechanism for the differences in effects of manipulating insulin signaling in polyQ0 and polyQ128 is increased basal insulin signaling in polyQ128 as a result of its protein load. However, we propose this is unlikely to be the mechanism underlying the observed differences. We see no difference in lifespan between empty vector control (L4440) treated polyQ0 and polyQ128 lifespan (Figure 2.2A). This is not surprising given that mechanosensory neurons do not seem to modulate lifespan (Chalfie et al., 1985). Further, microarray analysis of polyQ128 FACS-purified P_{mec-3} cells (mechanosensory neurons) showed no apparent dysregulation of genes in the insulin signaling pathway compared to non-toxic huntingtin:polyglutamine-expressing controls (Tourette and Neri, personal communication). Thus, the differences in neuron morphology and function seen in empty vector control treated polyQ0 and polyQ128 animals are likely due to some mechanism other than insulin signaling.

We have seen that with age, the effects on touch response and mechanosensory morphology are negatively correlated in polyQ0 and polyQ128 models (Vayndorf et al., 2016). We showed that this correlation between increased morphological aberrations and decreased function remains in all RNAi treated polyQ128 animals (Figure 2.5). However, when polyQ0 animals receive RNAi treatment targeting components of the insulin signaling pathway, touch response and accumulation of aberrant morphology are no longer negatively correlated (Figure 2.4). Interestingly, while only *daf-2* RNAi showed overall significant effects on mechanosensory morphology and function in polyQ0 animals, RNAi treatment of polyQ128 animals yielded a higher number of significant changes. Also, we observed empty vector control polyQ128 animals decreased touch response and increased changes in neuron morphology when compared to polyQ0 animals. Perhaps the decreased baseline neuronal function and worsened baseline neuron morphology of the polyQ128 animals makes them more susceptible to changes in expression of insulin signaling pathway proteins, whereas naturally aging animals have more

ability to compensate with other signaling pathways when there are changes in insulin signaling protein expression.

Overall, our findings suggest that improving neuronal aging outcomes and neuronal dysfunction associated with elevated protein aggregate stress may not be as simple as decreasing classical insulin signaling. This is not surprising because there are 40 insulin ligands with different expression levels in various cell types all vying for binding sites at the *C. elegans* insulin receptor, DAF-2. Others have shown that this insulin network is complex and works together to respond to varying stresses (Ritter et al., 2013), including protein misfolding and dysfunction as in our polyQ128 model. In addition, in mammalian and cell culture models, huntingtin is a phosphorylation substrate for AKT/PKB (Humbert et al., 2002; Dong et al., 2012). AKT can be modified and even cleaved into an inactive form in a rat model of Huntington's disease (Colin et al., 2005). Thus, in systems with endogenous huntingtin, unlike *C. elegans*, complex interactions between insulin signaling, expanded polyglutamine huntingtin aggregation, and neuron morphology and function may be operative. Further genetic studies of the huntingtin polyQ128 model in *C. elegans* have the potential to elucidate mechanisms that influence morphological changes during neuronal aging.

2.6 Acknowledgements

The authors would like to thank Dr. Marton Toth for the *zdIs5* strain, Leena Shah for helping with the strain crosses, Dr. Kriya Dunlap and Theresia Schnurr for training on and use of the microplate reader, and Jason Neuswanger for statistical consulting and the ImageJ macro used for aggregate analysis. Work was supported by NIH NINDS 2U54NS041069-06AI (EMV), NIH 8P20GM103395-12 (BET), ANR -08-MNPS-024-01 (CN), and NIH 1R01AG046358, R21 NS076868-01 (MD).

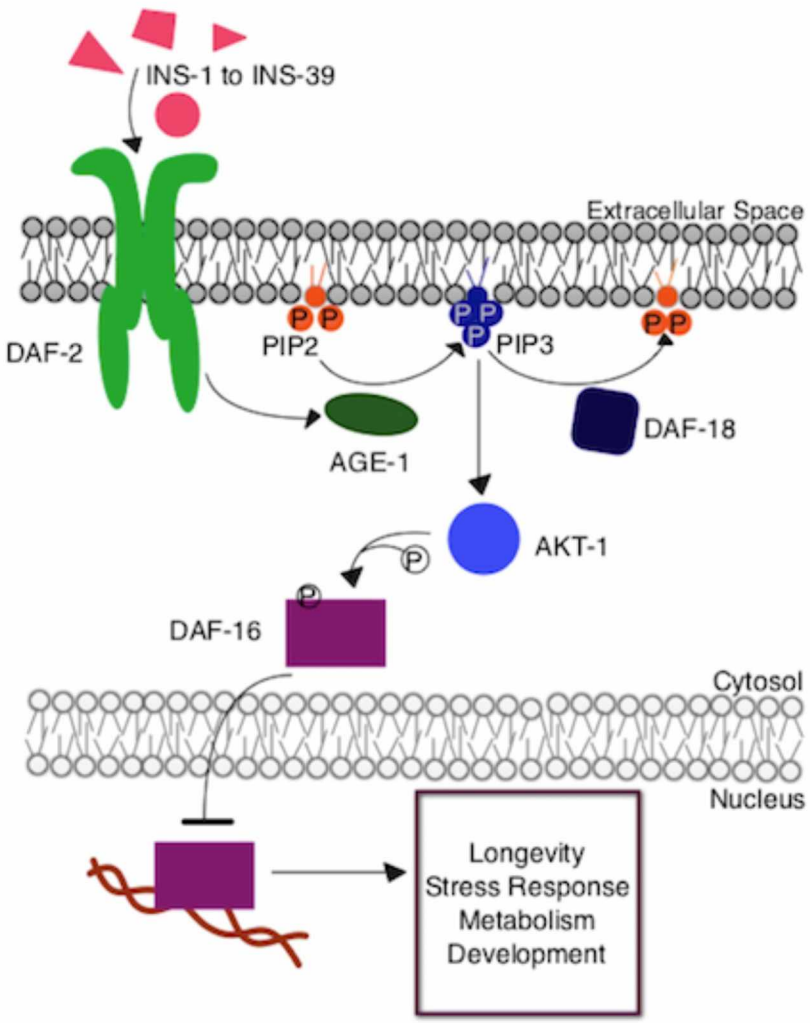

Figure 2.1 The insulin signaling pathway in *Caenorhabditis elegans*.

Upon insulin ligand binding to the DAF-2 insulin receptor in *C. elegans*, AGE-1 (homolog to mammalian PI3-K) is activated and converts PIP_2 to PIP_3 at the cellular membrane. PIP_3 activates the central kinase AKT-1 (ortholog to mammalian PKB), which phosphorylates DAF-16, the *C. elegans* FOXO transcription factor, preventing its entry into the nucleus where it would otherwise regulate the expression of genes contributing to longevity, stress response, and metabolism. The DAF-18 (homolog to mammalian PTEN) phosphatase negatively regulates the system by decreasing the amount of PIP_3 present at the membrane by reconverting it to PIP_2.

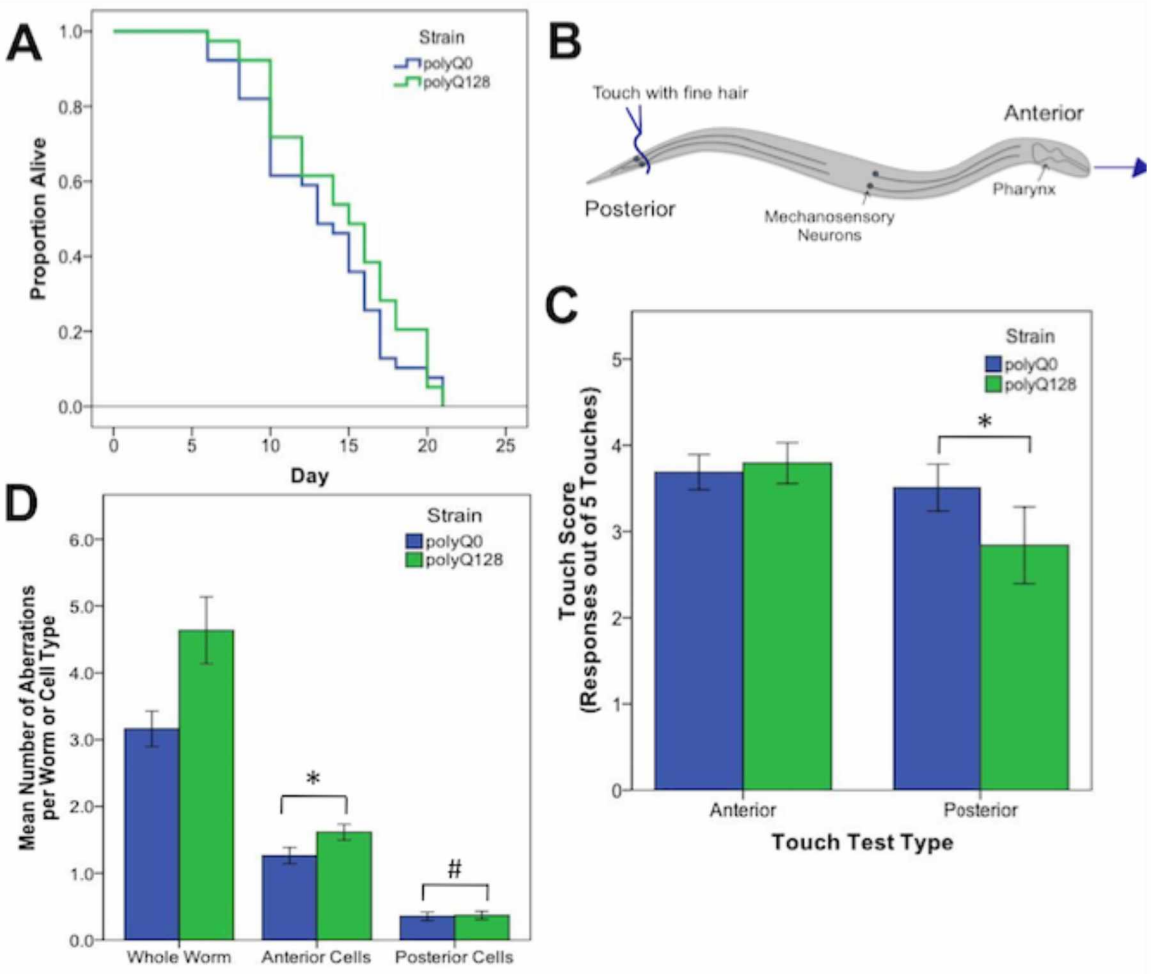

Figure 2.2 PolyQ0 and polyQ128 exhibit basal differences in mechanosensory neuron morphology and function without altered lifespan.

(A) Kaplan-Meier survival curves for one representative survival experiment shown for empty vector (L4440) treated polyQ0 and polyQ128 animals. Mean and median lifespan do not differ between the two strains. (B) Schematic of posterior touch test; an animal is touched at the tail and normally moves forward, gaining 1 positive response to touch (out of 5). For anterior touch test, animals are touched at the head and scored for backwards movement. Mechanosensory neurons (PLMs and ALMs) and pharynx shown. (C) Anterior and posterior touch test scores for empty vector control individuals. Each bar represents the mean number of positive responses out of 5 to soft touch. (D) Total number of aberrations (e.g. number of outgrowths and branches and presence of abnormal cell body and punctae) per worm and cell type for each empty vector control group. Whole worm bars represent the mean values of the sum of all 4 neurons scored (ALML, ALMR, PLML, and PLMR) for each individual. Anterior and posterior bars represent the mean values for individual anterior (ALML or ALMR) or posterior (PLML or PLMR) neurons. * denotes significance of $p<0.01$ and # denotes significance of $p<0.10$ following Mann-Whitney U comparison. Each bar shows mean ± SE for N=69 (polyQ0) and N=84 (polyQ128) animals.

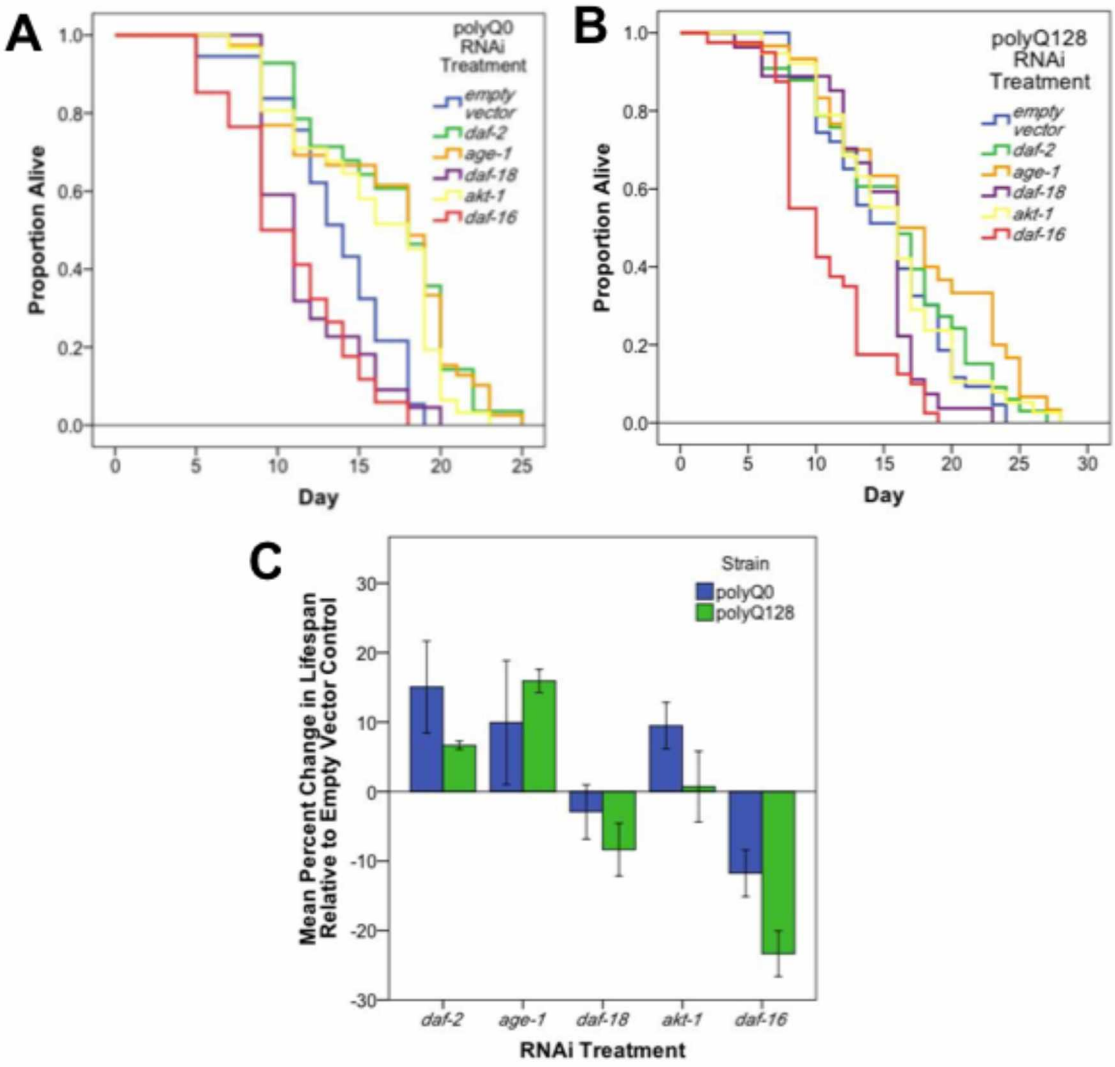

Figure 2.3 Neuronal and systemic insulin signaling mediates lifespan of both healthy (polyQ0) and proteotoxically stressed (polyQ128) animals.

Kaplan-Meier survival curves for one representative survival experiment shown for polyQ0 (A) and polyQ128 (B) animals with RNAi knockdown of the indicated insulin signaling pathway gene. Mean lifespan, sample size, and significance reported as Replicate 1 for each strain in Table 2.2. (C) Mean percent change in lifespan with RNAi treatment for polyQ0 and polyQ128 animals pooled across biological replicates. Only *daf-16* RNAi showed a significant impact on lifespan for polyQ128 animals when compared to polyQ128 empty vector controls (23.3±4.1% for 3 replicates of 45-50 animals). Each bar represents mean ± SE.

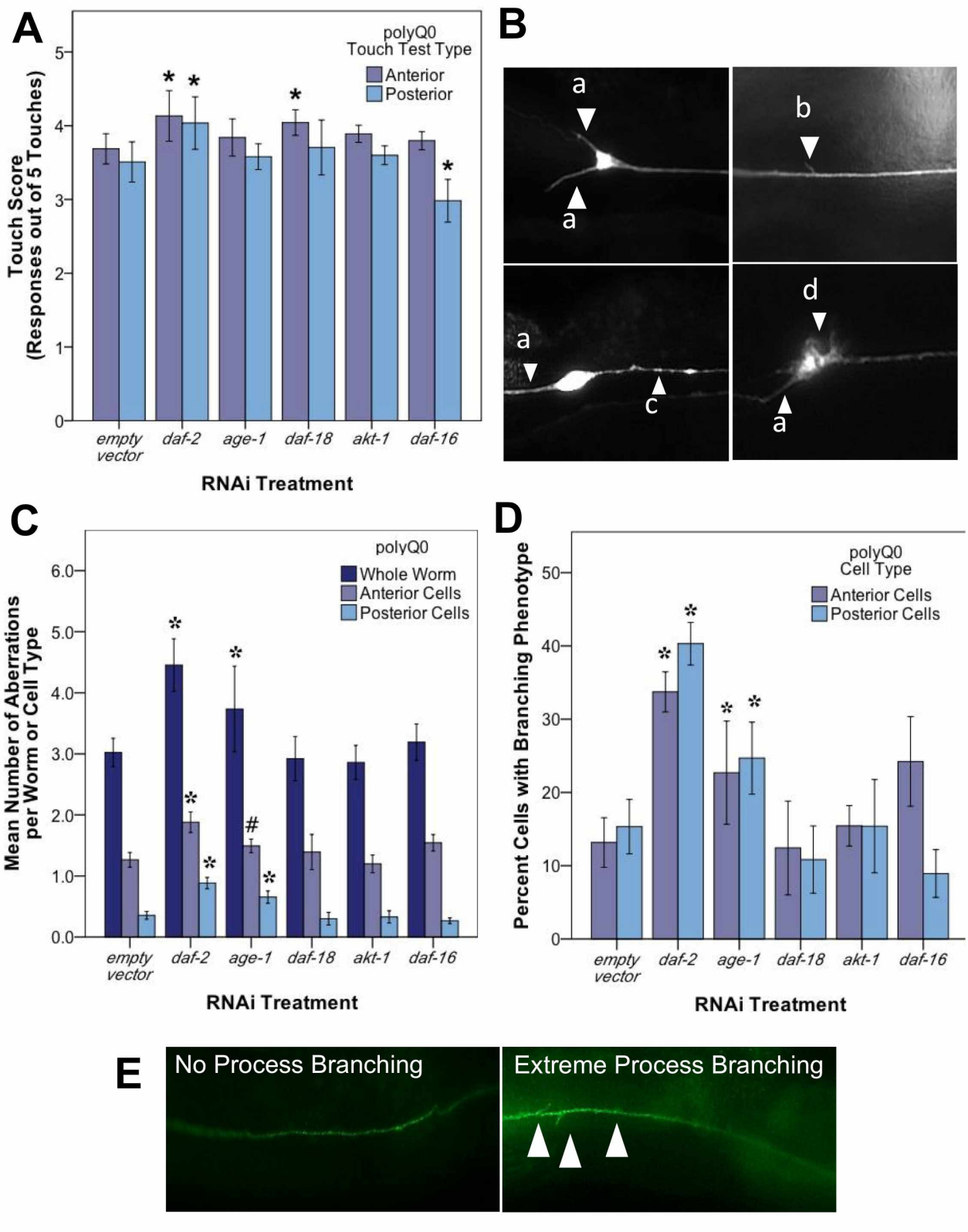
A
polyQ0
Touch Test Type
Anterior
Posterior
Touch Score
(Responses out of 5 Touches)
0
1
2
3
4
5
empty vector
daf-2
age-1
daf-18
akt-1
daf-16
RNAi Treatment
B
a
a
b
a
c
d
a
C
polyQ0
Whole Worm
Anterior Cells
Posterior Cells
Mean Number of Aberrations per Worm or Cell Type
0.0
1.0
2.0
3.0
4.0
5.0
6.0
empty vector
daf-2
age-1
daf-18
akt-1
daf-16
RNAi Treatment
D
polyQ0
Cell Type
Anterior Cells
Posterior Cells
Percent Cells with Branching Phenotype
0
10
20
30
40
50
empty vector
daf-2
age-1
daf-18
akt-1
daf-16
RNAi Treatment
E
No Process Branching
Extreme Process Branching

Figure 2.4 *daf-2* RNAi mediates mechanosensory neuron morphology and function in polyQ0 animals.

(A) Anterior and posterior touch test scores of polyQ0 animals following RNAi treatment. Each bar represents the mean number of positive responses to 5 soft touches. (B) Representative examples of outgrowths (a), branching (b), punctae (c), and abnormal cell body (d) phenotypes seen in aging mechanosensory neurons of polyQ0 and polyQ128 individuals. (C) Mean number of neuronal aberrations per whole animal (sum of all 4 neurons scored in an individual) and individual cell type (anterior [ALML or ALMR] and posterior [PLML or PLMR]). (D) Percentage of neurons with branching phenotype for each RNAi treatment. Neurons with this phenotype may have more than one branch (data not shown). (E) Representative images of mechanosensory neuron processes and process branching (white arrows) in polyQ0 animals. * denotes significance of $p<0.01$ and # denotes significance of $p<0.10$ relative to appropriate empty vector control following a generalized linear model with a log link function (Poisson regression) and Wald tests for significance of treatment effects. Each bar represents mean ± SE for N=49-70 animals.

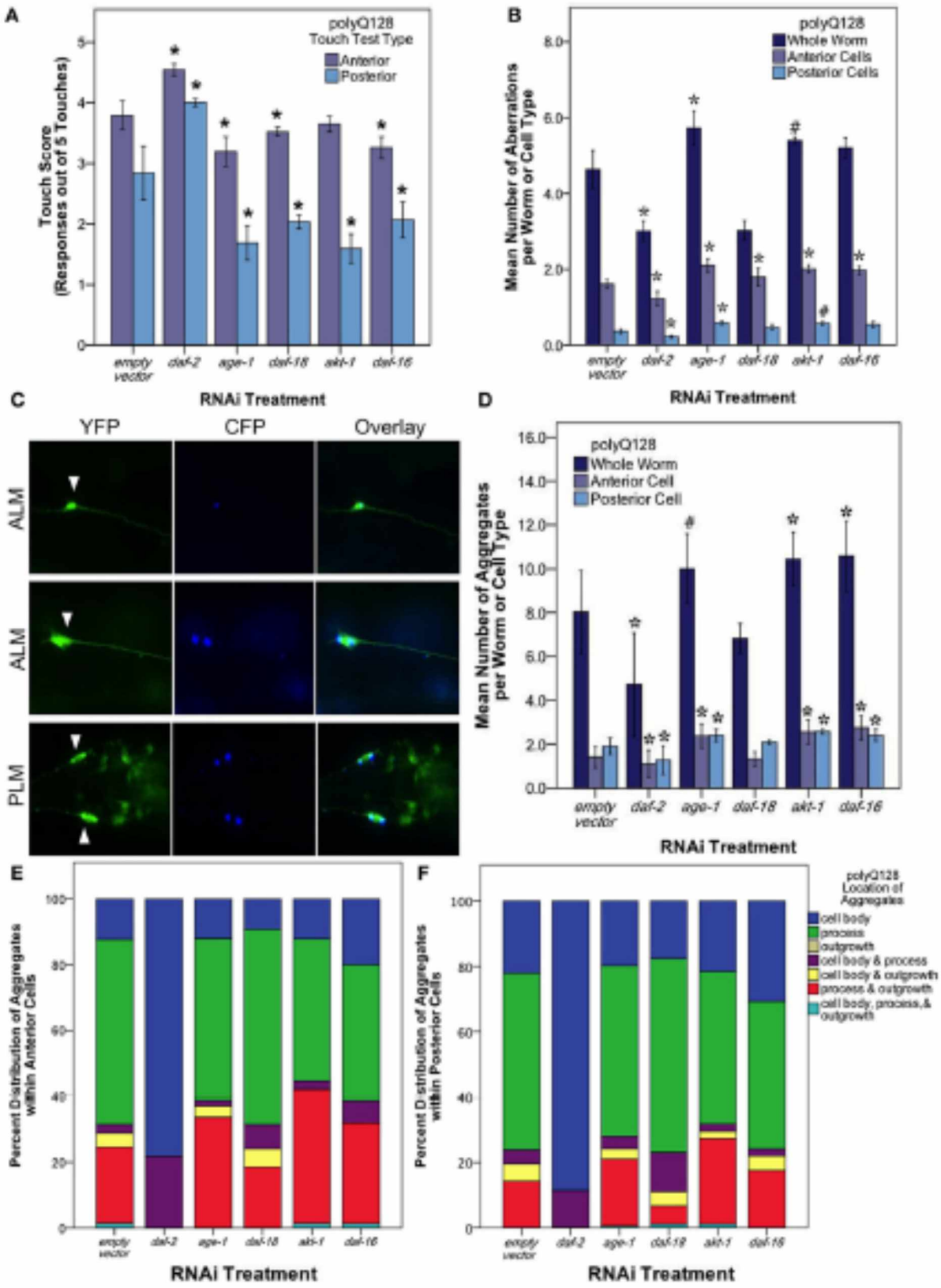
A
polyQ128
Touch Test Type
Anterior
Posterior
Touch Score
(Responses out of 5 Touches)
empty vector
daf-2
age-1
daf-18
akt-1
daf-16
RNAi Treatment
B
polyQ128
Whole Worm
Anterior Cells
Posterior Cells
Mean Number of Aberrations per Worm or Cell Type
RNAi Treatment
C
YFP
CFP
Overlay
ALM
ALM
PLM
D
polyQ128
Whole Worm
Anterior Cell
Posterior Cell
Mean Number of Aggregates per Worm or Cell Type
RNAi Treatment
E
Percent Distribution of Aggregates within Anterior Cells
RNAi Treatment
F
Percent Distribution of Aggregates within Posterior Cells
RNAi Treatment
polyQ128
Location of Aggregates
cell body
process
outgrowth
cell body & process
cell body & outgrowth
process & outgrowth
cell body, process, & outgrowth

Figure 2.5 The insulin signaling pathway mediates mechanosensory neuron morphology and function in polyQ128 animals.

(A) Anterior and posterior touch test scores, representing the number of positive responses to 5 soft touches, following RNAi treatment for indicated insulin signaling pathway gene of polyQ128 animals. (B) Mean number of neuronal aberrations per whole animal (sum of all 4 neurons scored in an individual) and individual cell type (anterior [ALML or ALMR] and posterior [PLML or PLMR]). (C) Representative image of polyQ128 aggregate (CFP, blue panels) accumulation within anterior (ALM) and posterior neurons (PLM) (YFP, green panels). White arrows in YFP panels indicate the location of the cell body of each neuron. (D) The effect of RNAi treatment on the number of distinct CFP-labeled extended polyglutatmine huntingtin protein aggregates in whole animal and anterior and posterior neurons of polyQ128 animals. (E) Sub-cellular localization of poyQ128 aggregates within anterior neurons of polyQ128 animals that contained aggregates. (F) Location of polyQ128 aggregates in posterior neurons of polyQ128 animals. * denotes significance of $p<0.01$ and # denotes significance of $p<0.10$ relative to appropriate empty vector control following generalized linear model analysis with a log link function (Poisson regression) and Wald tests for significance of treatment effects. Each bar represents mean ± SE.

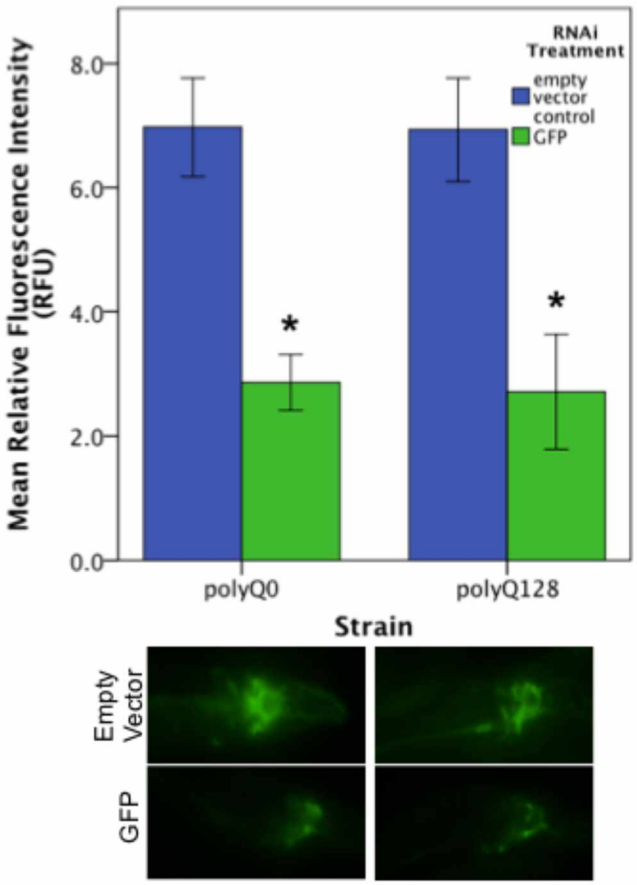

Supplemental Figure 2.1 polyQ0 and polyQ128 neurons are sensitive to RNAi treatments.

Representative data and images of both polyQ0 and polyQ128 embryos treated with GFP RNAi treatment compared to empty vector controls. * denotes $p<0.001$ when compared to empty vector control following unpaired t-test. This experiment was repeated with similar results for each replicate of each RNAi experiment. Each bar represents mean relative fluorescence in arbitrary units (RFU) ± SE.

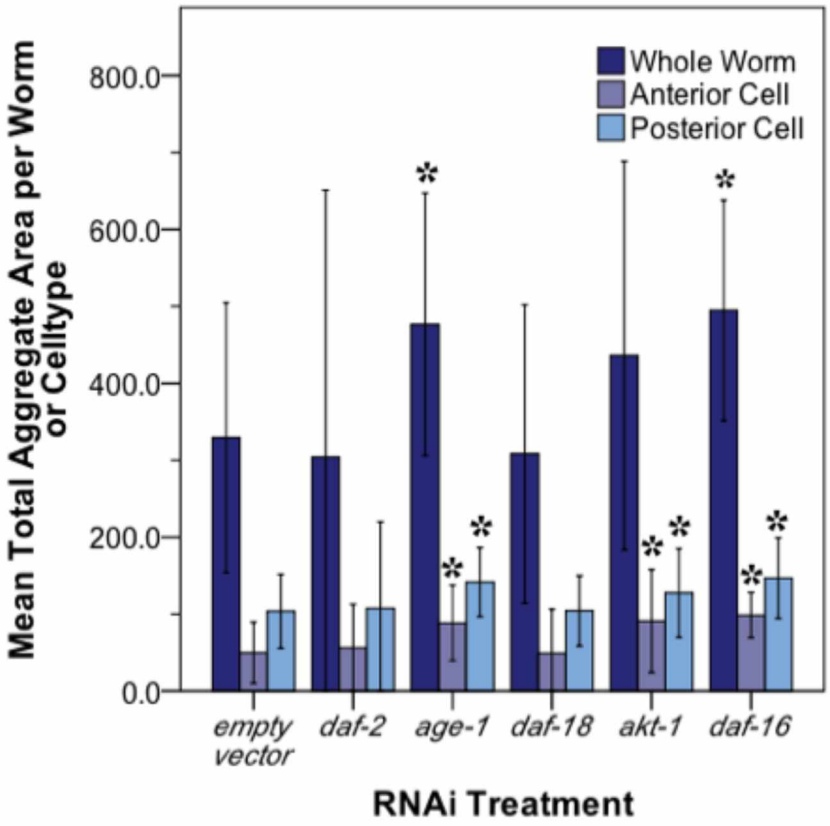

Supplemental Figure 2.2 Insulin signaling mediates poly128 aggregate area.

Mean aggregate area per cell type and whole animal for each RNAi treatment. Aggregate area calculated using ImageJ. * denotes significance of <0.01 and # denotes significance of <0.10 relative to appropriate empty vector control following ANOVA and Tukey post-hoc analysis. Each bar represents mean ± SE.

Table 2.1 Effect of RNAi treatment on polyQ0 and polyQ128 motility.

Number of individuals falling into A, B, or C class motility for each treatment group is shown. A class indicates normal, voluntary sinusoidal movement, B class indicates locomotion following gentle prodding, and C class indicates inability to locomote. Overall, polyQ128 animals have higher incidence of B class motility than polyQ0. Only polyQ128 *daf-18(RNAi)* results in a significant difference in motility compared to control.

Strain	RNAi Treatment	Number per Motility Class			Total *N*
		A	B	C	
polyQ0	Empty Vector	65	4	0	69
	daf-2	53	0	0	53
	age-1	67	4	0	71
	daf-18	47	2	0	49
	akt-1	50	1	0	51
	daf-16	48	3	0	51
polyQ128	Empty Vector	69	15	0	84
	daf-2	87	6	0	93
	age-1	77	18	0	95
	daf-18	47	0	0	47
	akt-1	31	15	1	47
	daf-16	51	20	1	72

Table 2.2 Effects of RNAi treatment targeting insulin signaling on polyQ0 and polyQ128 animals' mean lifespan.

Mean lifespan in days ± SE of each RNAi treatment replicate for the polyQ0 and polyQ128 strains are shown. Each replicate of 6 treatments (empty vector control, DAF-2, AGE-1, DAF-18, AKT-1, and DAF-16) was run one strain at a time. Entries with * are significantly different ($p<0.05$) from the strain- and replicate-matched empty vector control following Kaplan Meier log-rank survival statistics. Replicate with missing data (N/A) was censored from experiment.

Strain	RNAi Treatment	Replicate 1 *N*	Replicate 1 Mean Lifespan days ± SE	Replicate 2 *N*	Replicate 2 Mean Lifespan days ± SE	Replicate 3 *N*	Replicate 3 Mean Lifespan days ± SE
polyQ0	Empty Vector	50	13.7 ± 0.56	60	14.3 ± 0.58	55	13.5 ± 0.66
	daf-2	40	16.8 ± 0.83*	*N/A*	*N/A*	48	16.3 ± 1.04*
	age-1	51	16.3 ± 0.82*	59	16.9 ± 0.61*	*N/A*	*N/A*
	daf-18	30	11.7 ± 0.70	60	14.8 ± 0.57	50	13.5 ± 0.62
	akt-1	40	15.8 ± 0.79*	60	16.2 ± 0.52*	48	13.4 ± 0.50
	daf-16	46	11.0 ± 0.61*	60	12.1 ± 0.53*	51	12.9 ± 0.68
polyQ128	Empty Vector	50	15.2 ± 0.71	50	15.1 ± 0.61	56	13.4 ± 0.55
	daf-2	51	16.1 ± 0.94	50	16.2 ± 0.89*	*N/A*	*N/A*
	age-1	40	17.9 ± 1.01*	*N/A*	*N/A*	59	15.0 ± 0.89*
	daf-18	38	15.6 ± 0.79	50	14.5 ± 0.66	59	11.4 ± 0.42*
	akt-1	47	15.8 ± 0.79	25	14.4 ± 1.15	56	11.4 ± 0.44*
	daf-16	48	10.9 ± 0.60*	50	12.8 ± 0.63*	61	10.4 ± 0.39*

Table 2.3 RNAi treatments targeting the insulin signaling pathway differentially effect polyQ128 specific mechanosensory neuron aberrations.

Table depicts mean number and significant difference for anterior (ALML or ALMR) and posterior (PLML or PLMR) mechanosensory neurons following RNAi treatment for each specific neuronal aberration observed (i.e. cell body outgrowths, process branching, presence of process punctae, and cell body abnormality). *p* values indicate significance compared to appropriate empty vector control following generalized linear model analysis. Sample sizes for anterior ($N_{anterior}$) and posterior ($N_{posterior}$) neurons of each RNAi treatment are shown. Example outgrowths (A), branching (B), punctae (C), and abnormal cell body (D) are shown in Figure 2.4B.

Specific Types of Aberrations per	**Cell Type**	**RNAi Treatment on polyQ128 animals**									
		Empty Vector ($N_{anterior}$ = 226; $N_{posterior}$ = 217)	***daf-2*** ($N_{anterior}$ = 199; $N_{posterior}$ = 202)		***age-1*** ($N_{anterior}$ = 185; $N_{posterior}$ = 185)		***daf-18*** ($N_{anterior}$ = 92; $N_{posterior}$ = 94)		***akt-1*** ($N_{anterior}$ = 93; $N_{posterior}$ = 92)		***daf-16*** ($N_{anterior}$ = 143; $N_{posterior}$ = 140)	
		Mean±SE	Mean±SE	*p* value	Mean±SE	*p* value	Mean±SE	*p* value	Mean ±SE	*p* value	Mean±SE	*p* value
Number of Cell Body Outgrowths	anterior	1.11±0.05	0.86±0.04	*0.00	1.32±0.06	*0.01	1.21±0.08	*n.s.*	1.24±0.08	*n.s.*	1.29±0.06	*0.03
	posterior	0.01±0.01	0.01±0.03	*n.s.*	0.03±0.03	*n.s.*	0.01±0.01	*n.s.*	0.00±0.00	*n.s.*	0.01±0.01	*n.s.*
Number of Branches	anterior	0.15±0.03	0.09±0.02	*0.05	0.16±0.03	*n.s.*	0.23±0.05	*n.s.*	0.10±0.03	*n.s.*	0.13±0.03	*n.s.*
	posterior	0.07±0.02	0.05±0.02	*n.s.*	0.08±0.02	*n.s.*	0.05±0.02	*n.s.*	0.03±0.02	*n.s.*	0.05±0.02	*n.s.*
Presence of Punctae	anterior	0.14±0.02	0.04±0.02	*0.00	0.37±0.02	*0.00	0.27±0.03	*0.02	0.39±0.03	*0.00	0.33± 0.02	*0.00
	posterior	0.71±0.03	0.90±0.03	*0.00	0.59±0.04	*0.02	0.65±0.05	*n.s.*	0.55±0.05	*0.01	0.58±0.04	*0.01
Presence of Abnormal Cell Body	anterior	0.13±0.01	0.03±0.01	*0.00	0.19±0.01	*n.s.*	0.10±0.02	*n.s.*	0.15±0.02	*n.s.*	0.11±0.01	*n.s.*
	posterior	0.00±0.01	0.02±0.01	*0.02	0.03±0.01	*0.01	0.02±0.02	*n.s.*	0.00 ±0.02	*n.s.*	0.03±0.01	*0.02

2.7 References cited

Alcedo, J., Flatt, T., and Pasyukova, E.G. (2013). Neuronal inputs and outputs of aging and longevity. *Front Genet* 4(71), 1-14.

Brenner, S. (1974). The Genetics of *Caenorhabditis elegans*. *Genetics* 77(1), 71–94.

Broughton, S., and Partridge, L. (2009). Insulin/IGF-like signalling, the central nervous system and aging. *Biochem J* 418, 1–12.

Calixto, A., Chelur, D., Topalidou, I., Chen, X., and Chalfie, M. (2010). Enhanced neuronal RNAi in C. elegans using SID-1. *Nat Methods* 7, 554–559.

Chalfie, M., Sulston, J.E., White, J.G., Southgate, E., Thomson, J.N., and Brenner, S. (1985). The neural circuit for touch sensitivity in Caenorhabditis elegans. *J Neurosci* 5, 956–964.

Cohen, E., Du, D., Joyce, D., Kapernick, E.A., Volovik, Y., Kelly, J.W., and Dillin, A. (2010). Temporal requirements of insulin/IGF-1 signaling for proteotoxicity protection. *Aging Cell* 9, 126–134.

Cohen, E., Paulsson, J.F., Blinder, P., Burstyn-Cohen, T., Du, D., Estepa, G., Adame, A., Pham, H. M., Holzenberger, M., Kelly, J. W., et al. (2009). Reduced IGF-1 signaling delays age-associated proteotoxicity in mice. *Cell* 139, 1157–1169.

Colin, E., Régulier, E., Perrin, V., Dürr, A., Brice, A., Aebischer, P., Déglon, N., Humbert, S., and Saudou, F. (2005). Akt is altered in an animal model of Huntington's disease and in patients. *Eur J Neurosci* 21, 1478–1488.

Dillin, A., and Cohen, E. (2011). Ageing and protein aggregation-mediated disorders: from invertebrates to mammals. *Philos Trans R Soc Lond B Biol Sci* 366, 94–98.

Dong, G., Callegari, E., Gloeckner, C.J., Ueffing, M., and Wang, H. (2012). Mass spectrometric identification of novel posttranslational modification sites in Huntingtin. *Proteomics* 12, 2060–2064.

Faber, P.W., Alter, J.R., MacDonald, M.E., and Hart, A.C. (1999). Polyglutamine-mediated dysfunction and apoptotic death of a *Caenorhabditis elegans* sensory neuron. *PNAS* 96, 179–184.

Freude, S., Hettich, M.M., Schumann, C., Stöhr, O., Koch, L., Köhler, C., Udelhoven, M., Leeser, U., Müller, M., Kubota, N., Kadowaki, T., Krone, W., Schroder, H., Bruning, J.C., and Schubert, M. (2009). Neuronal IGF-1 resistance reduces Abeta accumulation and protects against premature death in a model of Alzheimer's disease. *FASEB J* 23, 3315-3324.

Friedman, D.B., and Johnson, T.E. (1988). Three mutants that extend both mean and maximum life span of the nematode, *Caenorhabditis elegans*, ddefine the Age-1 gene. *J Gerontol* 43 , B102–B109.

Gerstbrein, B., Stamatas, G., Kollias, N., and Driscoll, M. (2005). *In vivo* spectrofluorimetry reveals endogenous biomarkers that report healthspan and dietary restriction in *Caenorhabditis elegans*. *Aging Cell* 4, 127–137.

Hertweck, M., Göbel, C., and Baumeister, R. (2004). *C. elegans* SGK-1 is the critical component in the Akt/PKB kinase complex to control stress response and life span. *Dev Cell* 6, 577–588.

Hsu, A.L., Murphy, C.T., and Kenyon, C. (2003). Regulation of aging and age-related disease by DAF-16 and heat-shock factor. *Science* 300, 1142–1145.

Humbert, S., Bryson, E.A., Cordelie, F.P., Connors, N.C., Datta, S.R., Finkbeiner, S., and Greenberg, M.E. (2002). The IGF-1/Akt pathway is neuroprotective in Huntington's disease and involves huntingtin phosphorylation by Akt. *Dev Cell* 2, 831–837.

Kenyon, C.J. (1993). A *C. elegans* mutant that lives twice as long as wild type. *Nature* 366, 461–464.

Killick, R., Scales, G., Leroy, K., Causevic, M., Hooper, C., Irvine, E.E., Choudhury, A.I., Drinkwater, L., Kerr, F., Al-Qassab, H., Stephenson, J., Yilmaz, Z., Glese, K.P., Brion, J.P., Withers, D.J., and Lovestone, S. (2009). Deletion of Irs2 reduces amyloid deposition and rescues behavioural deficits in APP transgenic mice. *Biochem Biophys Res Commun* 386, 257–262.

Lejeune, F., Mesrob, L., Parmentier, F., Bicep, C., Vazquez, R., Parker, A., Vert, J.P., Tourette, C., and Neri, C. (2012). Large-scale functional RNAi screen in *C. elegans* identifies genes that regulate the dysfunction of mutant polyglutamine neurons. *BMC Genomics* 13(91), 1-14.

Libina, N., Berman, J.R., and Kenyon, C. (2003). Tissue-specific activities of *C. elegans* DAF-16 in the regulation of lifespan. *Cell* 115, 489–502.

Morley, J.F., Brignull, H.R., Weyers, J.J., and Morimoto, R.I. (2002). The threshold for polyglutamine-expansion protein aggregation and cellular toxicity is dynamic and influenced by aging in *Caenorhabditis elegans*. *PNAS* 99, 10417–10422.

Mukhopadhyay, A., Oh, S.W., and Tissenbaum, H. (2006). Worming pathways to and from DAF-16/FOXO. *Exp Gerontol* 41, 928–934.

Neri, C. (2012). Role and therapeutic potential of the pro-longevity factor FOXO and its regulators in neurodegenerative disease. *Front Pharmacol* 3(15), 1-15.

Newman, A.B., and Murabito, J.M. (2013). The epidemiology of longevity and exceptional survival. *Epidemiol Rev* 35, 181-197.

Oh, S.W., Mukhopadhyay, A., Dixit, B.L., Raha, T., Green, M.R., and Tissenbaum, H.A. (2006). Identification of direct DAF-16 targets controlling longevity, metabolism and diapause by chromatin immunoprecipitation. *Nat Genet* 38, 251–257.

Pan, C.L., Peng, C.Y., Chen, C.H., and McIntire, S. (2011). Genetic analysis of age-dependent defects of the *Caenorhabditis elegans* touch receptor neurons. *PNAS* 108, 9274–9279.

Parker, J.A, Connolly, J.B., Wellington, C., Hayden, M., Dausset, J., and Neri, C. (2001). Expanded polyglutamines in *Caenorhabditis elegans* cause axonal abnormalities and severe dysfunction of PLM mechanosensory neurons without cell death. *PNAS* 98, 13318–13323.

Parker, J.A., Arango, M., Abderrahmane, S., Lambert, E., Tourette, C., Catoire, H., and Neri, C. (2005). Resveratrol rescues mutant polyglutamine cytotoxicity in nematode and mammalian neurons. *Nat Genet* 37, 349–350.

Parker, J.A., Vazquez-Manrique, R.P., Tourette, C., Farina, F., Offner, N., Mukhopadhyay, A., Orfila, A.-M., Darbois, A., Menet, S., Tissenbaum, H.A, and Neri, C. (2012). Integration of β-catenin, sirtuin, and FOXO signaling protects from mutant huntingtin toxicity. *J Neurosci* 32, 12630–12640.

Ritter, A.D., Shen, Y., Fuxman Bass, J., Jeyaraj, S., Deplancke, B., Mukhopadhyay, A., Xu, J., Driscoll, M., Tissenbaum, H.A, and Walhout, A.J.M. (2013). Complex expression dynamics and robustness in *C. elegans* insulin networks. *Genome Res* 23, 954–965.

Taguchi, A., Wartschow, L.M., and White, M.F. (2007). Brain IRS2 signaling coordinates life span and nutrient homeostasis. *Science* 317, 369–372.

Taguchi, A., and White, M.F. (2008). Insulin-like signaling, nutrient homeostasis, and life span. *Annu Rev Physiol* 70, 191–212.

Tank, E.M.H., Rodgers, K.E., and Kenyon, C. (2011). Spontaneous age-related neurite branching in *Caenorhabditis elegans*. *J Neurosci* 31, 9279–9288.

Toth, M., Melentijevic, I., Shah, L., Bhatia, A., Lu, K., Talwar, A., Naji, H., Ibanez-Ventoso, C., Ghose, P., Jevince, A., Xue, J., Herndon, L.A., Bhanot, G. Rongo, C., Hall, D.H., and Driscoll, M. (2012). Neurite sprouting and synapse deterioration in the aging *Caenorhabditis elegans* nervous system. *J Neurosci* 32, 8778–8790.

Vayndorf, E.M., Scerbak, C., Hunter, S., Neuswanger, J.R., Toth, M., Parker, A.J., Neri, C., Driscoll, M., and Taylor, B.E. (2016). Morphological remodeling of *C. elegans* neurons during aging is modified by compromised protein homeostasis. *NPJ Aging Mech Dis* 2, 16001.

Chapter 3

Differential Mechanosensory Neuron Aging Trajectories and Lifespan Extension Following Medicinal Alaskan Berry and Fungal Treatments in *Caenorhabditis elegans*[2]

3.1 Abstract

Many nutritional interventions that increase lifespan are also proposed to postpone age-related declines in motor and cognitive function. Potential sources of anti-aging compounds are the plants and fungi that have adapted to extreme environments. We studied the effects of four commonly consumed and culturally relevant Interior Alaska berry and fungus species (bog blueberry, lowbush cranberry, crowberry, and chaga) on the decline in overall health and neuron function and changes in touch receptor neuron morphology associated with aging. We observed increased wildtype *Caenorhabditis elegans* lifespan and improved markers of healthspan upon treatment with Alaskan blueberry, lowbush cranberry, and chaga extracts. Interestingly, although all three treatments increased lifespan, they differentially affected the development of aberrant morphologies in touch receptor neurons. Blueberry treatments decreased anterior mechanosensory neuron (ALM) aberrations (i.e. extended outgrowths and abnormal cell bodies) while lowbush cranberry treatment increased posterior mechanosensory neuron (PLM) aberrations, namely process branching. Chaga treatment both decreased ALM aberrations (i.e. extended outgrowths) and increased PLM aberrations (i.e. process branching and loops). These results support the large body of knowledge positing that there are multiple cellular strategies and mechanisms for promoting health with age. Importantly, these results also demonstrate that although an accumulation of abnormal neuron morphologies is associated with aging and

[2] Authorship for this chapter is as follows: Courtney Scerbak, Elena Vayndorf, Alicia Hernandez, Colin McGill, and Barbara Taylor. In preparation for submission.

decreased health, not all of these morphologies are detrimental to neuronal and organismal health.

3.2 Introduction

Aging is a ubiquitous process affecting the health of increasing numbers of aged individuals throughout the world. Gradual declines in many physiological functions accompany increased chronological age and are associated with increased mortality. Thus, development of strategies to improve tissue, system, and organismal function during aging is an increasing public health priority. Alaskan traditional ecological knowledge holds that a diverse array of local berries, plants, and fungi benefit health and wellness. While plant matter consists of a low proportion of total energy intake in traditional Alaska Native diets (<3% compared to 90% from fish and game meat and fat; (Bersamin et al., 2007), plants and fungi historically were and currently are highly valued by Alaska Native traditional healers (Loring and Gerlach, 2009). Various berries, plant greens, and fungi are consumed as part of a standard subsistence diet and used by traditional healers and contemporary herbalists to combat health problems ranging from stomach and muscle pain to bleeding and snow blindness. An increasing number of studies show that transitioning away from Alaska Native traditional diets and lifestyles is associated with increased incidence of age-associated disorders, including cardiovascular disease (Loring and Gerlach, 2009; Ebbesson et al., 2005). Importantly, cultures throughout the world value plants and fungi related to Alaskan species in traditional foods and medicines (Kim and Song, 2014; Iriti et al., 2010).

Modifying diet, specifically consuming fruits, vegetables, nuts, and specific spices (e.g. tumeric, which contains curcumin), is proposed to be a practical method to lower age-related cognitive decline (Joseph et al., 2009). Alaskan plant and fungus species have adapted to extreme environments, in part by producing a wide variety of secondary metabolites, bioactive molecules not required for plant growth and development (Elks et al., 2013; Wink, 2003).

Various plant and fungal extracts composed of secondary metabolites interact with specific molecular targets to improve health and to slow the progression of aging and age-related disease damage (Youl et al., 2010; Wiegant et al., 2008; Liu et al., 2005). For example, a large body of research describes the anti-inflammatory and antioxidant activity of polyphenolic compounds, such as anthocyanins (Zafra-Stone et al., 2007). Berries in particular have been heavily studied for their impact on brain signaling and neurodegeneration (Miller and Shukitt-Hale, 2012; Shukitt-Hale, 2012; Spencer, 2008).

Alaskan berry species consistently contain higher levels and activity of antioxidant and anti-inflammatory compounds (e.g. phenolic, flavonoid, and anthocyanin compounds) than other commercially grown, temperate species (Grace et al., 2014; Dinstel et al., 2013; Kalt et al., 2001). The selected berries in this study, bog blueberry (*Vaccinium uliginosum*, also known as bog bilberry), lowbush cranberry (*Vaccinium vitis-idaea*, also known as lingonberry), and crowberry (*Empetrum nigrum*, also known as blackberry or mossberry), are found throughout Alaska and the circumpolar north in bogs, woodlands, and spruce stands. Non-Alaskan species of lowbush blueberries (*Vaccinium angustifolium)* prevent and reverse object-recognition memory loss in aging rats (Joseph et al., 1999) and improve memory in both children (Whyte et al., 2015) and older humans (Krikorian et al., 2010). Blueberry polyphenols (*V. angustifolium)* also extend wildtype *Caenorhabditis elegans* lifespan (Wilson et al., 2006). The American cranberry (*Vaccinium macrocarpon)* extends *C. elegans* lifespan in a dose-dependent manner (Guha et al., 2012). Crowberry contains higher total anthocyanins than other well-studied berries, such as blueberries, raspberries, and cranberries (Ogawa et al., 2008), but little is known about its biological actions. Thus, it is logical to suspect and investigate the benefits of consuming Alaskan berries.

Chaga (*Inonotus obliquus*, also known as cinder conk) is a parasitic fungus found on birch trees; it has a long history of a wide variety of medicinal uses in Asia and Eastern Europe, as well as in Alaska. Chaga extracts exhibit high antioxidant activity (Cui et al., 2005) and

protect rat neuronal cells against oxidative stress (Giridharan et al., 2011). Korean traditional knowledge heralds chaga for its anti-cancer effects (Kim and Song, 2014) and ergosterol peroxide extracted from chaga was recently shown to inhibit cell growth by promoting apoptosis in a colorectal cancer cell model (Kang et al., 2015). Taken together, consumption of plants and fungi, especially those biochemically adapted to life in the Arctic, is a promising approach to combating age-related declines in function and development of disease.

The nematode *C. elegans* has homologous neuronal features to humans that are vital for nervous system function, which makes these animals a powerful model for studying neuronal aging *in vivo*. Healthy brain and neuron aging in humans and *C. elegans* is not characterized by cell death (Yankner et al., 2008; Herndon et al., 2002). Instead, age-related cognitive and functional decline in the human brain is associated with neuroanatomical changes, such as decreased white matter (i.e. myelinated neuron axons, glial cells), altered dendritic branching, and decreased synapse density (Yankner et al., 2008). Recently, certain classes of *C. elegans* neurons were also shown to change morphologically with age (Toth et al., 2012; Pan et al., 2011; Tank et al., 2011). Specifically, aging touch receptor neurons develop novel outgrowths from the soma, axon, and dendrites and deteriorated synapses when observed with fluorescent (GFP transgenes) and electron microscopy (Toth et al., 2012; Pan et al., 2011; Tank et al., 2011). By assessing neuron function and phenotypes within an individual, we have a powerful model for exploring mechanisms of neuronal aging and neurological effects of medicinal Alaskan berries and fungus.

The current study aims to describe the influence of Alaskan medicinal berry and fungal treatments on the aging process. We tested the hypothesis that treatments with blueberry, lowbush cranberry, crowberry, and chaga increase wildtype *C. elegans* lifespan and alter touch receptor neuron aging, potentially through different cellular mechanisms. Specifically, we tested the impact of specific treatments on lifespan and healthspan (i.e. motility, touch response, endogenous ROS). By examining the six *C. elegans* touch receptor neurons throughout

adulthood using fluorescence microscopy, we also described the effects of the treatments on age-related morphological changes. Studying the impact of these culturally relevant foods on aging not only provides further support for their ethnomedicinal use, but also gives unique insights into the mechanisms of whole organism and neuronal aging.

3.3 Materials and methods

3.3.1 *C. elegans* strains and maintenance

The following strains were used in this study: N2 (Bristol), ZB154 (zdIs5 [P*mec*-4GFP*; lin-15(+)*]), and TJ375 (*gpIs1*[hsp-16.2::GFP]). We used standard methods to maintain and manipulate *C. elegans* populations (Brenner, 1974). Stock populations were cultured at room temperature (about 22ºC) on Nematode Growth Media agar plates (1L NGM: 2.5g peptone, 17g agar, 3g NaCl, 975mL double distilled water, 1mL 5mg/mL cholesterol, 1mL 1M $CaCl_2$, 1mL 1M $MgSO_4$, 25mL 1M $KHPO_4$, and 0.5mL 100mg/mL streptomycin) seeded with live bacteria (*E. coli* strain OP50-1 cultured in Luria Broth) that were allowed to form a lawn for 48h at room temperature and then stored at 4°C until use.

3.3.2 Berry and fungus extract preparation

We collected wild specimens of the selected species of natural berries and fungus from Fairbanks, Alaska in late summer and early fall 2012. A local Alaskan fungi expert verified the identity of the chaga (*Inonotus obliquus)* specimen. We prepared crude berry extracts by blending and homogenizing a known mass of berries with a known volume of chilled 80% aqueous acetone (~4°C) for 10min and removing the acetone with a rotary evaporator (~90min). We prepared crude chaga extract by steeping the fungus in boiling water and straining out leftover particulates, to mimic common consumption of the fungus as a tea-like infusion. We determined the stock concentrations of extracts using a ratio of the starting mass berry or fungus to the final volume of extract. Extracts were then aliquoted and stored at -80°C. Freeze

thaw cycles were limited to one (thawed from -80°C then aliquoted and frozen at -20°C until use) to ensure maximal preservation of bioactive components (Lohachoompol et al., 2004). Because seasonal weather patterns and location (e.g. bog versus mountain) have been shown to influence the chemical makeup of various botanicals (Howell et al., 2001), all experiments were conducted using extracts prepared from the same extraction batch to eliminate the potential for differences in the chemical properties of the extracts.

3.3.3 Biochemical quantification of extracts

We quantified total phenolic content of each of the Alaskan berry and fungus extracts using a Folin-Ciocalteu assay with a gallic acid standard curve adapted for 96-well plate analysis (Herald et al., 2012). We also measured flavonoid content with a $NaNO_2$/Al/NaOH assay with a catechin standard curve (Herald et al., 2012). The gallic acid and catechin standard curves used for comparison had R^2 values of 0.98 and 0.96, respectively. We quantified anthocyanin content by pH-differential assay with cyanidin-3-glucoside equivalent (Song et al., 2013). Each measurement included at least 3 technical replicates.

3.3.4 Berry and fungus treatment administration

To administer Alaskan berry and fungus treatments, we created treatment agar plates by mixing the appropriate concentration of extract into NGM after the agar cooled but prior to it solidifying. Control plates consisted of NGM plates with no extract. We seeded all plates with live OP50-1 *E. coli.* During all experiments, we ensured that the experimenter was blinded to the treatment groups. In the following described experiments (unless otherwise mentioned), synchronous populations of the appropriate *C. elegans* strains were created on standard, untreated NGM agar plates using the egg lay method (i.e. allow 30 gravid adults to lay eggs for 4h, then removing the adults), fed standard live OP50-1 *E. coli*, and cultured at 25°C. We transferred experimental populations by hand to treatment plates at the late L4 larval stage, just

before adulthood (48h at 25°C after egg lay), allowing the animals to ingest the extract after normal larval development.

3.3.5 Lifespan analysis

Following the production of age-synchronous L4 populations via egg lay, we transferred 2 replicates of 25 animals onto plates for each berry and fungus treatment. We continued to transfer animals at least every other day of adulthood to fresh, seeded agar plates with the appropriate treatment. After all treatment groups stopped producing eggs, we continued to determine survival at least every other day by visual observation or gentle prodding with a platinum wire. At any point during the experiment, animals with protruding intestines, internal live young, or that crawled off the plates were censored. Survival experiments always included an untreated control in parallel with berry and fungus treatments and were repeated at least 3 times. For lifespan experiments using UV irradiated bacteria, berry and fungus treatment administration and agar plate preparation were performed in the same manner as all other experiments with the additional step of exposing prepared OP50-1 lawns to 9999J/m^2 254nm UV light using a UV Stratalinker 1800 and testing for survival before use. We used Kaplan-Meier log-rank survival statistics to analyze differences in mean survival between treatment groups. For this and all other statistical analyses described, we used the statistical software SPSS (version 20) and considered a *p*-value of less than 0.05 statistically significant.

3.3.6 Motility measurement

We divided aging individuals' motility into 3 classes: A, B, and C, following the methods of Herndon et al. (2002). Class A individuals moved spontaneously in a normal, sinusoidal pattern. Class B individuals moved in markedly non-sinusoidal movements and may have required prodding to encourage movement. Class C individuals moved their head and/or tail in response to prodding, but were unable to move across the agar. Treatment effects were compared to their age-matched no treatment control using an ordinal logistic statistics model.

3.3.7 Reactive oxygen species quantification

To begin treatment on large age-matched populations, we washed late L4 populations (48h after bleaching at 25°C) onto treatment plates with M9 (autoclaved 3g KH_2PO_4, 5g NaCl, 6g Na_2HPO_4*$7H_2O$ and sterile 1mL 1M $MgSO_4$ in 1L H_2O). On test day (48h after treatment, day 3 of adulthood), we isolated 300-500 adult worms from each treatment group by washing populations through a 50µm filter with M9. We then quantified reactive oxygen species (ROS) using H_2DCF-DA (Halliwell and Whiteman, 2004). To do this, we: transferred the live adults into labeled 2mL tubes using 1.5mL M9 buffer; allowed them to settle by gravity; removed the supernatant such that 500µL of M9 was left in the tube; and pipetted 3 aliquots of 50µL of the well-mixed M9-worm solution to the appropriate 96-well plate well. Immediately before loading the plate into the Biotek Synergy™ HT Multi-Mode Microplate Reader, we added 50µL of 100mM 2', 7'-Dichlorofluorescin diacetate (DCF-DA, Sigma) in M9 to each well. We recorded basal fluorescence (excitation 485nm, emission 520nm), stored the plate in the dark at room temperature on a shaker for 1h, and recorded final fluorescence. We normalized fluorescence results to basal worm and basal DCF-DA fluorescence (50µM DCF-DA in M9 buffer). Results were also normalized to total protein in each tube (using the leftover 200µL of M9-worm solution in the 2mL tube, described above) using the Pierce BCA Protein Assay on the supernatant following worm lysis (20µL 1M NaOH to each tube incubated for 25min at 70°C). This ROS quantification protocol was performed 3 times and was adapted from other published protocols (Braeckman et al., 2002; Schulz et al., 2006).

3.3.8 Fecundity measurement

To determine whether fecundity, specifically the number of viable progeny produced, was affected by treatments, we performed progeny count assays. We individually plated and transferred age-matched adults each day to fresh plates until the end of their reproductive phase or death. We allowed embryos left behind by the adults each day to develop for 48h at

25°C and then manually counted the number of progeny produced by each individual on each day. We compared the total number of progeny produced per treatment and control using one-way ANOVA and Tukey post-hoc comparisons. We tested for treatment effects on each day of adulthood using a Poisson log linear statistical model.

3.3.9 Mechanosensory neuron aging assay

We performed neuron aging assays (i.e. soft touch response and mechanosensory neuron imaging) using the *C. elegans* strain *zdIs5*, which expresses green fluorescent protein (GFP) in each of the 6 touch receptor neurons (Figure 3.5A). On days 5, 7, 9, and 11 of adulthood, we randomly selected individuals from a synchronous population, tested for touch sensitivity, and imaged the number and type of specific neuronal aberrations seen in the 6 fluorescently labeled neurons. We measured soft touch sensitivity and observed mechanosensory neuron aberrations as established by Toth et al. (2012), by counting the number of positive responses an individual had to 5 alternating touches at each the anterior and posterior ends (10 total touches). To image the fluorescently labeled neurons, we then mounted that individual on a labeled coverslip with 36% Pluronic solution and quantified neuron morphology with an Olympus FSX100 inverted fluorescent microscope at 20x magnification. Neuron morphologies observed included those previously described (Scerbak et al., 2014; Toth et al., 2012; Pan et al., 2011; Tank et al., 2011), such as various lengths of outgrowths from the soma, branches from the process, abnormally shaped soma, punctae on the process, and soma in the wrong location. This assay of mechanosensory neuron form and function was repeated at least 3 times for each selected Alaskan berry and fungus lifespan-extending treatment and each replicate contained its own distinct untreated control group. We performed Poisson log linear (for count data, i.e. number of outgrowths) or logistic regression (for bimodal data, i.e. presence of abnormal cell soma) statistical models to test for treatment and age effects on touch

sensitivity and neuron morphologies. Pairwise comparisons with $p \leq 0.05$ were considered significant.

3.3.10 *hsp16-2*::GFP gene expression assay

hsp-16.2::GFP gene expression assays were performed on age-matched day 3 adults cultured on appropriate berry and fungus treatment plates at 20°C using 8x magnification and constant exposure. Positive control animals were heat shocked at 37°C for 90min, 20h before imaging (Rea et al., 2005). To detect treatment effects, we used an ordinal logistic statistics model.

3.4 Results

3.4.1 Standardization of Alaskan plant and fungus extracts

Polyphenolic compounds, including flavonoids and anthocyanins, exhibit potent antioxidant and anti-inflammatory properties (Joseph et al., 2014). We quantified three measures of phenolic content to compare our extracts with others shown to have bioactive properties and other Alaskan berry extracts shown to contain high phenolic content. Total phenolic content (Folin-Ciocalteu assay with gallic acid equivalent), flavonoid content ($NaNO_2$/Al/NaOH assay with catechin equivalent), and anthocyanin content (pH-differential with cyanidin-3-glucoside) of each extract were measured using established methods (Table 3.1; Song et al., 2013; Herald et al., 2012). The *relative* abundance of total phenolics and anthocyanins of blueberry compared to lowbush cranberry levels was the same as previously reported for Alaskan blueberry and lowbush cranberry (Grace et al., 2014); total phenolic content was 443% higher in lowbush cranberry than blueberry while anthocyanin content was 137% higher in blueberry than cranberry (Table 3.1). Our crowberry extract contained the highest levels of total phenolics and anthocyanins of all our extracts. In contrast, our chaga

extract contained the lowest levels of total phenolics, flavonoids, and anthocyanins of all our extracts.

3.4.2 Alaskan berry and fungus treatments extend *C. elegans* lifespan

Under our laboratory culture conditions (i.e. 25°C, solid media, live OP50-1 *E. coli* food source), *C. elegans* untreated control mean lifespan was 10.2±0.4 days. Three of the four tested Alaskan berry and fungus treatments resulted in wildtype *C. elegans* lifespan extension: blueberry, lowbush cranberry, and chaga treatments extended lifespan at varying doses and to different extents when compared to untreated control populations (Figure 3.1 and Table 3.2). Blueberry treatment elicited the highest increase in lifespan of all tested Alaskan berries and fungus; an average of 30% and up to 47% (200µg/mL treatment) when compared to untreated control. Blueberry was also the only treatment for which an entire range of doses tested (60-400µg/mL) resulted in lifespan extension (Figure 3.1D). In a representative trial, mean lifespan significantly increased over the no treatment control to 12.4±0.6, 11.2±0.6, 12.4±0.7, and 11.2±0.6 days upon treatment with 60, 100, 200, and 400µg/mL Alaskan blueberry extract, respectively ($p<0.05$, Kaplan-Meier log-rank test). Treatment with 800µg/mL blueberry did not consistently, statistically increase lifespan.

Both lowbush cranberry (Figure 3.1E) and chaga (Figure 3.1F) treatments resulted in a bimodal response in lifespan extension. Two of the five selected lowbush cranberry treatment doses significantly increased lifespan: 50 and 400µg/mL. Both 50 and 400µg/mL lowbush cranberry treatments reliably, statistically increased lifespan up to 22% when compared to control. Treatment with 50, 200, and 800µg/mL chaga extract significantly increased mean lifespan to 13.1±0.6, 12.9±0.5, and 12.9±0.6 days, respectively, compared to a control of 10.7±0.5 days in a representative trial ($p<0.05$, Kaplan-Meier log-rank test). In addition to the effective chaga treatments doses shown in Figure 3.1C, we observed no significant change in mean or median lifespan at several additional doses (10, 20, and 100µg/mL; Figure 3.1F).

Crowberry treatment was also tested for lifespan extension at similar treatment doses as blueberry, but no significant effect was observed (Supplemental Figure 3.1).

Next, we investigated whether the lifespan-extending effects of blueberry, lowbush cranberry, and chaga were primarily due to secondary responses in *C. elegans* to an altered food source, OP50-1 *E. coli* exposed to the same treatment. OP50-1 *E. coli* growth in liquid culture was unaffected by the presence of Alaskan nutraceuticals at *C. elegans* lifespan-extending doses (data not shown). We also measured *C. elegans* lifespan on Alaskan berry and fungus treatments with UV irradiated OP50-1 *E. coli*. Both blueberry and lowbush cranberry treatments resulted in extended wildtype lifespan when compared to untreated control, even with UV-killed bacteria ($p<0.05$; Kaplan Meier log-rank test; Supplemental Figure 3.2). However, chaga treatment did not extend lifespan when *C. elegans* were fed UV-killed bacteria ($0.09<p<0.4$; Kaplan Meier log-rank test).

3.4.3 Alaskan berry and fungus treatments improve healthspan

Interventions that increase lifespan do not necessarily increase health with age nor decrease the proportion of time spent living in a frail state (Bansal et al., 2015). To address this possibility with our Alaskan berry and fungus treatments that extended lifespan (Figure 3.1), we studied several measures of healthspan. In *C. elegans*, the ability to move spontaneously and actively (i.e. motility) declines stochastically (Herndon et al., 2002). At mid-life (day 5 of adulthood), both control and lifespan-extending Alaskan berry and fungus treatments tested had nearly 100% normal motility, as expected (Figure 3.2A-C). However, all of the lifespan-extending Alaskan berry and fungus treatments maintained healthy motility well into late adulthood (day 11) by significantly increasing the ratio of normally, spontaneously moving adults (Class A) to abnormally, non-spontaneously moving (Class B) and frail, immobile (Class C) adults ($p<0.01$ ordinal logistic model; Figure 3.2D-F). There were no dose-dependent effects on motility within blueberry and lowbush cranberry treatments ($p>0.2$, ordinal logistic model).

800µg/mL chaga treatment significantly decreased the incidence of Class C adults at Day 11 of adulthood when compared to control, 50, and 200µg/mL chaga (p<0.001, ordinal logistic model).

The ability to sense and respond to touch (i.e. touch response) also decreases with age in *C. elegans*. We observed a significant age-related decrease in both anterior and posterior touch response (i.e. the number of positive responses to 5 touches at the anterior or posterior end of the animal) in all control groups, as expected (Figure 3.3, black bars). Overall, lifespan-extending Alaskan berry and fungus treatments slowed this decline in mechanosensation by late adulthood (day 9 or day 11; Figure 3.3). Both blueberry treatments robustly improved anterior (1.75±0.15 control vs. 2.5±0.15 60µg/mL and 2.4±0.16 200µg/mL; p<0.02) and posterior touch response (2.7±0.14 control vs. 3.4±0.13 60µg/mL and 3.2±0.14 200µg/mL; p<0.02) at day 11 when compared to age-matched control. Low dose lowbush cranberry treatment (50µg/mL) improved both anterior and posterior touch response over control at day 11 of adulthood (anterior: 1.7±0.14 vs. 2.2±0.18; posterior: 3.1±0.11 vs. 3.3±0.11; p<0.05). The higher lowbush cranberry treatment (400µg/mL) improved posterior touch response at day 9 of adulthood (3.75±0.11 vs. 3.9±0.11; p<0.02), then dropped to control levels at day 11 (3.1±0.11 vs. 3.26±0.11; Figure 3.3E). Two of the three lifespan-extending chaga treatments improved touch response: both 50 (2.63±0.18) and 200µg/mL (2.82±0.21) chaga treatments significantly improved anterior (but not posterior) touch response compared to control (2.0±0.16) at day 11 (p<0.05).

Reactive oxygen species (ROS) are considered a biomarker of overall health and are associated with aging (Campos et al., 2014; Stuart et al., 2014; Kregel and Zhang, 2007). To test the hypothesis that lifespan-extending berry and fungus treatments decrease damaging ROS early in life, we measured ROS within whole, live young adult (day 2) *C. elegans* populations using H_2DCF-DA. Blueberry, lowbush cranberry, and chaga treatments differentially influenced endogenous management of ROS (Figure 3.4A). Treatment with blueberry trended

toward increasing ROS levels (113.7% of control; p=0.085; One-way ANOVA) while chaga treatment strikingly decreased ROS (53.5% of control; p=0.06; One-way ANOVA). Lowbush cranberry treatment had no effect on ROS early in adulthood when compared to control (p=1.0; One-way ANOVA), although lowbush cranberry-mediated ROS levels were not significantly different from chaga treatments. Increased expression of the heat shock protein HSP-16.2 is a marker for ROS stress within *C. elegans*. To further describe ROS stress in young adults treated with lifespan-extending Alaskan berry and fungus treatments, we measured the *hsp-16.2*::GFP gene reporter fluorescence in the pharynx (Figure 3.4B-G). These results generally align with the H_2DCF-DA ROS measurements (Figure 3.4A). Blueberry treatment significantly increased *hsp-16.2*::GFP expression (146% of control; p<0.05; One-way ANOVA). Both chaga and lowbush cranberry treatments did not significantly alter *hsp-16.2*::GFP gene expression (p>0.2; One-way ANOVA).

Interventions that increase aging are often associated with a decrease in fecundity (Jafari and Rose, 2006). We found that lifespan-extending Alaskan berry and fungus treatments did not influence total progeny produced per individual (p>0.7; One-way ANOVA; N=24 per treatment; Table 3.3). When we considered the number of progeny produced per individual on specific days of adulthood, several treatment doses had numerically small (<15 progeny) but significant effects (p<0.05; One-way ANOVA with Tukey post-hoc analysis). However, no treatments extend the number of days individuals produced viable progeny (Supplementary Figure 3.3).

3.4.4 Alaskan berry and fungus treatments differentially alter mechanosensory neuron aging

C. elegans mechanosensory neurons sense soft touch and exhibit changes in morphology with age and with modifications in cellular signaling (Toth et al., 2012; Pan et al., 2011; Tank et al., 2011). To visualize these morphological changes with age, we used a *C.*

elegans strain with GFP-labeled touch receptor neurons (*zdIs5* [mec-4p::GFP]). There are six *C. elegans* touch receptor neurons: two anterior lateral (ALML, ALMR), one anterior ventral (AVM), two posterior lateral (PLML, PLMR), and one posterior ventral (PVM), which are illustrated in Figure 3.5A. This study focused on the two pairs of lateral neurons because they are the most sensitive to change with age. The four lateral neurons (ALML, ALMR, PLML, PLMR) are typified by a circular cell body (soma) and a single, straight process (representing the axon and dendrites) extending towards the anterior end of the animal. Posterior neurons have an additional outgrowth from the soma towards the posterior of the animal. We considered any morphological deviations from this norm to be "neuronal aberrations," but did not assume that these aberrations were functionally deleterious.

In all treatments, we observed similar morphological changes with age in the untreated control groups, as expected (Figures 3.5-7; black bars). Notably, as they aged, all control populations exhibited significantly increased numbers of total aberrations per anterior cell (day 11 is 179% of day 5 levels; $p<0.05$; Poisson log linear model; Figure 3.5B; black bars) and total aberrations per posterior cell (day 11 is 3154% of day 5 levels; $p<0.05$; Poisson log linear model; Figure 3.6A; black bars). In anterior cells, the total number of extended outgrowths increased with age (day 11 is 469% of day 5 levels; $p<0.05$; Poisson log linear model; Figures 3.5D and 3.7B; black bars). In posterior cells, an increase in process branching was the primary driver for the increased total aberrations per cell (increased from no occurrences at day 5 to 23.2% occurrence at day 11; $p<0.05$; Poisson log linear model; Figure 3.6B; black bars). These findings generally align with previously described age-related morphological changes observed in touch receptor neurons (Toth et al., 2012; Pan et al., 2011; Tank et al., 2011).

Blueberry treatments that significantly extended lifespan (60 and 200µg/mL) decreased the total number of aberrations observed per animal relative to control by day 11 of adulthood (79.2% and 71.8% of control; $p<0.05$; Poisson log linear model). At the cellular level, only anterior lateral neuron morphology was altered with blueberry treatment (86.2% and 76.2% of

control; $p<0.05$; Poisson log linear model; Figure 3.5B). The primary aberration driving this difference in anterior neuron morphology with blueberry treatment was soma outgrowths (90.9% and 77.6% of control levels; $p<0.05$; Poisson log linear model; Figure 3.5C), specifically extended soma outgrowths (<2x soma diameter; Figure 3.5D). The percent of anterior cell somas with an abnormal shape or location significantly decreased with 200µg/mL blueberry treatment day 11 of adulthood (67.4% and 56.5% of control; $p<0.05$ Poisson log linear model; Figure 3.5G) and was the only other specific aberration significantly altered with blueberry treatment. Conversely, on day 5 of adulthood, low dose blueberry (60µg/mL) treatment significantly increased extended outgrowths and significantly decreased percent cells with abnormal cell bodies ($p<0.05$; Poisson log linear model), suggesting that a relationship between these two aberrations exists early in life. Posterior touch receptor neuron aging was unaffected by blueberry treatment ($p>0.8$; Poisson log linear model).

In contrast to blueberry treatment, lowbush cranberry treatment increased only posterior cell aberrations (Figure 3.6A). Treatment with low dose lowbush cranberry (50µg/mL) significantly increased total posterior cell aberrations both at mid-life (day 5; 719% of control) and old age (day 11; 177% of control; $p<0.01$; Poisson log linear model). This increase in total aberrations was due solely to increased posterior cell process branching compared to control by day 11 of adulthood (Figure 3.6B). Anterior cell aberration development with age was unaffected by 50µg/mL lowbush cranberry treatment ($p>0.8$; Poisson log linear model). The higher lowbush cranberry treatment (400µg/mL), which also increased lifespan, had no effect on age-related development of posterior cell aberrations ($p>0.1$; Poisson log linear model). 400µg/mL lowbush cranberry treatment significantly decreased the number of anterior cell aberrations by day 11 of adulthood, similar to 200µg/mL blueberry treatment (83.1% of control; $p<0.05$; Poisson log linear model), but we are unable to relate this decrease to any specific type of neuronal aberration.

Treatment with lifespan-extending chaga doses elicited effects similar to both blueberry and lowbush cranberry treatments: both anterior cell soma outgrowths and posterior cell process outgrowth events were impacted (Figure 3.7). While chaga treatment did not significantly alter the accumulation of total anterior cell outgrowths with age ($p>0.8$; Poisson log linear model; Figure 3.7A), these treatments did affect the lengths of the soma outgrowths observed. In all three chaga treatments, the occurrence of extended outgrowths (≥2x soma diameter) significantly decreased compared to control at day 11 of adulthood (43.3%-52.8% of control; $p<0.05$; Poisson log linear model; Figure 3.7B). Conversely, short soma outgrowths (<1x soma diameter) increased by day 11 with chaga treatment (153-210% of control; $p<0.05$; Poisson log linear model; Figure 3.7C). Posterior cell process outgrowths, which consist of both straight branches pointing away from the process and branches that loop back to the process (i.e. loops), were affected by all three chaga treatments later in life (166-403% of control; $p<0.05$; Poisson log linear model; Figure 3.7D). Branching events were the primary driver of these posterior cell process outgrowths, but the unique presence of loops in the process warrants consideration. Specifically, treatment with low dose chaga (50µg/mL) significantly reduced posterior cell process outgrowths at day 9 of adulthood (8.3% of control; $p<0.05$; Poisson log linear model), but these aberrations rose to control levels at day 11 ($p>0.2$; Poisson log linear model). Treatment with 200µg/mL chaga quadruples the occurrence of posterior cell process outgrowths at day 11 of adulthood compared to control (403% of control; $p<0.05$; Poisson log linear model). High dose chaga treatment (800µg/mL) caused a significant decrease in posterior cell process outgrowths at day 9 of adulthood compared to control and a significant increase by day 11 (241% of control; $p<0.05$; Poisson log linear model).

3.5 Discussion

Compared to the modern “Western” lifestyle, traditional North American Native and subsistence lifestyles are associated with lower incidence of age-related and chronic disorders,

particularly cardiovascular disease (Mohatt et al., 2007; Ebbesson et al., 2005). Differences in the diet of these two lifestyles are proposed factors for the improved health. To further explore the influence of traditional food sources on the functional aging process, we tested the effects of Alaskan berry and fungus extracts on *C. elegans* lifespan, healthspan, and markers of touch receptor neuron aging. Alaskan blueberry, lowbush cranberry, and chaga treatment increased lifespan at varying doses (i.e. 50 to 800µg/mL; Figure 3.1 and Table 3.2). Increased lifespan may be uncoupled from improved health in old age (e.g. healthspan), thus measuring length of life alone does not necessarily provide an accurate portrayal of aging (Bansal et al., 2015). We find that measures of healthspan are either improved (i.e. motility, touch response; Figure 3.2-3.3) or not affected (i.e. total viable progeny produced; Table 3.3) throughout the lifespan of animals treated with Alaskan berries and fungus. Each of the Alaskan berry and fungus treatments resulted in varied touch receptor neuron aging trajectories, with both decreased incidence of anterior neuron (ALM) soma outgrowths and increased incidence of posterior neuron (PLM) process branching (Figure 3.8). Nonetheless, both changes correlated with improved touch response (Figures 3.3 and 3.5-3.8). Importantly, this suggests that the development of specific touch receptor neuron morphologies impact neuronal and organismal function differently and reflects the importance of examining multiple healthspan markers in aging studies. Our findings demonstrate that beneficial nutritional lifespan interventions differentially impact touch receptor neuron aging and, thus, support the body of research describing numerous cellular strategies leading to increased lifespan and improved health (reviewed in Lopez-Otin et al., 2013).

Alaskan blueberry treatment effects are distinct from the other treatments; blueberry elicited the greatest increase in lifespan (up to 47%) and improved both anterior and posterior touch response late in life, while only impacting ALM morphology (i.e. decreased extended soma outgrowths and incidence of abnormal cell bodies; Figure 3.5). There is also a time-dependent and dose-dependent response to blueberry treatment that is unique from the other

Alaskan nutraceutical treatments. First, middle-aged adults (day 5) treated with 60µg/mL blueberry exhibit a touch receptor neuron phenotype associated with decreased health later in life (i.e. increased incidence of extended outgrowths from anterior cell somas; Figure 3.5D) and no improvement in other markers of healthspan (i.e. motility, Figure 3.2A; touch response, Figure 3.3A and 3.3D). Second, the higher 200µg/mL treatment elicited a significant decrease in extended outgrowths by late life (day 11), while 60µg/mL did not (Figure 3.5D). Also, in young adults (day 2) treated with 200µg/mL blueberry, we observed increased levels of damaging ROS within live animals and increased *hsp-16.2*::GFP expression, a marker of ROS stress when compared to controls (Figure 3.4). Importantly, heat-shock treatments, which induce *hsp-16.2*::GFP expression, are known to result in improved stress response via hormetic mechanisms (Link et al., 2009). Blueberry treatment (200µg/mL) also slightly, but significantly, decreased the number of progeny produced on day 2 of adulthood (27±13.1 fewer progeny than control; Supplemental Figure 3.3) but did not impact total progeny produced over reproductive lifespan; again suggesting that early in life, blueberry treatment induces stress-response signaling.

These dose- and time-dependent results indicate an involvement of two interesting biological phenomenon in the blueberry treatment effects: hormesis and xenohormesis. Hormesis describes the dose-dependent effect wherein low doses of a treatment elicit a beneficial response while high doses of the same treatment are elicit a negative response or are toxic. Xenohormesis is the adaptive, defensive response of animals to consuming secondary metabolites produced by environmentally stressed plants (e.g. polyphenols; Howitz and Sinclair, 2008). Xenohormesis may also be described as one organism (i.e. the consumer) benefiting from the stress response, or hormesis, of another organism (i.e. the plant). This intra-species signaling is proposed to activate stress-response signaling in animals via interactions with signaling molecules (as opposed to general antioxidant effects), which improves the health and survival of the consumer (Howitz and Sinclair, 2008). Xenohormesis may be involved in the

blueberry treatment effects because of the increased *C. elegans* lifespan following the consumption of Alaskan blueberry extract, which is known to have elevated polyphenolic content relative to other blueberry species (Grace et al., 2014), indicative of UV-stress. Additionally, our observation of a detrimental neuronal phenotype coupled with increased markers of ROS stress and decreased progeny early in life followed by improved lifespan, healthspan, and touch receptor neuron health late in life suggests that hormesis within the worm is likely also occurring.

Others have proposed that polyphenols, including extracts from blueberry, exert their effects on stress-response and longevity through mechanisms other than antioxidant activity, such as hormesis and xenohormesis. For example, Elks et al. (2011) observed that feeding a hypertensive rat model a blueberry-enriched diet improved renoprotection and oxidative stress markers in the long term (6 or 12 weeks) but *increased* oxidative stress in the short term (2 days). These authors also proposed xenohormesis as a mechanism of blueberry treatment effects. Additionally, Wilson et al. (2006) found that treatment with non-Alaskan, wild lowbush blueberry polyphenols not only increased lifespan but also improved response to heat stress and thermotolerance, processes that are markers of an adaptive response to a stressor (Gems and Partridge, 2008). Blueberry extracts have also been shown to modulate biological responses (e.g. inhibition of inflammation) at treatment doses low enough to preclude the action of antioxidants as ROS scavengers as the sole explanation of their effects in neuronal cell culture (Gustafson et al., 2012). Interactions of specific polyphenolic compounds with diverse cellular signaling pathways outside of antioxidant signaling involved in aging have also been described (e.g. quercitin from apples and insulin signaling; Youl et al., 2010). Our results and these previous examples suggest that blueberry treatment elicits health benefits through signaling mechanisms outside, or at least in addition to, antioxidant signaling and scavenging.

Lowbush cranberry treatment increased lifespan to a lower extent than blueberry (22% compared to 30-47%), improved both anterior and posterior touch response late in life, and only

impacted PLM neuron aging (i.e. increased posterior process branching). Chaga treatment resulted in bimodal lifespan extension to a similar magnitude as lowbush cranberry (up to 24%), only improved anterior touch response, and both decreased extended ALM soma outgrowths and increased PLM process branching and loop events late in life. Interestingly, there is not a clear relationship between total phenolic, flavonoid, and anthocyanin contents and these lifespan, healthspan, and neuron aging results (Table 3.1), suggesting that the concentrations of these compounds alone is not enough to predict anti-aging bioactivity. Although both lowbush cranberry and chaga treatments resulted in a similar magnitude of lifespan extension, the lowbush cranberry extract contained nearly 3x, 7x, and 29x more total phenolic, flavonoid, and anthocyanin content, respectively, than the chaga extract. Also, the extract containing the highest levels of all three polyphenols, crowberry, did not extend the lifespan of wildtype animals at the doses tested. This lack of lifespan extension may be due to either testing doses with too high of polyphenolic content or the presence of competing, non-beneficial molecules in the crowberry extract that are not in the blueberry or lowbush cranberry extracts.

Chaga extract contained the lowest polyphenolic compound levels of the studied extracts, yet, our ROS results support previous studies demonstrating that extracts from chaga exert potent antioxidant effects (Figure 3.4; Giridharan et al., 2011; Cui et al., 2005). While chaga contains novel polyphenolic compounds (Lee et al., 2007), it is interesting to note that the fungus also contains unique non-polyphenolic bioactive secondary compounds, such as steroid derivatives. Ergosterol peroxide, a steroid derivative unique to fungi, lichens, yeast, and sponges, was recently shown to have anti-cancer activity in a model of colorectal cancer (Kang et al., 2015). The low polyphenolic content in our chaga extract when compared to berry extracts coupled with the observed beneficial effects on aging (e.g. decreased ROS and increased lifespan) suggest that such a compound may be central to the health properties of chaga. The lack of correlation between the polyphenolic content in our extracts and ROS levels with the observed effects on whole animal and neuron aging suggests that the general

antioxidant effect (i.e. removal of ROS) by these compounds may not be central to their involvement in healthy neuron aging. Rather, chaga-induced healthy neuron aging may be due to the interaction of polyphenolic and non-polyphenolic compounds with cellular signaling pathways distinct from antioxidant signaling pathways, another potential example of xenohormesis.

Anterior and posterior mechanosensory neurons respond to aging with different morphological changes: ALM neurons exhibit increased soma outgrowths and abnormal soma shapes while PLM neurons exhibit increased process outgrowths with age (i.e. branching, loops; Vayndorf et al., 2016; Toth et al., 2012; Pan et al., 2011; Tank et al., 2011). Our association of distinctly different mechanosensory neuron morphologies with improved health is novel. We found that both *decreased* outgrowth from anterior neuron somas (i.e. soma outgrowths) and *increased* outgrowth from posterior neuron axons (i.e. process branching) late in life are associated with improved mechanosensory neuron function (i.e. touch response), improved motility, and increased lifespan (Figure 3.8). Thus, increased incidence of these age-related morphologies is not directly correlated with poorer health: both decreased incidence of ALM aberrations (i.e. soma outgrowths, abnormal soma shape) and increased incidence of PLM aberrations (i.e. process branching and loops) correlate with increased lifespan, improved motility, and improved touch response. Others have shown that specific genetic mutations known to be involved in aging (e.g. insulin signaling) seem to regulate specific mechanosensory neuron morphologies (Scerbak et al., 2014; Toth et al., 2012; Tank et al., 2011; Pan et al., 2011). Because of the apparent different cellular controls of these morphological changes, a synergy in maintaining organismal health with age may exist between the anterior and posterior neurons. Aspects of this potential synergy are evident in the treatment effects of chaga, which impacted both ALM and PLM neurons: although chaga treatment was not the most effective at extending lifespan at the doses tested (Figure 3.1), it maintained motility the best out of treatments tested (Figure 3.2) and maintained anterior touch response better than cranberry

(Figure 3.3). What remains to be determined is whether increased incidence of morphological aberrations (e.g. PLM process branching) is a stimulatory response that *actively promotes* healthy aging or whether this phenotype occurs as a *consequence* of good health and aging. The ALM and PLM pairs of touch receptor neurons consistently respond to the aging process different manners; reflecting the multifaceted controls of aging at the cellular level.

These data and conclusions also bring up an exciting aspect of studying the impacts of medicinal foods on aging: the opportunity to study biological complexities that can rarely be fully recapitulated by single genetic manipulations. Studying the impact of culturally valued foods, such as Alaskan berries and fungi, not only supports the traditional ecological knowledge that these foods are beneficial to health, but provides novel insights into the mechanisms of neuronal aging and aging in general.

3.6 Acknowledgements

The authors would like to thank Dr. Marton Toth for the ZB154 strain, Dr. Gary Laursen for chaga identification, Dr. Tom Green for berry extraction assistance, Ian Herriott for UAF Core Lab support, and members of the Taylor/Harris laboratory for their support. Some *C. elegans* strains were provided by the CGC, which is funded by NIH Office of Research Infrastructure Programs (P40 OD010440). Work reported in this publication was supported by the National Institute of General Medical Sciences of the National Institutes of Health (1) under an Institutional Development Award (IDeA; grant number P20GM103395) and (2) under a Building Infrasturcture Leading to Diversity Award (BUILD; three linked grants numbered RL5GM118990, TL4 GM118992 and 1UL1GM118991). The work is solely the responsibility of the authors and does not necessarily represent the official view of the National Institutes of Health.

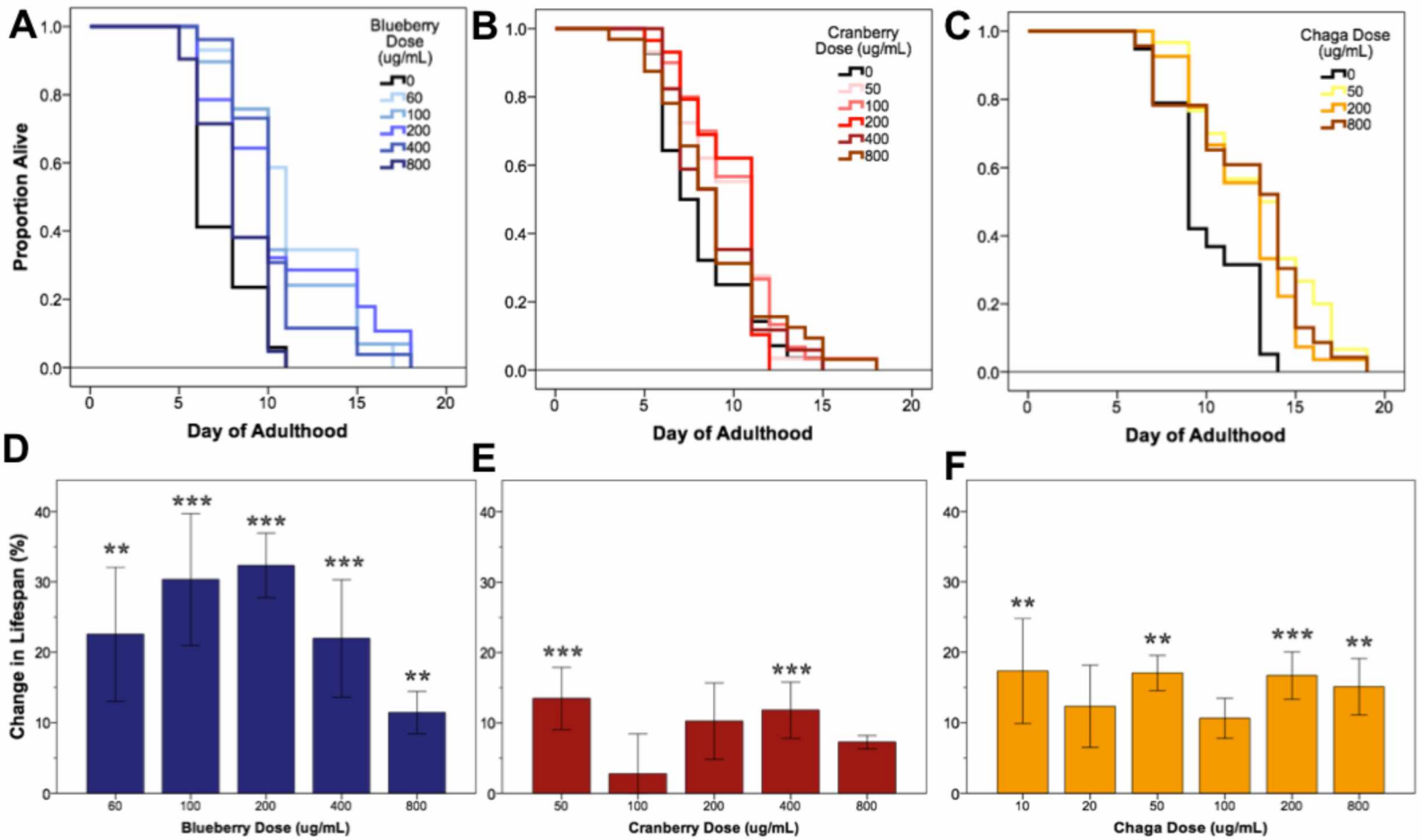

Figure 3.1 Alaskan berry and fungus treatments extend wildtype *C. elegans* lifespan.

Representative survival curves for each berry and fungus treatment (A-C) and induced percent change in lifespan relative to control for all replicates (D-F) are shown (N=50 per treatment group). Asterisks denote significant lifespan extension ($p<0.05$; Kaplan Meier log-rank test) from control in 75% or more (***) and 60% or more (**) of 4-6 independent trials. Bars represent mean ± standard error of the mean between all replicates of a treatment dose.

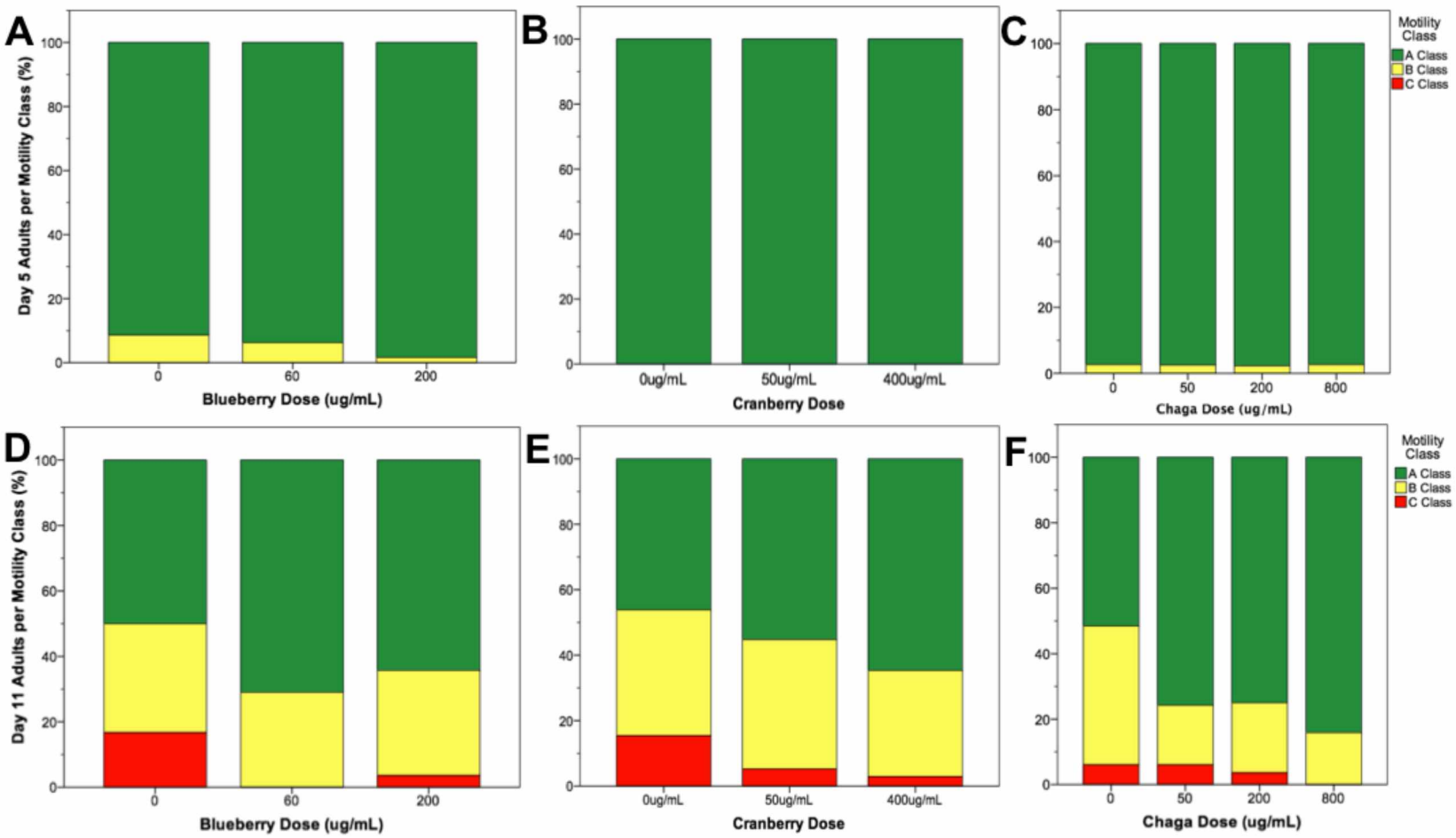

Figure 3.2 Lifespan-extending Alaskan berry and fungus treatments improve wildtype *C. elegans* motility late in life.

Percent per motility class of middle age (day 5 adults; A-C) and old age (day 11 adults; D-F) for lifespan-extending Alaskan blueberry (A, D), lowbush cranberry (B, E), and chaga (C, F) are shown. Class A animals (green bars) moved normally and spontaneously, class B animals (yellow bars) moved abnormally and may have required prodding, and class C animals (red bars) were unable to translocate. N=28-58 animals from at least 3 separate biological replicates per treatment group.

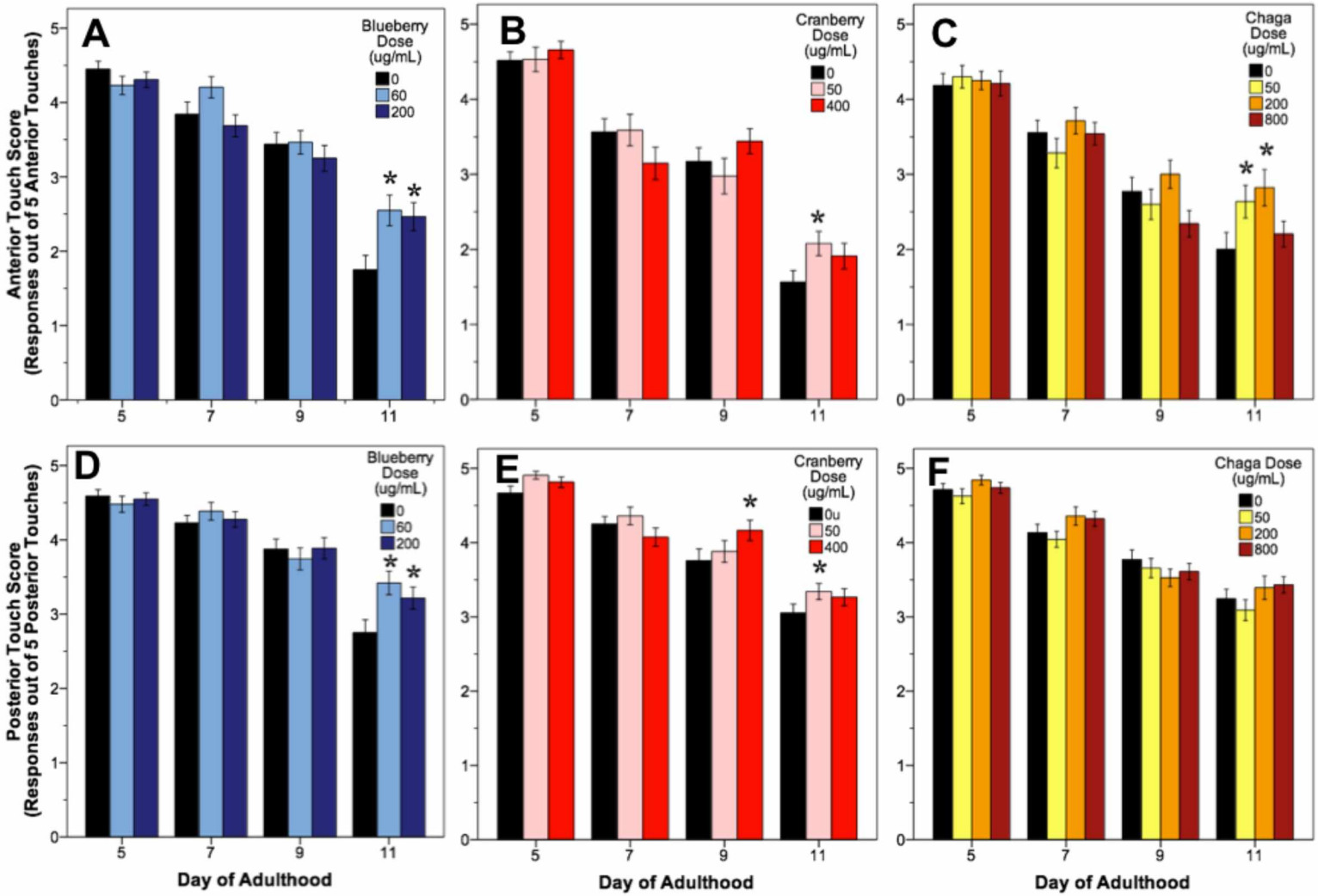

Figure 3.3 Lifespan-extending Alaskan berry and fungus treatments improve wildtype *C. elegans* gentle touch response late in life.

Anterior (A-C) and posterior (D-F) mean touch score for each treatment group is shown. Asterisks denote significance from age-matched control ($p<0.05$; Poisson log linear model). Bars represent mean ± standard error of the mean. N=28-58 animals from at least 3 separate biological replicates per treatment group.

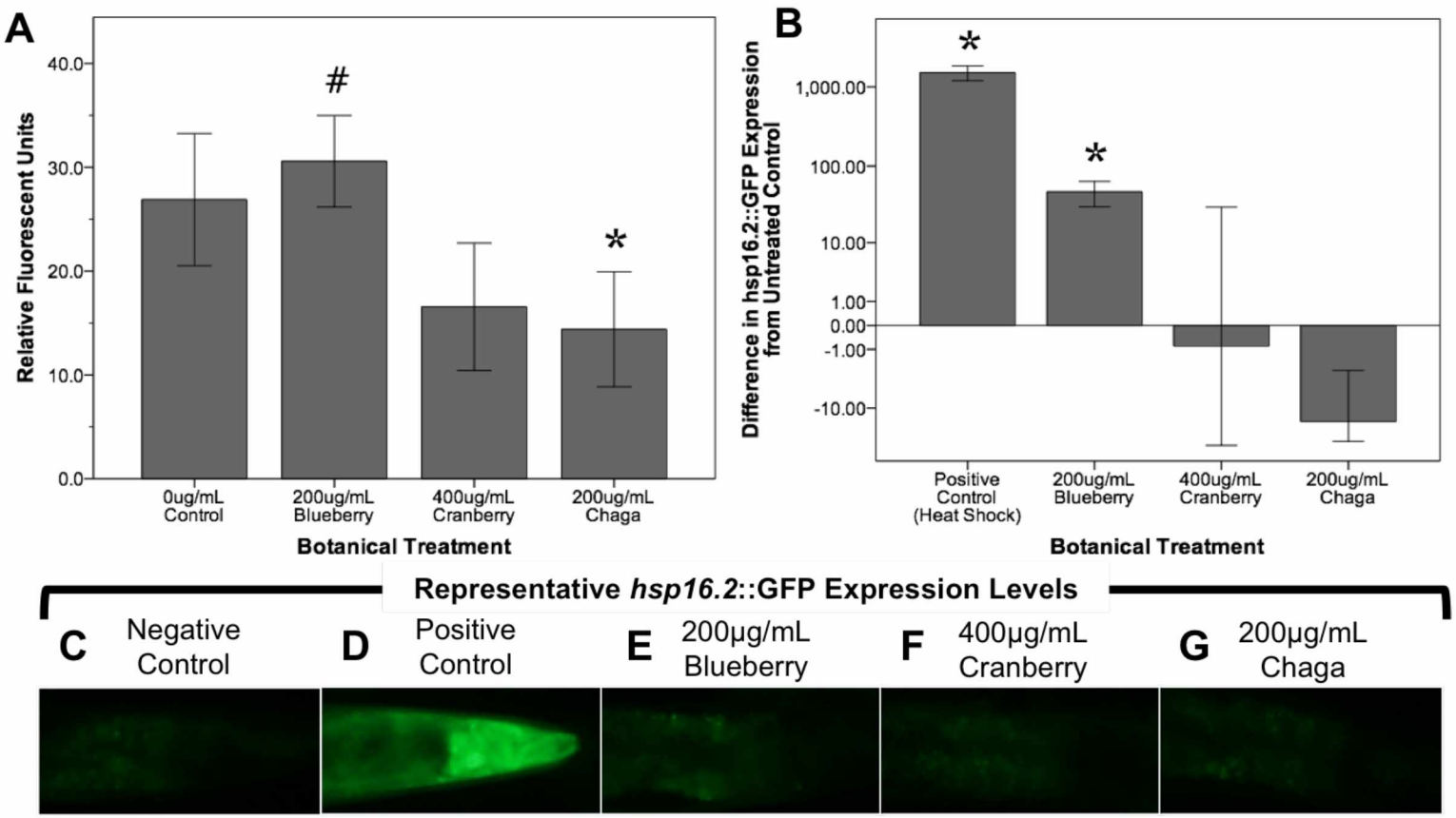

Figure 3.4 Lifespan-extending Alaskan berry and fungus treatments change endogenous reactive oxygen species (ROS) levels in young wildtype *C. elegans*.

(A) The change in endogenous ROS measured by DCF-DA after treating young adults for 48h with selected lifespan-extending Alaskan berry and fungus treatments is shown. The percent change on a logarithmic scale of *hsp16.2*::GFP expression in the pharynx region of young adults treated for 48h with selected berry and fungus treatments relative to untreated control (B) and representative images (C-G) are also shown. Note the extreme increase in *hsp16.2*::GFP expression in response to heat shock. Bars represent mean ± standard error of the mean of each replicate, each with 2 or 3 technical replicates for the DCF-DA assay. Hashtag (p=0.085) and asterisks (p<0.06; one-way ANOVA with Tukey post-hoc) denote significance from 0µg/mL control.

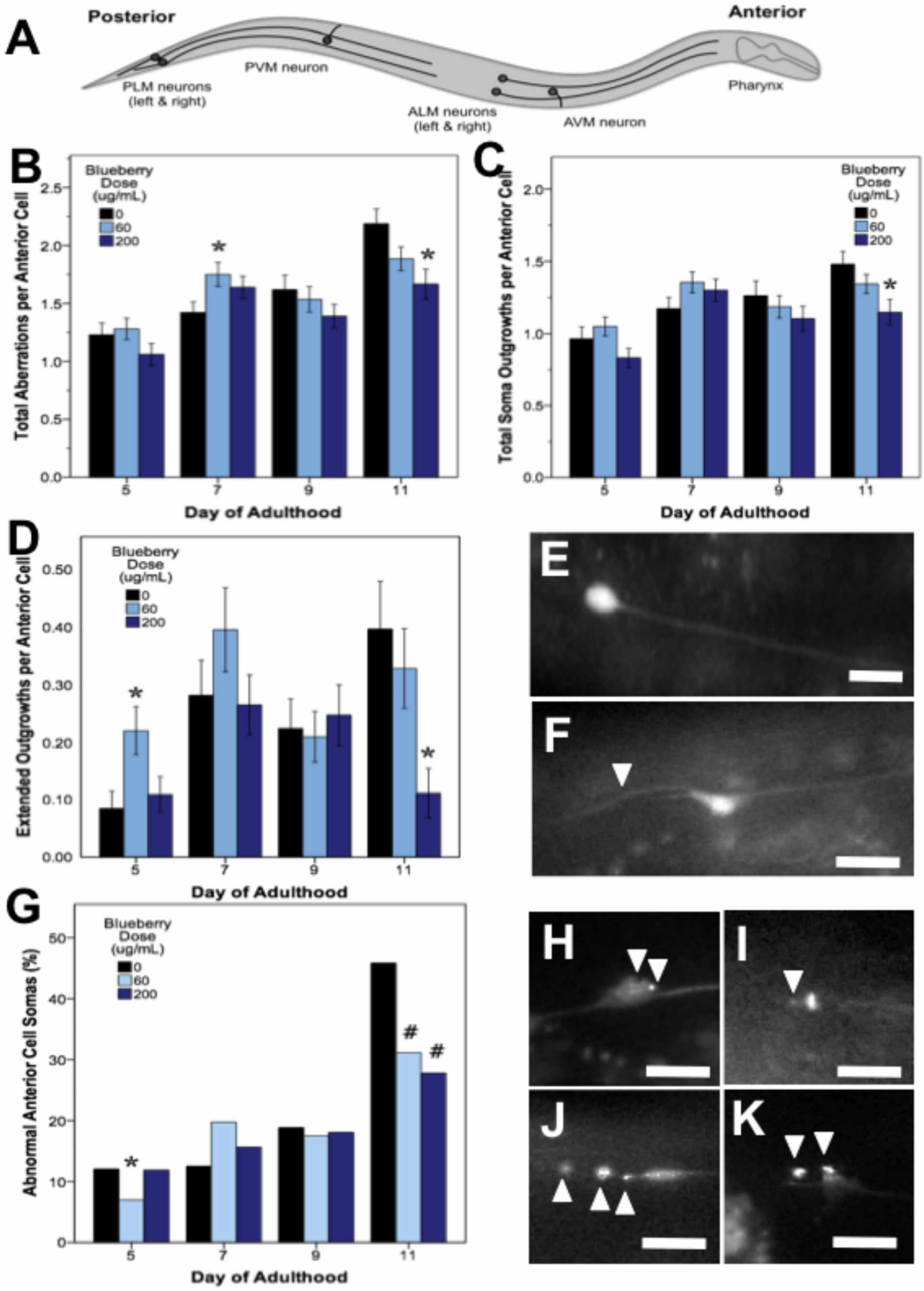
A
Posterior
Anterior
PVM neuron
PLM neurons
(left & right)
ALM neurons
(left & right)
AVM neuron
Pharynx
B
Blueberry
Dose
(ug/mL)
0
60
200
Total Aberrations per Anterior Cell
Day of Adulthood
C
Total Soma Outgrowths per Anterior Cell
Day of Adulthood
D
Extended Outgrowths per Anterior Cell
Day of Adulthood
E
F
G
Abnormal Anterior Cell Somas (%)
Day of Adulthood
H
I
J
K

Figure 3.5 Alaskan blueberry treatments alter the accumulation of aberrations in aging anterior touch receptor neurons.

Animals from control and lifespan-extending blueberry treatments (60 and 200µg/mL) were imaged for touch receptor neuron aberrations at days 5, 7, 9, and 11 of adulthood. A schematic of the locations of the 6 GFP-labeled touch receptor neurons (A) is shown. Neuron aging markers in order of broad to more specific effects are shown: Mean number of total aberrations (B), soma outgrowths (of all lengths) (C), extended outgrowths (≥2x longer than soma diameter) per anterior (ALM) neuron (D) are shown along with representative images of ALM somas free of aberrations (E) and with extended outgrowth (F). Percent of all anterior cells imaged with abnormal somas (G) is shown along with example ALM neurons with abnormal somas (H-K). Bars represent mean ± standard error of the mean. Asterisks ($p<0.05$) and hashtags ($p<0.08$) denote significance from age-matched control. Nworms= 28-62 and Nanterior cells= 48-101 per bar. White arrowheads denote location of specific aberration. All images were collected at 20x magnification and were cropped to the same scale (no other image processing was performed). White scale bars are 10µm.

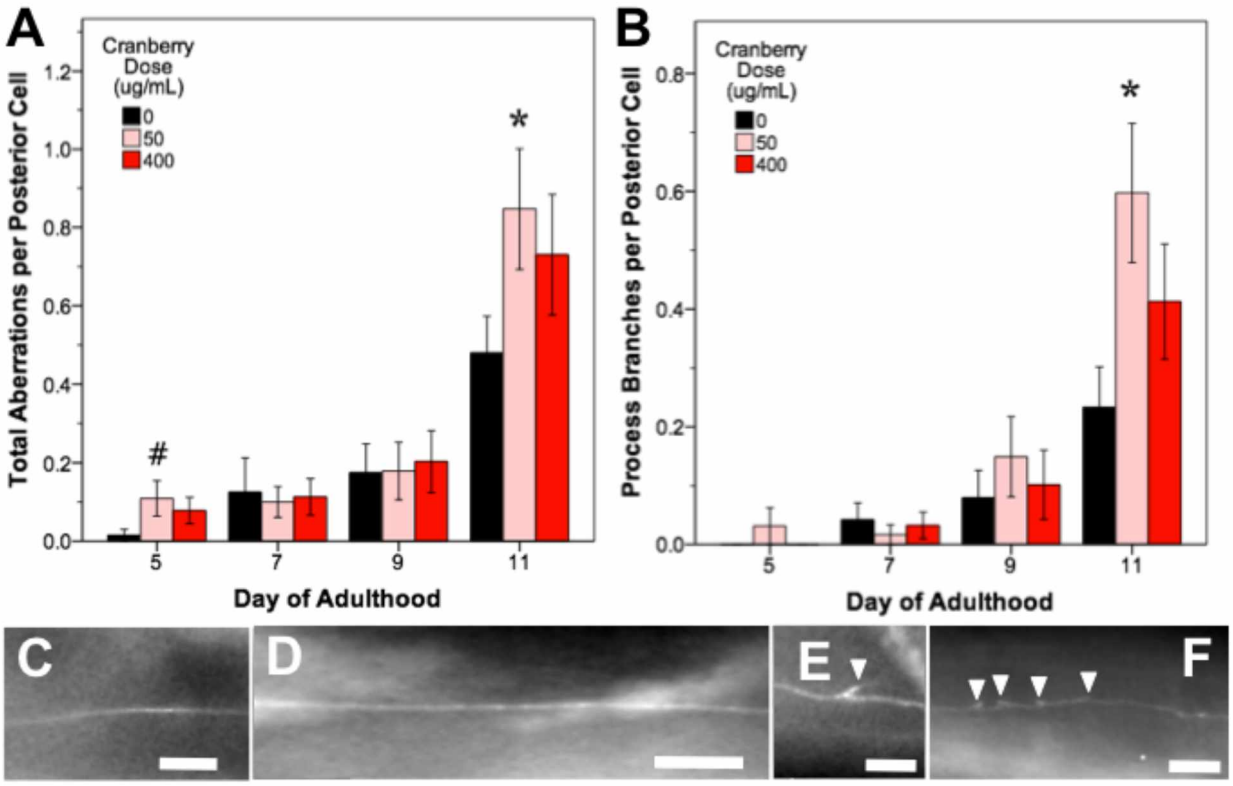

Figure 3.6 Alaskan lowbush cranberry treatments increase occurrence of process branching in aging posterior touch receptor neurons.

Animals from control and lifespan-extending lowbush cranberry treatments (50 and 400μg/mL) were imaged for touch receptor neuron aberrations at days 5, 7, 9, and 11 of adulthood. Mean number of total aberrations (A) and branches observed on the dentrite/axon per posterior lateral touch receptor (PLM) neuron (B) are shown. Representative images of posterior neuron processes with no aberrations (C, D), with one process branch (E), and with multiple process branching events (F) are also shown. Bars represent mean ± standard error of the mean. Asterisks ($p<0.05$) and hashtags ($p<0.085$) denote significance from age-matched control. Nposterior cells= 48-73 per bar. In all images, the anterior end of the animal is to the right and posterior lateral touch receptor (PLM) neurons are shown. All images were collected at 20x magnification and were cropped to the same scale (no other image processing was performed). White scale bars are 10μm.

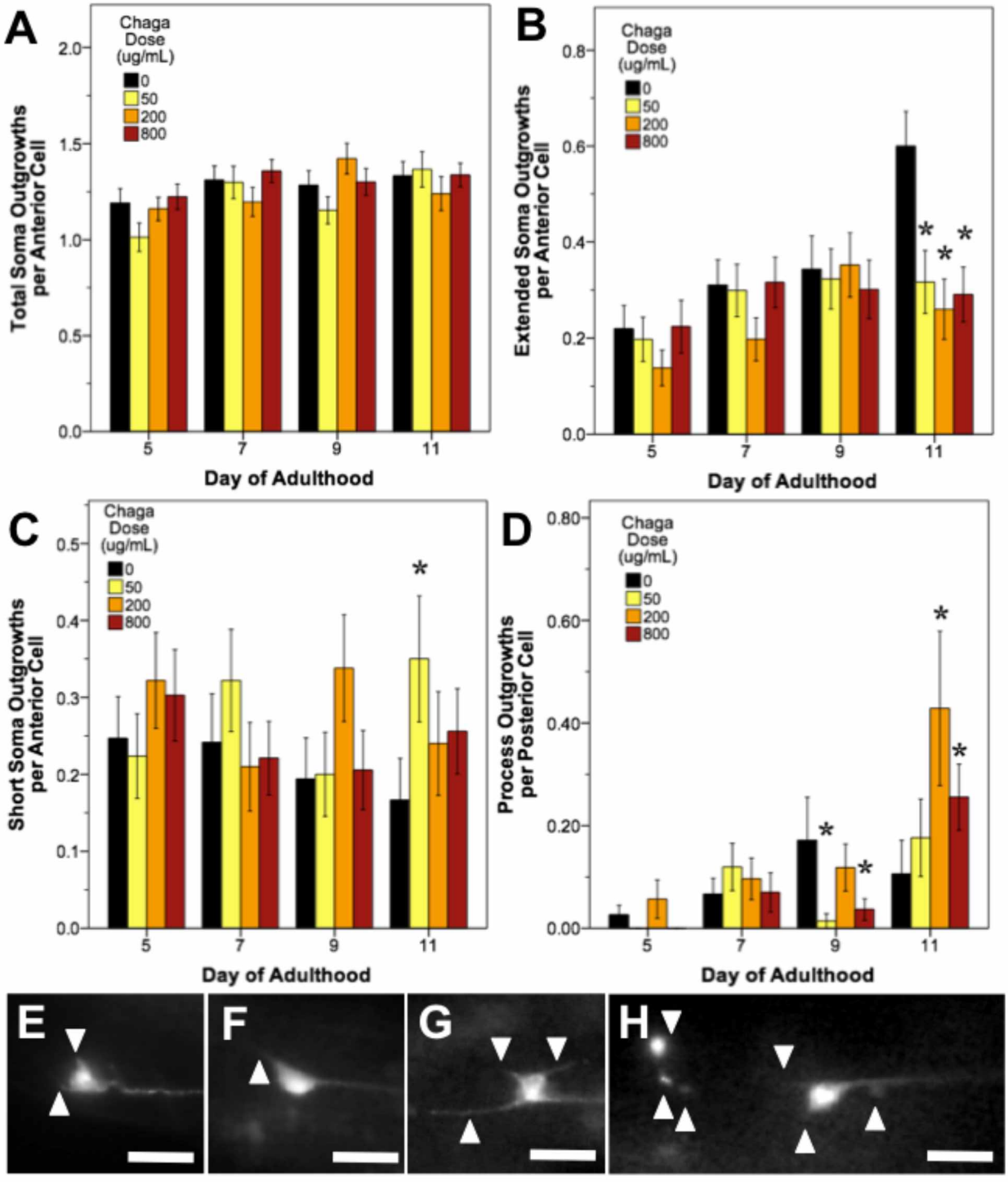
A
Chaga Dose (ug/mL)
0
50
200
800
Total Soma Outgrowths per Anterior Cell
Day of Adulthood
B
Extended Soma Outgrowths per Anterior Cell
Day of Adulthood
C
Short Soma Outgrowths per Anterior Cell
Day of Adulthood
D
Process Outgrowths per Posterior Cell
Day of Adulthood
E
F
G
H

Figure 3.7 Alaskan chaga treatments impact aging anterior and posterior touch receptor neurons.

Animals from control and lifespan-extending chaga treatments (50, 2, and 800µg/mL) were imaged for touch receptor neuron aberrations at days 5, 7, 9, and 11 of adulthood. The total number of anterior cell soma outgrowths was unchanged with chaga treatment (A), but the mean number of extended outgrowths (≥2x longer than soma diameter) (B) and short soma outgrowths (<1x soma diameter) per anterior cell (C) were impacted. Posterior cell process outgrowths (D) represents branching or loop phenotypes observed from the axon and/dendrites of the two posterior lateral neurons (PLM). Representative images of short soma outgrowths (E), standard soma outgrowth (1x soma diameter; F), different length soma outgrowths (G) and extreme aberrations (H) are also shown. Bars represent mean ± standard error of the mean. Asterisks ($p<0.05$) denote significance from age-matched control. Nworms= 28-50, Nanterior cells= 50-95, and Nposterior cells= 56-100 per bar. . All images were collected at 20x magnification and were cropped to the same scale (no other image processing was performed). White scale bars are 10µm.

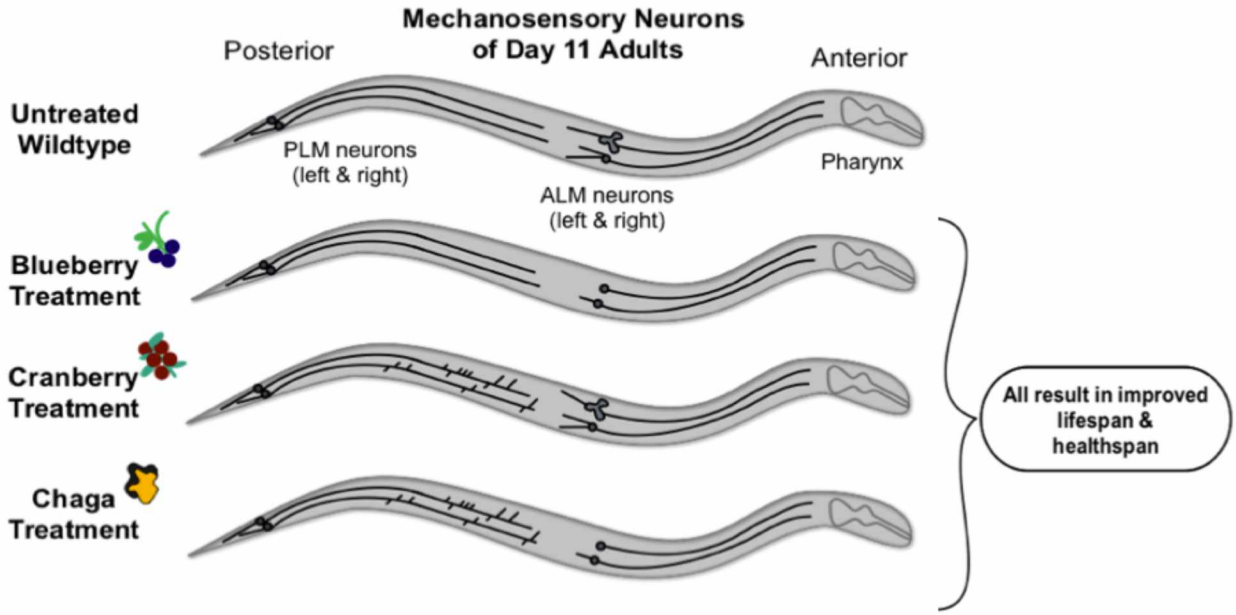

Figure 3.8 Schematic summary of results.

Non-treated wildtype aging C. elegans touch receptor neurons exhibit increased extended outgrowths from the anterior neuron (ALM) soma and increased abnormal ALM soma by late life (day 11 of adulthood). Alaskan berry and fungus treatments impact this neuron aging trajectory by blocking accumulation of ALM aberrations (i.e. blueberry), increasing the incidence of posterior neuron (PLM) aberrations (i.e. lowbush cranberry), or both (i.e. chaga) when compared to age-matched controls. Nevertheless, all 3 treatments significantly increase lifespan and improve markers of healthspan (i.e. motility and touch response late in life).

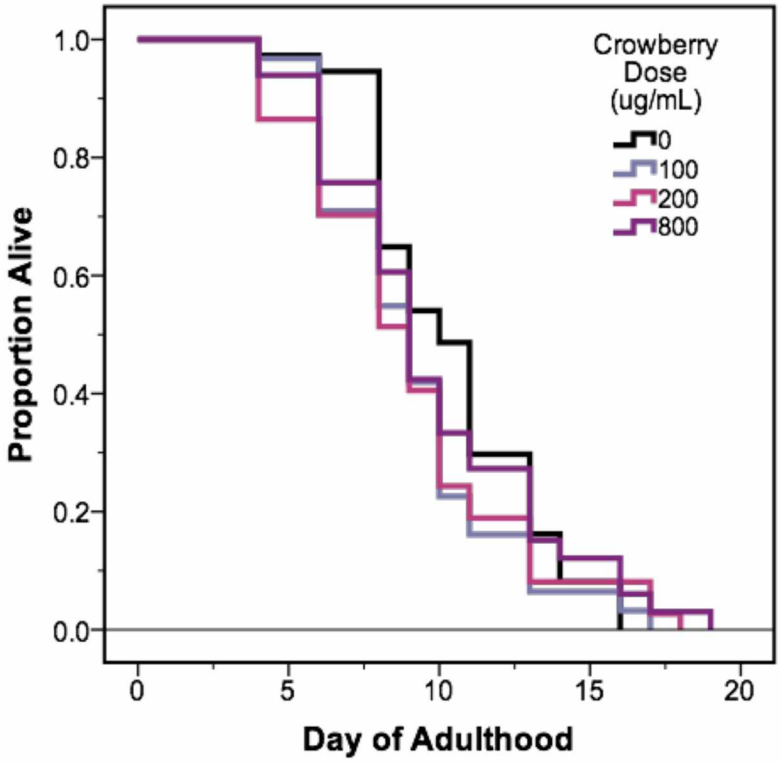

Supplemental Figure 3.1 Crowberry treatment does not affect wildtype *C. elegans* lifespan.

Treatment with 100, 200, and 800µg/mL crowberry mixed into NGM agar did not significantly affect mean or median lifespan at 25°C ($0.13<p<0.78$), Kaplan-Meier log-rank test; 3 replicates). Representative survival curves are shown (N=50 per treatment group).

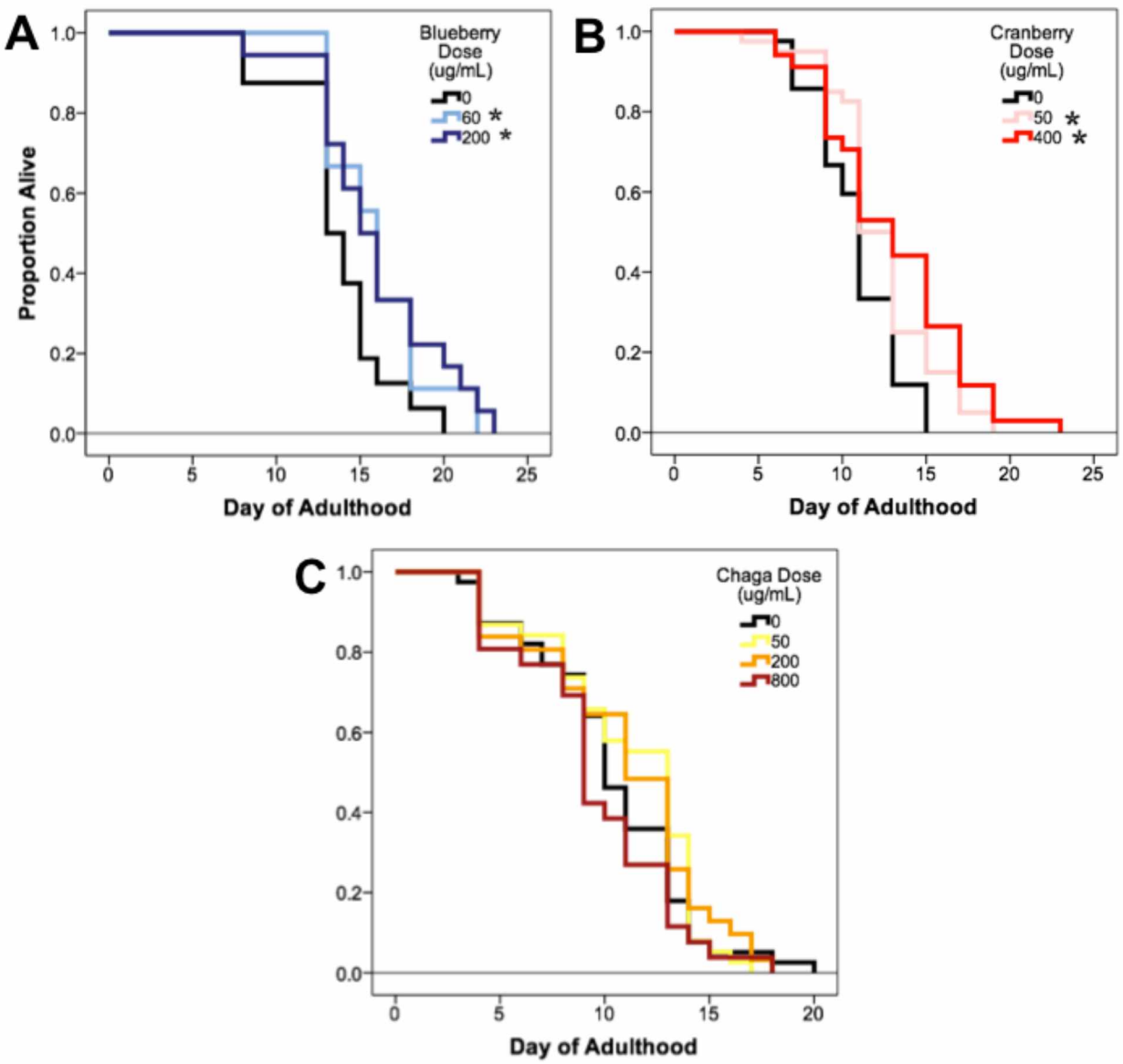

Supplemental Figure 3.2 Blueberry and lowbush cranberry treatments increase wildtype *C. elegans* lifespan even with UV killed bacterial food source.

Mean *C. elegans* lifespan cultured on UV killed bacteria increased from 10.2±0.3 to 11.4±0.6 and 12.3±0.3 days (11.7% and 20.2% increase) upon treatment with 60 and 200µg/mL blueberry, respectively ($p<0.05$, Kaplan Meier log-rank test). 50 and 400µg/mL lowbush cranberry treatment increased lifespan to 12.6±0.5 and 13.2±0.7 days (14.2% and 19.9% increase), respectively, from 11.1±0.3 days in the presence of UV killed bacteria ($p<0.01$, Kaplan Meier log-rank test). Treatment with 50, 200, and 800µg/mL chaga did not significantly alter lifespan in the presence of UV killed bacteria ($p>0.25$, Kaplan Meier log-rank test, 3 replicates). Asterisks represent significance from untreated control ($p<0.05$, Kaplan Meier log-rank test). Representative survival curves are shown (N=50 for each treatment group).

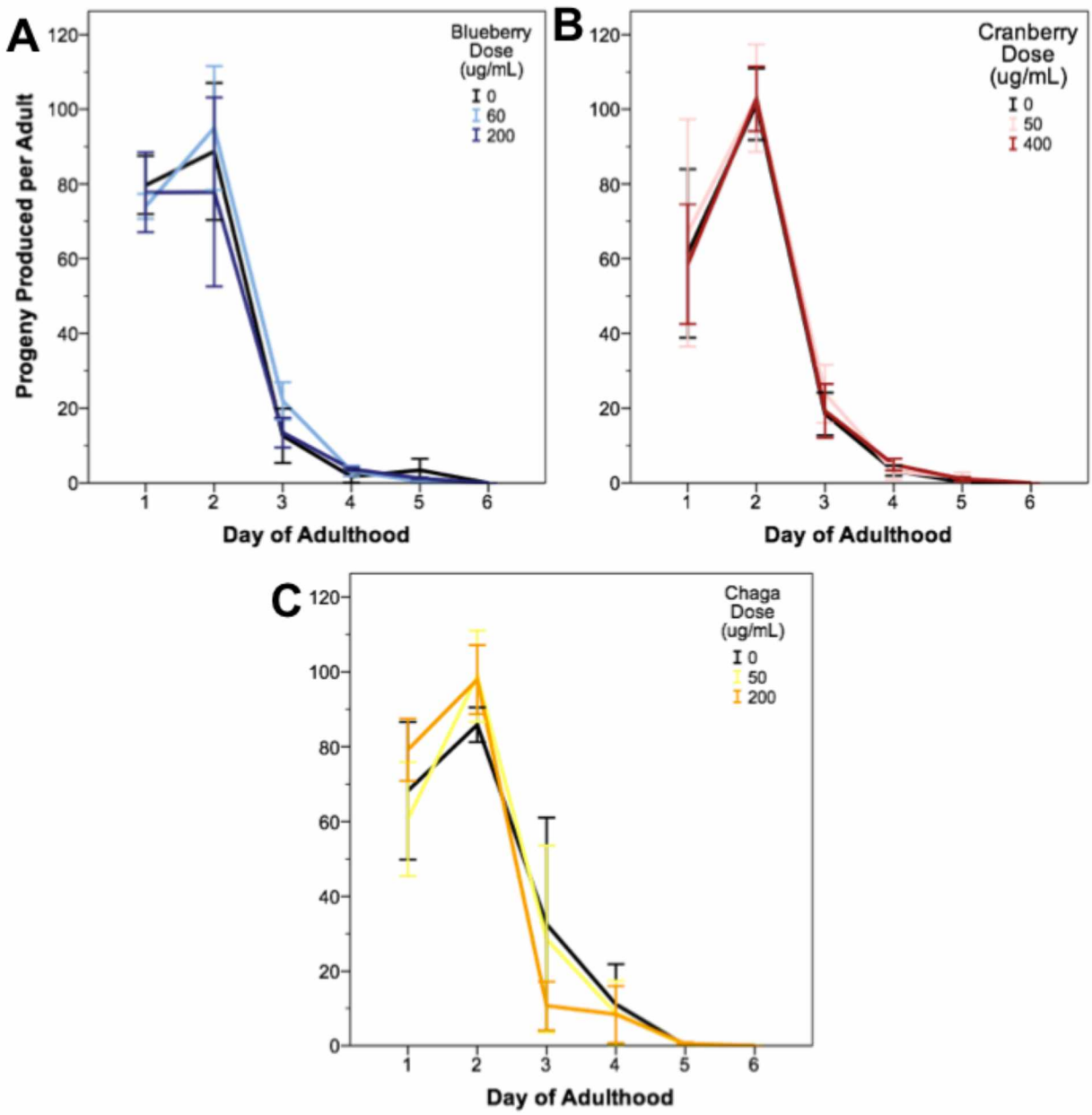

Supplementary Figure 3.3 Lifespan-extending Alaskan berry and fungus treatments alter wildtype *C. elegans* daily progeny production, but not total progeny produced.

Blueberry (A), lowbush cranberry (B), and chaga (C) treatments differentially affected the number of progeny produced per adult per day on days 2, 3, and 1 of adulthood, respectively ($p<0.05$; Poisson log linear model), but did not alter the total number of progeny produced per adult (Table 3.3). Peak progeny production in all groups was observed at day 2 of adulthood (48h after treatment administration) and all animals ceased viable progeny production by day 6 of adulthood.

Table 3.1 Biochemical quantification of crude extracts.

Total phenolic content (quantified by Folin-Ciocalteu assay with gallic acid equivalent), flavonoid content (quantified by NaNO2/Al/NaOH assay with catechin equivalent), and anthocyanin content (quantified by pH-differential with cyanidin-3-glucoside) ± standard error of the mean for each berry and fungus extract is reported.

	Total Phenolic Content (mg GAE g-1 FW)	Flavonoid Content (mg CAE 100g-1 FW)	Anthocyanin Content (mg C3G L-1 FW)
Blueberry	190.4 ± 4.0	202.3 ± 1.4	217.4 ± 5.3
Lowbush cranberry	219.6 ± 6.4	896.2 ± 8.6	158.4 ± 5.3
Chaga	74.9 ± 3.3	125.9 ± 3.1	5.5 ± 2.6
Crowberry	365.3 ± 9.2	453.2 ± 30.1	713.9 ± 45.2

Table 3.2 Alaskan berry and fungus treatments extend wildtype *C. elegans* lifespan.

Percent change in lifespan relative to control, significance from the representative survival curves shown in Figure 3.1A-C. The highest and lowest percent increase in lifespan relative to control in all replicates is also reported. Experiments were repeated in multiple independent trials (≥3), all with the same directional effect and similar magnitude of effect. Statistical significance (p value) calculated with Kaplan-Meier log-rank test.

Treatment	N	Mean Lifespan ± S.E.M.	Percent of Control	*p* value	Highest Increase Observed	Lowest Increase Observed
Blueberry dose (µg/mL)						
0	60	9.48±0.31				
60	66	12.4±0.56	156%	<0.0001	128%	107%
100	60	11.2±0.59	147%	<0.0001	144%	111%
200	51	12.4±0.73	146%	0.001	147%	120%
400	58	11.2±0.58	139%	<0.0001	139%	120%
800	60	9.31±0.28	109%	0.341	117%	109% (n.s.)
Lowbush cranberry dose (µg/mL)						
0	50	11.3±0.58				
50	50	13.9±0.91	122%	0.012	122%	116%
100	51	11.1±0.50	102%	0.868	116%	104% (n.s.)
200	50	12.5±0.49	110%	0.123	119%	106%
400	50	13.9±0.89	122%	0.016	122%	108%
800	50	12.5±0.28	107%	0.229	119%	108% (n.s)
Chaga dose (µg/mL)						
0	50	10.7±0.50				
50	49	13.1±0.60	122%	0.002	122%	113%
200	50	12.9±0.55	121%	0.005	124%	117%
800	47	12.9±0.65	121%	0.003	121%	116%

Table 3.3 Alaskan berry and fungus treatments do not alter total progeny produced by wildtype *C. elegans*.

Experiments were repeated in 3 independent trials each with N=8 parents per treatment group, all with no significant effect observed.

Treatment		**Total Progeny Produced per Adult (Mean ± S.E.M.)**
Blueberry dose (ug/ml)	0	190.7±27.5
	60	198.2±13.9
	200	195.2±38.0
Lowbush cranberry dose (ug/ml)	0	183.4±19.3
	50	201.7±10.2
	400	198.3±7.2
Chaga dose (ug/ml)	0	173.4±7.47
	50	174.9±14.7
	200	188.1±4.6

3.7 References cited

Bansal, A., Zhu, L., Yen, K., and Tissenbaum, H. (2015). Uncoupling lifespan and healthspan in Caenorhabditis elegans longevity mutants. *Proceedings of the National Academy of Sciences* 122, E277–E286.

Bersamin, A., Zidenberg-Cherr, S., Stern, J., and Luick, B. (2007). Nutrient intakes are associated with adherence to a traditional diet among Yup`ik Eskimos living in remote Alaska Native communities: the CANHR Study. *International Journal of Circumpolar Health* 66(1), 62-70.

Braeckman, B.P., Houthoofd, K., De Vreese, A., and Vanfleteren, J.R. (2002). Assaying metabolic activity in ageing Caenorhabditis elegans. *Mechanims of Ageing and Development* 123, 105–119.

Brenner, S. (1974). The genetics of *Caenorhabditis elegans*. *Genetics* 77, 71–94.

Campos, P., Paulsen, B., and Rehen, S. (2014). Accelerating neuronal aging in in vitro model brain disorders: a focus on reactive oxygen species. *Frontiers in Aging Neuroscience 6,* 1-14.

Cui, Y., Kim, D.S., and Park, K.C. (2005). Antioxidant effect of *Inonotus obliquus*. *Journal of Ethnopharmacology* 96, 79–85.

Dinstel, R., Cascio, J., and Koukel, S. (2013). The antioxidant level of Alaska's wild berries: high, higher and highest. *International Journal of Circumpolar Health 72*, e2188

Ebbesson, S., Adler, A., Risica, P., Ebbesson, L., Yeh, J.-L., Go, O., Doolittle, W., Ehlert, G., Swenson, M., and Robbins, D. (2005). Cardiovascular disease and risk factors in three Alaskan Eskimo populations: the Alaska-Siberia project. *International Journal of Circumpolar Health* 64, 365–386.

Elks, C.M., Reed, S.D., Mariappan, N., Shukitt-Hale, B., Joseph, J.A., Ingram, D.K., and Francis, J. (2011). Blueberry-enriched diet attenuates nephropathy in a rat model of hypertension via reduction in oxidative stress. *Public Library of Science One* 6(9), e24028.

Elks, C.M., Francis, J., Stull, A., Cefalu, W., Shukitt-Hale, B., and Ingram, D. (2013). Overview of the Health Properties of Blueberries. Bioactives in Fruit: Health Benefits and Functional Foods. eds. M. Skinner and D. Hunter (John Wiley & Sons), 251–271.

Gems, D. and Partridge, L. (2008). Stress-response hormesis and aging: "That which does not kill us makes us stronger." *Cell Metabolism* 7(3), 200-203.

Giridharan, V., Thandavarayan, R., and Konishi, T. (2011). Amelioration of scopolamine induced cognitive dysfunction and oxidative stress by *Inonotus obliquus* – a medicinal mushroom. *Food and Function 2*, 320–327.

Grace, M.H., Esposito, D., Dunlap, K.L., and Lila, M.A. (2014). Comparative analysis of phenolic content and profile, antioxidant capacity, and anti-inflammatory bioactivity in wild Alaskan and commercial Vaccinium berries. *Journal of Agricultural Food Chemistry*. 62, 4007–4017.

Guha, S., Cao, M., Kane, R., Savino, A., Zou, S., and Dong, Y. (2012). The longevity effect of cranberry extract in Caenorhabditis elegans is modulated by daf-16 and osr-1. *AGE* 35(5), 1559-1574.

Gustafson, S.J., Dunlap, K.L., McGill, C.M., Kuhn, T.B. (2012). A nonpolar blueberry fraction blunts NADPH oxidase activation in neuronal cells exposed to tumer necrosis factor-α. *Oxidative Medicine and Cellular Longevity* 12, 1-12.

Halliwell, B., and Whiteman, M. (2004). Measuring reactive species and oxidative damage in vivo and in cell culture: how should you do it and what do the results mean? *British Journal Pharmacology 142*, 231–255.

Herald, T., Gadgil, P., and Tilley, M. (2012). High‐throughput microplate assays for screening flavonoid content and DPPH‐scavenging activity in sorghum bran and flour. *Journal of the Science of Food and Agriculture*. 92, 2326–2331.

Herndon, L., Schmeissner, P., Dudaronek, J., Brown, P., Listner, K., Sakano, Y., Paupard, M., Hall, D., and Driscoll, M. (2002). Stochastic and genetic factors influence tissue-specific decline in ageing *C. elegans*. *Nature* 419, 808–814.

Howell, A, Kalt, W, Duy, JC, and Forney, CF. (2001). Horticultural factors affecting antioxidant capacity of blueberries and other small fruit. *Horitechnology* 11(4), 523-528.

Howitz, K.T. and Sinclair, D.A. (2008). Xenohormesis: Sensing the chemical cues of other species. *Cell* 133, 387-391.

Iriti, M., Vitalini, S., Fico, G., and Faoro, F. (2010). Neuroprotective herbs and foods from different traditional medicines and diets. *Molecules* 15(5), 3517-3555.

Jafari, M. and Rose, M. (2006). Rules for the use of model organisms in antiaging pharmacology. *Aging Cell* 5, 17–22.

Joseph, J.A., Shukitt-Hale, B., and Denisova, N.A. (1999). Reversals of age-related declines in neuronal signal transduction, cognitive, and motor behavioral deficits with blueberry, spinach, or strawberry dietary supplementation. *Journal of Neuroscience* 19(18), 8114-8121.

Joseph, J., Cole, G., Head, E., and Ingram, D. (2009). Nutrition, brain aging, and neurodegeneration. *Journal of Neuroscience* 29, 12795–12801.

Joseph, S., Edirisinghe, I., and Burton-Freeman, B. (2014). Berries: Anti-inflammatory effects in humans. *Journal of Agricutural and Food Chemistry* 62, 3886–3903.

Kalt, W., Ryan, D., Duy, Prior, R.L., Ehlenfeldt, M.K., and Kloet, S.P.V. (2001). Interspecific variation in anthocyanins, phenolics, and antioxidant capacity among genotypes of highbush and lowbush blueberries (*Vaccinium section cyanococcus spp.*). *Journal of Agricultural and Food Chemistry* 49, 4761-4767.

Kang, J.H., Jang, J.E., Mishra, S.K., Lee, H.J., Nho, C.W., Shin, D., Jin, M., Kim, M.K., Choi, C., and Oh, S.H. (2015). Ergosterol peroxide from chaga mushroom (*Inonotus obliquus*) exhibits anti-cancer activity by down-regulation of the B-catenin pathway in colorectal cancer. *Journal of Ethnopharmacology* 173, 303-312.

Kim, H. and Song, M.J. (2014). Analysis of traditional knowledge for wild edible mushrooms consumed by residents living in Jirisan National Park (Korea). *Journal of Ethnopharmacology* 153, 90–97.

Kregel, K. and Zhang, H. (2007). An integrated view of oxidative stress in aging: basic mechanisms, functional effects, and pathological considerations. *American Journal of Physiology - Regulatory, Integrative and Comparative Physiology* 292, R18–R36.

Krikorian, R., Shidler, M., Nash, T., Kalt, W., Vinqvist-Tymchuk, M., Shukitt-Hale, B., and Joseph, J. (2010). Blueberry supplementation improves memory in older adults. J*ournal of Agricultural and Food Chemistry 58*, 3996–4000.

Lee, I.K.K., Kim, Y.S.S., Jang, Y.W.W., Jung, J.Y.Y., and Yun, B.S.S. (2007). New antioxidant polyphenols from the medicinal mushroom *Inonotus obliquus*. *Bioorganic Medicinal Chemistry Letters* 17, 6678–6681.

Link, C.D., Cypser, J.R., Johnson, C.J. and Johnson, T.E. (1999). Direct observation of stress resonse in *Caenorhabditis elegans* using a reporter transgene. *Biological Sciences and Medicinal Science* 57, B109-B114.

Liu, Z., Schwimer, J., Liu, D., Greenway, F., Anthony, C., and Woltering, E. (2005). Black raspberry extract and fractions contain angiogenesis inhibitors. *Journal of Agricultural and Food Chemistry* 53, 3909–3915.

Lohachoompol, V., Srzednicki, G., and Craske, J. (2004). The change of total anthocyanins in blueberries and their antioxidant effect after drying and freezing. *BioMedical Research International* 2004(5), 248-252.

Lopez-Otin, C., Blasco, M.A., Partridge, L., Serrano, M., and Kroemer, G. (2013). The hallmarks of aging. *Cell* 153, 1194-1217.

Loring, P. and Gerlach, S.C. (2009). Food, culture, and human health in Alaska: an integrative health approach to food security. *Environmental Science and Policy* 12, 466–478.

Miller, M. and Shukitt-Hale, B. (2012). Berry fruit enhances beneficial signaling in the brain. *Journal of Agricultural and Food Chemistry* 60, 5709–5715.

Mohatt, G., Plaetke, R., Klejka, J., Luick, B., Lardon, C., Bersamin, A., Hopkins, S., Dondanville, M., Herron, J., and Boyer, B. (2007). The Center for Alaska Native Health Research Study: a community-based participatory research study of obesity and chronic disease-related protective and risk factors. *International Journal of Circumpolar Health* 66, 8–18.

Ogawa, K., Sakakibara, H., Iwata, R., Ishii, T., Sato, T., Goda, T., Shimoi, K., and Kumazawa, S. (2008). Anthocyanin composition and antioxidant activity of the crowberry (*Empetrum nigrum*) and other berries. *Journal of Agricultural and Food Chemistry* 56, 4457–4462.

Pan, C.L., Peng, C.Y., Chen, C.H., and McIntire, S. (2011). Genetic analysis of age-dependent defects of the *Caenorhabditis elegans* touch receptor neurons. *Proceedings of the National Academy of Sciences of the United States of America* 108, 9274–9279.

Scerbak, C., Vayndorf, E., Parker, A., Neri, C., Driscoll, M., and Taylor, B. (2014). Insulin signaling in the aging of healthy and proteotoxically stressed mechanosensory neurons. *Frontiers in Genetics* 5(12), 1-14.

Schulz, T., Zarse, K., Voigt, A., Urban, N., Birringer, M., and Ristow, M. (2006). Glucose restriction extends *Caenorhabditis elegans* life span by inducing mitochondrial respiration and increasing oxidative stress. *Cell Metabolism* 6(4), 280-293.

Shukitt-Hale, B. (2012). Blueberries and neuronal aging. *Gerontology* 58, 518–523.

Song, B., Sapper, T., Burtch, C., Brimmer, K., Goldschmidt, M., and Ferruzzi, M. (2013). Photo- and thermodegradation of anthocyanins from grape and purple sweet potato in model beverage systems. *Journal of Agricultural and Food Chemistry* 61, 1364–1372.

Spencer, J. (2008). Food for thought: the role of dietary flavonoids in enhancing human memory, learning and neuro-cognitive performance. *Proceedings of the Nutrition Society* 67, 238–252.

Stuart, J., Maddalena, L., Merilovich, M., and Robb, E. (2014). A midlife crisis for the mitochondrial free radical theory of aging. *Longevity and Healthspan* 3(1), 4.

Tank, E., Rodgers, K., and Kenyon, C. (2011). Spontaneous age-related neurite branching in *Caenorhabditis elegans*. *Journal of Neuroscience* 31, 9279–9288.

Toth, M., Melentijevic, I., Shah, L., Bhatia, A., Lu, K., Talwar, A., Naji, H., Ibanez-Ventoso, C., Ghose, P., Jevince, A., Xue, J., Herndon, L.A., Bhanot, G. Rongo, C., Hall, D.H., and Driscoll, M. (2012). Neurite sprouting and synapse deterioration in the aging *Caenorhabditis elegans* nervous system. *Journal of Neuroscience* 32, 8778–8790.

Vayndorf, E.M., Scerbak, C., Hunter, S., Neuswanger, J.R., Toth, M., Parker, A.J., Neri, C., Driscoll, M., and Taylor, B.E. (2016). Morphological remodeling of *C. elegans* neurons during aging is modified by compromised protein homeostasis. *NPJ Aging Mech Dis* 2, 16001.

Whyte, A., Schafer, G., and Williams, C. (2015). Cognitive effects following acute wild blueberry supplementation in 7- to 10-year-old children. *European Journal of Nutrition*, *ePub ahead of print.*

Wiegant, F., Surinova, Ytsma, Langelaar-Makkinje, Wikman, and Post (2008). Plant adaptogens increase lifespan and stress resistance in *C. elegans*. *Biogerontology* 10, 27–42.

Wilson, M.A., Shukitt-Hale, B., Kalt, W., Ingram, D.K., Joseph, J.A., and Wolkow, C.A. (2006). Blueberry polyphenols increase lifespan and thermotolerance in *Caenorhabditis elegans*. *Aging Cell* 5, 59-68.

Wink, M (2003). Evolution of secondary metabolites from an ecological and molecular phylogenetic perspective. *Phytochemistry* 64, 3-19.

Yankner, B., Lu, T., and Loerch, P. (2008). The aging brain. *Annual Review of Pathology* 3, 41–66.

Youl, E., Bardy, G., Magous, R., Cros, G., Sejalon, F., Virsolvy, A., Richard, S., Quignard, J.F., Gross, R., Petit, P., Bataille, D., and Oiry, C. (2010). Quercetin potentiates insulin secretion and protects INS-1 pancreatic β-cells against oxidative damage via the ERK1/2 pathway. *British Journal of Pharmacology* 161, 799–814.

Zafra-Stone, S., Yasmin, T., Bagchi, M., Chatterjee, A., Vinson, J., and Bagchi, D. (2007). Berry anthocyanins as novel antioxidants in human health and disease prevention. *Molecular Nutrition and Food Research* 51, 675–68

Chapter 4

Neuronal Aging in *Caenorhabditis elegans* is Modulated via Distinct Cellular Signaling and Genetic Mechanisms: Insights from Alaskan Berry and Fungal Treatments[1]

4.1 Abstract

We previously described the beneficial effects of three commonly consumed and culturally relevant Interior Alaskan plant and fungus species (bog blueberry, lowbush cranberry, and chaga fungus) on the decline in *Caenorhabditis elegans* overall health, mechanosensation, and touch receptor (mechanosensory) neuron morphology associated with aging. Here, we describe the cellular and molecular mechanisms underlying these health effects. Only lowbush cranberry treatment caused marked activation of the central aging-related transcription factor DAF-16/FOXO. Further, DAF-16 activity is required for the observed lowbush cranberry treatment-mediated lifespan extension and touch receptor neuron functional improvements and morphological changes. We then utilized next generation sequencing to conduct a non-biased comparison of gene expression in control, blueberry-treated, and chaga-treated young adults (day 3), with the goal of testing the involvement of genes differentially regulated early in life in the aging processes of touch receptor neurons. Of the nearly 40,000 transcripts in *C. elegans*, we detected 206 genes with significant changes between control and treatments and between the two treatments. From these 206 genes, we selected 12 genes with known neuron-related functions (e.g. axon guidance, cytoskeleton regulation, metabolism) and tested the impact of these genes on touch receptor neuron morphology and function in aged animals (day 11) using RNA interference. Of the 12 selected candidate genes, 8 (*max-1*, *pck*-1, *stn*-1, ttx-*1*, *tub-1*, unc-*115*, *unc-44*, ZK418.3) have roles in aging touch receptor neurons. These results indicate that

[1] Authorship for this paper is as follows: Courtney Scerbak, Elena Vayndorf, Alicia Hernandez, Colin McGill, and Barbara Taylor. In preparation for submission.

the different touch receptor neuron phenotypes observed with Alaskan nutraceutical treatments reflect distinct cellular and molecular mechanisms. We demonstrate that multiple, novel cellular signaling pathways are involved in aging, specifically touch receptor neuron aberration development. Furthermore, we demonstrate that nutritional interventions may be used to discover and describe novel genes important in the biology of aging.

4.2 Introduction

Aging and nutrient consumption are tightly linked; the cellular signals and gene expression changes following the ingestion of nutrients impact biomarkers of aging. Epidemiological studies consistently show that dietary patterns rich in plant food sources are correlated with increased lifespan, decreased incidence of age-related diseases, or both (reviewed in Fleming et al., 2013). In model organisms, such as worms, flies, and rodents, many nutrients are studied for their impact on various biomarkers of aging (examples reviewed in Spencer, 2008; Zafra-Stone et al., 2007; Liu, 2004; Vayndorf et al., 2013). Alaskan traditional knowledge holds that a diverse collection of local plants and fungi benefit health and wellness (Garabaldi, 1999; Kari, 1995). Additionally, Alaskan plant and fungus species have adapted to extreme environments, in part by producing a wide variety of secondary metabolites (Elks et al., 2013), indicating that the molecular action of these food sources may provide novel insights into the aging process.

High-thoroughput RNA sequencing (RNAseq) is a widely applicable, non-biased technique used to sequence, align, and quantify gene expression levels using RNA sequences isolated from a biological sample. This non-biased approach also allows for the detection of candidate genes for specific functional studies that might otherwise not be selected. RNAseq has been used to further our understanding of molecular biology and genetics in a variety of complex biological scenarios: uncovering the heterogeneity of cancerous tumors (Patel et al., 2014); describing developmental differences in *Caenorhabditis elegans* gene expression (Li et

al., 2014; Spencer et al., 2011); and discovering cell specific gene expression networks regulated by transcription factors, such as DAF-16/FOXO in *C. elegans* (Kaletsky et al., 2016). RNAseq is a descriptive approach to discerning complex treatment effects at the molecular level.

In both humans and the model organism, *C. elegans,* neurons are known to change shape and function with age (rather than dying), which, due to the communication and integration function of the nervous system, impacts aging of the entire organism. One class of *C. elegans* neurons known to change shape and function with age are the mechanosensory or touch receptor neurons, which sense soft touch. These neurons develop novel outgrowths from the soma, additional branching on the axon/dentrites, and abnormal soma shapes with age (Toth et al., 2012; Pan et al., 2011; Tank et al., 2011). The age-related development of these morphologies are regulated, in part, by two signaling pathways central to the regulation of lifespan and healthspan: the insulin/IGF and Jun kinase pathways (Scerbak et al., 2014; Toth et al., 2012; Pan et al., 2011; Tank et al., 2011). However, the cellular mechanisms by which these pathways (and likely others) regulate aging-related changes in the morphology of touch receptor neurons have yet to be fully described.

We previously described the beneficial effects of commonly consumed and culturally relevant Interior Alaskan plant and fungus species (bog blueberry, lowbush cranberry and chaga fungus) on the decline in overall health, neuronal function, and touch receptor neuron morphology associated with aging. Here, we tested the involvement of the central aging-related transcription factor in the insulin signaling pathway, DAF-16/FOXO, in the development of the observed effects (e.g. lifespan, aging neuron morphologies). We also performed RNAseq on young adult *C. elegans* treated with lifespan-extending doses of Alaskan blueberry (*Vaccinium uliginosum*) and chaga (*Inonotus obliquus*) extracts to inform subsequent genetic screens of aging neuron morphology and function. Through the RNAseq results, we uncovered previously undescribed candidate neuron morphology modulators. Our findings support the growing

evidence that *C. elegans* touch receptor neuron aging is regulated via multiple mechanisms, including well-studied (e.g. insulin/IGF signaling) and novel pathways.

4.3 Materials and methods

4.3.1 *C. elegans* strains and maintenance

The *C. elegans* strains N2 (Bristol wildtype), TJ356 (DAF-16::GFP (zIs356 IV [*daf-16*p::*daf-16*a/b::GFP + *rol-6*])), OG497 (HSF-1::GFP (drSi13 II [*hsf-1*p::*hsf-1*::GFP::*unc-54* 3'UTR + Cbr-*unc-119*(+)]; *unc-119*(ed3) III)), GR1307 (*daf-16(mgdf50)),* ZB154 (zdIs5 [P*mec-*4GFP*; lin-15(+)*]), and ZB4064 (*zdIs5* [$P_{mec\text{-}4}$*GFP; lin-15(+)*]; *uIs57* [$P_{unc\text{-}119}$*SID-1*, $P_{unc\text{-}119}$*YFP*, $P_{mec\text{-}6}$*mec-6*]) were used in this study. Both ZB154 and ZB4064 exhibit GFP-labeled touch receptor neurons (Toth et al., 2012), and ZB4064 overexpresses the SID-1 transmembrane channel in all neurons (Calixto et al., 2010), rendering neurons susceptible to RNA interference treatment.

We used standard methods to maintain and manipulate *C. elegans* populations (Brenner, 1974). Stock populations were cultured at room temperature (about 22ºC) on Nematode Growth Media agar plates (1L NGM: 2.5g peptone, 17g agar, 3g NaCl, 975mL double distilled water, 1mL 5mg/mL Cholesterol, 1mL 1M $CaCl_2$, 1mL 1M $MgSO_4$, 25mL 1M $KHPO_4$, and 0.5mL 100mg/mL streptomycin) seeded with live bacteria (*E. coli* strain OP50-1 cultured in Luria Broth) that was allowed to form a lawn for 2 days at room temperature and then stored at 4°C until use.

4.3.2 Berry and fungus extract preparation and treatment administration

The Alaskan blueberry and chaga extract preparation and treatment administration herein are the same as described in Chapter 3. Briefly, extracts of wild Alaskan specimens of blueberry (*Vaccinium uliginosum)* and chaga *(Inonotus obliquus*) were prepared with 80% aqueous acetone and rotaevaporation (blueberry) or boiling water and straining (chaga).

Freeze thaw cycles were limited to one (thawed from -80°C then aliquoted and frozen at -20°C until use) to ensure maximal preservation of bioactive components. To administer berry and fungus treatments to *C. elegans* populations, we cultured synchronous, day 1 adult populations of the appropriate strain on NGM agar plates mixed with the appropriate concentration of extract and seeded with live OP50-1 *E. coli* at 25°C. Control populations were cultured on standard NGM plates without extract. For experiments involving aged populations, animals were hand transferred to fresh treatment plates to maintain synchrony and to avoid starvation and crowding.

4.3.3 Transcription factor activation assays

To visualize the activation of transcription factors, we utilized two previously described *C. elegans* strains: TJ356 (DAF-16::GFP; Henderson and Johnson, 2001) and OG497 (HSF-1::GFP; Morton and Lamitina, 2013). Synchronous populations were allowed to develop on NGM plates for 72h at 20°C and cultured on appropriate treatment plates until imaging (days 3 and 9 of adulthood). For animals expressing DAF-16::GFP, we imaged at 10x magnification to visualize the entire animal. Positive controls were heat shocked for 30min at 37°C on agar plates and imaged immediately thereafter. Each DAF-16::GFP animal was classified into 3 groups based on the nuclear foci observed: nuclear animals had foci seen throughout the animal with very little diffuse fluorescence (Figure 4.1C and 4.1D), and intermediate animals had at least three distinct DAF-16::GFP foci with mostly diffuse fluorescence (Figures 4.1E and 4.1G) (Oh et al., 2005). For animals expressing HSF-1::GFP, only 5 individuals were prepared for imaging at once, the epithelial cell layer in the bottom third of each animal was imaged at 40x and positive controls were heat shocked for 30min at 35°C after preparing for imaging. To detect treatment effects, we used an ordinal logistic statistics model.

4.3.4 RNA extraction and sample preparation

We collected total RNA from large, synchronous populations of day 3 adult *C. elegans* (2-3 100x20mm plates; ≥600 individuals) initiated via bleaching (i.e. isolation of embryos from healthy adults using a 5M NaOH and Chlorox 5% sodium hypochlorite solution and vortexing) and cultured 48h with 200µg/mL Alaskan blueberry extract, 200µg/mL Alaskan chaga extract, or no treatment. On the designated day, each adult population was isolated from their progeny by washing through a 50µm filter with M9 (autoclaved 3g KH_2PO_4, 5g NaCl, 6g $Na_2HPO_4*7H_2O$ and sterile 1mL 1M $MgSO_4$ in 1L H_2O) and allowed to settle by gravity and form a pellet before proceeding (≤2 min). The pellet was then pipetted into a ceramic pestle pre-chilled with liquid nitrogen, immediately crushed with a mortar to a fine powder, transferred to RNAase free 2mL eppendorf tubes (filling up to 1.3mL), and placed on ice. Liquid nitrogen was added to the pestle as needed to keep the sample frozen. After all populations had been crushed and frozen, we proceeded with the RNA Purification step of the PureLink RNA Mini Kit (Ambion; catalog number 12183025), which involves binding, washing, and elution of the RNA. We then aliquoted 2µL of each sample for prompt quality control analysis and immediately froze (-80°C) two 10µL aliquots of the remaining sample. Only samples determined to have a concentration ≥25µg/µL, RNA integrity value ≥7.0, and A260/A280 ratio ≥1.6 using a NanoDrop ND-1000 Spectrophotometer and Aligent 2100 Bioanalyzer were sequenced. This extraction procedure was repeated in three independent trials, each with all three treatments (i.e. control, blueberry, chaga) prepared and cultured in parallel.

4.3.5 RNA sequencing and analysis

RNA samples were sent to Expression Analysis (EA; Durham, NC) for sequencing and analysis. EA created the library and performed 50bp paired end sequencing using an Illumina next generation sequencing platform. Specifically, total RNA samples were converted into cDNA libraries using the TruSeq Stranded mRNA Sample Prep Kit (Illumina, #RS-122-2103). Starting

with 100ng of total RNA, polyadenylated RNA (primarily mRNA) was selected and purified using oligo-dT conjugated magnetic beads. This mRNA was chemically fragmented and converted into single-stranded cDNA using reverse transcriptase and random hexamer primers, with the addition of Actinomycin-D to suppress DNA-dependent synthesis of the second strand. Double-stranded cDNA was created by removing the RNA template and synthesizing the second strand in the presence of dUTP in place of dTTP. A single A base was added to the 3' end to facilitate ligation of sequencing adapters, which contain a single T base overhang. Adapter-ligated cDNA was amplified by polymerase chain reaction to increase the amount of sequence-ready library. Final cDNA libraries were analyzed for size distribution and using an Agilent Bioanalyzer (DNA 1000 kit, Agilent # 5067-1504), quantitated by qPCR (KAPA Library Quant Kit, KAPA Biosystems # KK4824), then normalized to 2 nM in preparation for sequencing.

17.4-28.8 million reads were generated per sample and were aligned to the *C. elegans* genome (Ensemble Caenorhabditis_elegans version 80). These reads were the processed and analyzed using the EA RNA analysis pipeline, version 9. Pairs of treatment groups (e.g. control vs. blueberry or chaga vs. blueberry) were then compared to determine differential expression by calculating fold change, unadjusted p-value, and false discovery rate (Supplementary Tables 4.1-4.3). Detected transcripts (≥5 counts in at least one group) with an FDR of ≤0.30 and unadjusted *p* value ≤0.01 were considered significantly impacted by treatment (Supplemental Table 4.4). Gene ontology analysis was performed on significantly impacted transcripts with the publically available DAVID Bioinformatics Resources (version 6.7; Huang et al., 2009).

4.3.6 RNA interference treatment

To administer RNA interference (RNAi) treatment, we cultured age-synchronous populations of *C. elegans* on RNAi agar plates (2.5g peptone, 17g agar, 3g NaCl, 1mL 5mg/mL cholesterol, 1mL 1M $CaCl_2$, 1mL 1M $MgSO_4$, 25mL 1M $KHPO_4$, 1mL 1M isopropyl beta-D-1-thiogalactopyranoside [IPTG], and 0.5mL 50mg/mL carbenicillin per 1L) seeded with 4x

concentrated L4440 (empty vector) HT115 *E. coli* protected from light at 25°C. All animals began RNAi (and berry or fungus treatment, if required) after normal development - 48h after egg lay at 25°C. All subsequent treatment and control plates consisted of RNAi plates mixed with varying concentrations of the appropriate extract as described above, seeded with 4x concentrated live HT115 bacteria from the Ahringer Library. Bacterial dsRNA production was induced by growing the HT115 bacterial lawn at room temperature (~22°C) for two days, allowing us to target the desired *C. elegans* mRNA for degradation. The experimenter was always blinded to the RNAi and extract treatment regimens until statistical analysis. To verify the RNAi treatment conditions for each experiment, we performed control experiments measuring fluorescence knockdown following GFP RNAi treatment (Supplemental Figure 4.2). RNAi clone identity was verified by sequencing (Macrogen Corp.; primer M13F) after plasmid extraction (QIA Spin Miniprep Kit; Qiagen; cat num 27104).

4.3.7 Touch receptor neuron morphology and touch response analysis

On day 11 of adulthood (10 days after beginning RNAi/extract treatment), ZB4064 individuals were randomly selected from a synchronous population and tested for motility, touch sensitivity, and touch receptor neuron aberrations. We assigned individuals into three classes based on their motility: Class A individuals moved normally and spontaneously; Class B individuals moved in markedly non-sinusoidal manner and, often, non-spontaneously; and Class C individuals were alive but unable to translocate (Herndon et al., 2002). We measured soft touch sensitivity by counting the number of positive responses an individual had to five alternating touches at each the anterior and posterior (10 total touches; Toth et al., 2012). Finally, to visualize the fluorescently labeled touch receptor neurons, we mounted individuals to a coverslip with 36% Pluronic solution and imaged the neurons with an Olympus FSX100 inverted fluorescent microscope at 20x magnification. We quantified the occurrence of abnormal morphologies in the anterior and posterior lateral touch receptor neurons (ALM and PLM) of

each individual and collected reference images. The neuron morphologies observed included those previously described (Scerbak et al., 2014; Toth et al., 2012; Pan et al., 2011; Tank et al., 2011), such as various lengths of outgrowths from the soma (e.g. short or extended), branches from the process, abnormally shaped soma, punctae on the process, and soma in the wrong location. Additional morphologies were also observed and included branches from the process that connect back to the process (i.e. loops) and deformed process sections (i.e. tangles). We performed Poisson log linear (for count data, i.e. touch response) or logistic regression (for bimodal data, i.e. presence of abnormal cell soma) statistical models to test for treatment and age effects on touch sensitivity and neuron morphologies using SPSS (version 20) statistical software. Pairwise comparisons with $p \leq 0.05$ were considered significant. We repeated this experiment in at least three independent trials for each combination of RNAi and extract treatment, each with a parallel empty vector L4440 no treatment control.

4.4 Results

4.4.1 Alaskan lowbush cranberry activates DAF-16/FOXO late in life

The well-studied DAF-16/FOXO and HSF-1 transcription factors are involved in longevity and stress response (reviewed in Hsu et al., 2003). Because of this, we tested the involvement of these central transcription factors in the Alaskan berry- and fungus-mediated effects we previously observed, namely lifespan extension and aging touch receptor neuron morphological and functional changes. *C. elegans* strains with GFP-tagged DAF-16 (strain TJ356) or HSF-1 (strain OG497) are available to visualize activation of these transcription factors in response to stress (Morton and Lamitina, 2013; Henderson and Johnson, 2001). In the DAF-16::GFP animals, DAF-16 can be visualized in the nuclei of cells as distinct foci in response to stressors, such as heat shock (Figures 4.1C and 4.1D). After 48 hours of treatment with lifespan-extending Alaskan berry and fungus treatments (day 3 of adulthood), we did not detect activation of DAF-16 into nuclear foci with any treatment (Supplemental Figure 4.1). However, at

day 9 of adulthood (after 8 days of treatment), we observed formation of DAF-16 nuclear foci in both lifespan-extending lowbush cranberry treatments (Figure 4.1; Table 4.1). Blueberry and chaga treatments did not lead to detectable DAF-16 nuclear foci early (Supplemental Figure 4.1) or late in life (data not shown).

In the HSF-1::GFP strain, HSF-1 is observed in nuclei under normal conditions and upon exposure to stress, forms distinct granules within nuclei, representing HSF-1 binding to DNA (Morton and Lamitina, 2013). We were unable to detect formation of HSF-1::GFP granules within nuclei following 48 hours of any lifespan-extending Alaskan berry and fungus treatment (Supplemental Figure 4.1). Interestingly, HSF-1::GFP animals had granules in all groups (including untreated control) later in adulthood (day 9), making it unfeasible for this method to determine whether HSF-1 is activated later in life due to Alaskan berry and fungus treatments.

4.4.2 Alaskan lowbush cranberry modulates DAF-16 to extend lifespan and influences touch receptor neuron aging

To examine whether the DAF-16::GFP nuclear foci observed after lowbush cranberry treatment reflect a requirement for functional DAF-16 in lowbush cranberry-mediated lifespan extension, we treated *C. elegans* DAF-16 mutant populations (strain GR1307; *daf-16(mgdf50)*; Ogg et al., 1997) with lowbush cranberry doses that extended wildtype lifespan (shown in Chapter 2 for the doses of 50 and 400µg/mL). These DAF-16 mutants did not respond with increased lifespan to lowbush cranberry treatment, which suggests that the requirement of a functional DAF-16/FOXO transcription factor is needed for lifespan extension via lowbush cranberry treatment (Figure 4.2A; Table 4.2).

In young adults, the two posterior lateral (PLM) and two anterior lateral (ALM) touch receptor neurons consist of a spherical cell soma with axon projections towards the head of the animal. With age, these neurons exhibit decreased function (i.e. touch response) and altered morphology; ALM neurons develop additional outgrowths from the soma and abnormal (non-

spherical) cell soma and PLM neurons develop addition growths on the axon (i.e. branches; Toth et al., 2012; Pan et al., 2011; Tank et al., 2011). We previously reported that lifespan-extending lowbush cranberry treatment increased the incidence of axon branching in posterior touch receptor neurons and improved touch response late in life. Thus, we also evaluated the involvement of DAF-16 in these lowbush cranberry-mediated touch receptor neuron aging effects. To do this, we compared the effects of lowbush cranberry, *daf-16*(RNAi), and lowbush cranberry-*daf-16*(RNAi) combination treatments on touch receptor neuron morphology and touch response in old (day 11) ZB154 animals (6 GFP-labeled touch receptor neurons). These experiments specifically tested the involvement of non-neuronal DAF-16 in the observed lowbush cranberry-induced increase in posterior cell branching events (as wildtype *C. elegans* neurons are not susceptible to RNAi; Calixto et al., 2010). We observed that *daf-16*(RNAi) completely blocked the observed increase in posterior touch response with empty vector lowbush cranberry treatments (p>0.8; Poisson log linear model; Figure 4.2B). *daf-16(*RNAi) and resulted in the same occurrence of posterior neuron process branching events as untreated empty vector control animals (p>0.1 Poisson log linear model; Figure 4.2C). Also, *daf-16*(RNAi) untreated and lowbush cranberry treated groups were not significantly different from untreated empty vector control in anterior touch response and most anterior neuron aberrations (p>0.1, Poisson log linear model). DAF-16 treatment did somewhat increase the number of anterior soma outgrowths observed at day 11 in all lowbush cranberry treatment groups; however, the change did not reach significance (111% of empty vector controls; 0.09>p>0.06 Poisson log linear model), suggesting that DAF-16 may be involved in the development of these aberrations through a mechanism not impacted by lowbush cranberry treatment (Figure 4.2D).

Others have observed that blueberry polyphenol-mediated lifespan extension does not require DAF-16 (Wilson et al., 2006). To test whether this is also the case with Alaskan blueberry treatments, we measured the lifespan of DAF-16 mutants (strain GR1307; *daf-16(mgdf50)*) with lifespan-extending blueberry treatments (60 and 200µg/mL). DAF-16 mutants

maintained blueberry-mediated lifespan extension similar to that of wildtype (p<0.05; Kaplan Meier log-rank test; Table 4.5), indicating that DAF-16 is most likely not required for lifespan extension from blueberry treatment. Interestingly, chaga-mediated lifespan extension did require DAF-16 (Table 4.2), but we were unable to detect DAF-16 activation in live animals early or late in life (Supplemental Figure 4.1).

4.4.3 Alaskan blueberry and chaga treatments differentially impact the transcriptome

To further describe the molecular role Alaskan blueberry and chaga treatments play in the aging process, we used whole animal RNA sequencing to quantify differential transcript expression following treatment with lifespan-extending Alaskan extracts. Specifically, we collected total RNA from three independent biological replicates of young adult *C. elegans* populations each treated with 200µg/mL blueberry extract, 200µg/mL chaga extract, or nothing (control) for 48 hours. We obtained 17.4-29.1 million reads per sample with 32.1-37.9% and 98.9-99.2% of those reads mapping to the current definition of the *C. elegans* transcriptome and genome, respectively, (Table 4.3).

We performed two separate pairwise statistical analyses to compare the transcriptome of control versus treatment (i.e. blueberry or chaga treated) populations (Figure 4.3A and 4.3B). The blueberry treatment induced small changes in the transcriptome when compared to control: 11 transcripts were significantly up-regulated and 6 were significantly down-regulated (FDR<0.3 and unadjusted p<0.0001; Figure 4.3A; Supplementary Table 4.1). Treatment with chaga resulted in the up-regulation of 86 transcripts and the down-regulation of 22 transcripts (FDR<0.3 and unadjusted p<0.001; Figure 4.3B; Supplementary Table 4.2). We then compared the transcripts significantly impacted by either blueberry or chaga treatment and found that only 5 transcripts were up-regulated in both treatments and there was no overlap in the down-regulated genes of either treatment (Figure 4.3C and 4.3D). To examine the molecular and biological function of transcripts regulated by each treatment, we used the gene ontology (GO;

gene function/description) functional annotation tool in the DAVID Bioinformatics Resources program (Huang et al., 2009). Blueberry treatment again impacted a small number of gene ontology terms, related to cellular membranes but with little to no functional descriptions (Figure 4.1E; blue bars). Of the transcripts significantly impacted by blueberry treatment, only 29% (5 of 17 transcripts) have a known or predicted GO molecular function and only 41% (7 of 17 transcripts) have a known or predicted GO biological function (PANTHER analysis; Huaiyu et al., 2013). Chaga treatment not only similarly impacted the same membrane GO terms as blueberry but also exhibited enriched (i.e. statistically overrepresented) GO terms in sensory perception of chemical stimulus, receptor activity, and molecular transducer activity (Figure 4.3E; orange bars). A high proportion of the transcripts regulated by chaga treatment had known functions: 60% (64 of 106 transcripts) had a known or predicted GO molecular function and 98% (104 of 106 transcripts) had known or predicted GO biological function (PANTHER analysis; Huaiyu et al., 2013).

To further compare the effects of Alaskan blueberry and chaga treatments on the transcriptome, we performed an additional pairwise statistical analysis to compare the transcriptomes of chaga-treated populations relative to blueberry-treated populations (Figure 4.4A; Supplemental Table 4.3). This comparison yielded 133 up-regulated and 22 down-regulated transcripts, relative to blueberry expression levels (FDR<0.3 and unadjusted p<0.001; Supplemental Table 4.3). A large number of GO terms were enriched in this comparison (N=65), many of which fall into DAVID functional annotation clusters, which group GO terms based on the genes that are shared between them (Figure 4.4B and 4.4C). Enriched GO terms in this comparison again included membrane, sensory perception, and molecular transducer activity terms. Additional signaling (e.g. cell communication and zinc finger domain) and behavior (e.g. locomotion and response to nutrients) GO terms were enriched in this chaga-versus blueberry-treated population comparison that were not uncovered in the comparisons with control groups. DAVID functional annotation clustering highlights important GO annotation

groups by their overrepresentation in a gene list (i.e. transcripts significantly impacted in the chaga- versus blueberry-treatment comparison), allowing the GO terms to be explored in groups (Huang et al., 2009). This analysis revealed several neuron-related, enriched clusters of GO terms: behavior and response to stimuli (10 GO terms; Cluster 2; purple bars) and neuron development and morphology (13 GO terms; Cluster 6; orange bars; Figure 4.4B and 4.4C).

4.4.4 Cytoskeleton- and metabolism-mediating candidate genes impact aging touch receptor neuron morphology and function

To relate gene expression changes early in life with aging touch receptor neuron morphology and function, we selected significantly impacted candidate genes from all three comparisons with enriched DAVID functional annotation clusters expressed in neurons and with homlogy to human genes (Supplemental Table 4.4). Genes selected included those known to be involved in neurotransmission, actin-binding processes, neuron differentiation and morphogenesis, and behavioral responses to stimuli (Table 4.4). To examine the effects of these genes on touch receptor neuron aging, we knocked down neuronal expression of the candidate genes after normal development with RNAi and examined neuronal aging phenotypes late in life (day 11) in ZB4064 animals (with GFP-labeled touch receptor neurons and neurons susceptible to RNAi treatment).

We previously demonstrated that lifespan- and healthspan-extending Alaskan nutraceutical treatments differentially impact touch receptor neuron morphology with age and our control treatments in this study replicate those results (even under RNAi treatment conditions: RNAi plates, HT115 *E. coli*, different *C. elegans* strain, ZB154*)*. Briefly, blueberry treatment decreases the occurrence of anterior neuron extended soma outgrowths (≥2x soma diameter; 44±0.1% versus 41±0.1% occurrence; $p<0.05$; binary logistic model; data not shown) and abnormal anterior cell somas (non-spherical shape; Figure 4.7D; second bar), which is again reflected in these data. Chaga treatment resulted in decreased occurrence of extended

soma outgrowth on anterior neurons (44±0.1% versus 19±0.1% occurrence; $p<0.05$; binary logistic model; data not shown) and increased process branching in posterior neurons (Figure 4.7B; third bar).

Only one gene significantly impacted by blueberry treatment had both a known or predicted function homologous to humans and RNAi clones available through the Ahringer library (ZK418.3; Table 4.4; Figure 4.5). This neuron-specific knockdown not only increased the proportion of mobile (Class A) relative to immobile (Class C) aged animals (day 11) when compared to no treatment control ($p<0.05$ ordinal logistic model; Figure 4.5A), it also specifically increased the accumulation of posterior touch receptor neuron aberrant morphologies, namely process branching ($p<0.01$ binary logistic model; Figure 4.5B) and loop events ($p<0.05$ binary logistic model; Figure 4.5C). The anterior touch response of ZK418.3(*RNAi)* animals was also increased over control levels, to the same extent as blueberry treatment (2.2±0.01 versus 2.6±0.1; <0.05 Poisson log-linear model; data not shown). Posterior touch response ($p>0.05$ Poisson log-linear model) and anterior neuron morphology ($p>0.05$ binary logistic model for all observed morphologies) of these animals were unaffected (data not shown).

We selected two candidate neuron morphology modulators from genes significantly impacted by chaga treatment: *nhr-35* and *pck-1* (Table 4.4; Figure 4.6). Neuronal knockdown of both genes improved motility of old (day 11) treated animals to equal that of chaga-treatment levels ($p<0.05$ ordinal logistic model; Figure 4.6A). However, only *pck-1*(RNAi) resulted in increased posterior neuron branching events when compared to control levels ($p<0.01$ binary logistic model; Figure 4.6B). These RNAi treatments did not impact any other tested phenotypes, including anterior and posterior touch response ($p>0.05$ Poisson log-linear model) and anterior neuron morphology ($p>0.05$ binary logistic model for all observed morphologies; data not shown).

We selected 9 genes for follow-up from the blueberry versus chaga treatment comparison (Figure 4.4): F44A2.5, *max-1, snt-1, stn-1, ttx-3, tub-1, unc-115, unc-2,* and *unc-44*

(Table 4.4; Figure 4.7). Motility and soft touch response were impacted by these RNAi treatments, but their effects (improvement versus regression) did not directly correlate with the neuron morphologies observed. 5 of the 9 neuronal RNAi treatments resulted in improved motility late in life (day 11), either similar to lifespan-extending blueberry (*ttx-3*) or chaga (*snt-1, stn-1, tub-1, unc-44*) treatments (Figure 4.7A). Anterior touch response was increased over control (2.1±0.1) in 6 treatments in a highly significant (*stn-1* [2.7±0.1]; $p<0.01$; Poisson log linear model) or significant manner (*max-1* [2.5±0.1], *snt-1* [2.5±0.1], *ttx-3* [2.5±0.1], *tub-1* [2.4±0.1], *unc-115* [2.5±0.1]; $p<0.05$; Poisson log linear model; data not shown). No treatments significantly improved posterior touch response ($p>0.05$; Poisson log linear model), but *max-1* treatment did significantly decrease posterior touch response relative to control (0.8±0.1 versus 0.5±0.1; $p<0.05$; Poisson log linear model; data not shown).

Although all 9 genes were upregulated with chaga treatment (compared to blueberry treatment), neuronal RNAi knockdown resulted in wide ranging effects on touch receptor neuron morphology. Many RNAi treatments increased the occurrence of posterior touch receptor neuron process branching to a similar extent as blueberry and chaga treatments (*ttx-3, tub-1, unc-115*) and to even statistically higher levels (*max-1, stn-1, unc-44*; $p<0.05$; binary logistic model; Figure 4.7B). Only *stn-1*(RNAi) increased the occurrence of anterior neuron soma outgrowths (between 1x and 2x soma diameter; $p<0.05$; binary logistic model) and only *tub-1*(RNAi) decreased soma outgrowths ($p<0.01$; binary logistic model; Figure 4.7C). No RNAi treatments significantly decreased the occurrence abnormal cell soma ($p>0.05$; binary logistic model; Figure 4.7E). However, two RNAi treatments (*ttx-3, unc-44*) resulted in drastically increased occurrence of abnormal cell somas ($p<0.05$; binary logistic model; Figure 4.7D). There is no direct correlation between occurrence of types of aberrations and touch response (e.g. improved touch response/motility is correlated with both increased and decreased incidence of anterior soma outgrowths), further supporting the idea that neuron morphologies have different biological consequences.

Only 4 candidate genes (F44A2.5, *snt-1, unc*-2; *nhr-35*) had no effect on touch receptor neuron morphology. F44A2.5 and *unc-2* RNAi treatments also had no effect on motility and touch response. However, *snt-1*(RNAi) induced a highly significant improvement in anterior touch response in old adults (2.1±0.1 versus 2.5±0.1; $p<0.01$; Poisson log linear model) and *nhr-35*(RNAi) improved motility of old adults relative to control (Figure 4.6A), suggesting that these genes may play other roles in aging touch receptor neurons.

4.5 Discussion

Through the application of transcriptional activity screening tools and a non-biased approach to uncovering cellular transcriptional activity (i.e. RNAseq), we uncovered (1) a specific mechanism for lowbush cranberry treatment effects (i.e. DAF-16/FOXO activation) and (2) novel genes involved in the development of age-related touch receptor neuron aberrations. After observing DAF-16 nuclear foci in aged (day 9) lowbush cranberry-treated populations, we examined lifespan and touch receptor neuron aging following DAF-16 knockdown with RNA interference (RNAi). We demonstrated that DAF-16 is required both for the lifespan extension and the increased posterior touch receptor neuron (PLM) branching caused by lowbush cranberry treatments (Figure 4.2). To examine cellular processes impacted by blueberry and chaga treatments with a non-biased experimental design, we measured changes in whole organism gene expression using RNAseq. Interestingly, chaga induced differential expression of a group of well-described transcripts (60-98% known or predicted GO functions), while blueberry treatment affected less understood transcripts (29-41% predicted GO functions; Figure 4.3). Whole organism transcriptome changes in young adults treated with lifespan-extending blueberry and chaga extracts are more different from each other than either is from the control transcriptome (Figures 4.3 and 4.4), supporting our original hypothesis that the two extracts exert their effects through distinct mechanisms. Also, the comparison of chaga- versus blueberry-treated transcriptomes resulted in more descriptive gene ontology enrichment than

either treatment versus control comparison and in enriched gene ontology terms particularly relevant to neuron development, maintenance, and aging, despite analyzing whole organism (versus neuron-specific) transcriptomes (Figure 4.2B). We then tested the hypothesis that candidate genes impacted by blueberry and/or chaga treatment early in life regulate aging touch receptor morphology and function, uncovering a role for several novel genes in touch receptor neuron aging with potential implications in the aging of the human nervous system (Figures 4.5-4.8 and Table 4.5).

The size and distribution of DAF-16::GFP foci observed (Figure 4.1) and the results of the systemic (vs. neuron-specific) DAF-16 RNAi experiments (Figure 4.2) suggest that, at least in part, a non-neuron specific pathway induces posterior neuron process branching. DAF-16, orthologous to human FOXO, is well known to operate in multiple tissues downstream of various cellular signaling pathways (e.g. insulin signaling) regulating the expression of genes that promote longevity, proteostasis, and stress response (Mukhopadhyay et al., 2006; Neri, 2012). The neuroprotective role of DAF-16 in healthy, untreated touch receptor neuron aging has also been explored (Scerbak et al., 2014; Toth et al., 2012; Tank et al., 2011). Toth et al. (2012) demonstrated that increased DAF-16 activity due to decreased insulin signaling (*daf-2(e1370)* mutant background) resulted in increased PLM process branching in otherwise untreated animals by late in life (day 10 of adulthood). Conversely, Tank et al. (2011) observed decreased posterior cell branching in the same genetic background. However, consistent with our results (Figure 4.2), removal of DAF-16 via genetic mutation and RNAi does not drastically disrupt aging touch receptor neuron morphologies, but does decrease touch response when compared to wildtype aging (Scerbak et al., 2014; Toth et al., 2012; Tank et al., 2011). While the involvement of DAF-16 in lifespan extension is well explored (albeit complex), our correlation of specific touch receptor neuron morphology (posterior neuron process branching) with berry- and fungus-induced DAF-16 activation is novel. What remains to be determined is whether PLM

process branching is a stimulatory response that *actively promotes* healthy aging or whether this phenotype occurs as a *consequence* of good health and aging.

The involvement of DAF-16 in the improved health with age upon Alaskan lowbush cranberry treatment is consistent with other work demonstrating that *C. elegans* lifespan extension upon American lowbush cranberry treatment requires DAF-16 (Guha et al., 2012). That we did not detect a requirement for DAF-16 for blueberry-mediated lifespan extension is not surprising; others have shown that DAF-16 is not required in lifespan extension in other species of wild blueberry (Wilson et al., 2006). Given that DAF-16 is a known modulator of *hsp-16.2* expression, it is interesting that we previously detected a significant increase in *hsp-16.2*::GFP expression but no detectable fluorescent DAF-16::GFP foci following blueberry treatment in young adults (Supplemental Figure 4.1). This supports the idea that *hsp-16.2* is regulated by additional signaling pathways and may be used as a general biomarker of aging (Rea et al., 2005). An alternative explanation is that our transcription factor activation assay only detects strong activation of DAF-16; however, given the assay's consistency and rapid time course, we remain convinced that it is a powerful preliminary screening tool when combined with additional bioassays.

Given the described involvement of DAF-16 in the development of lowbush cranberry treatment-induced posterior neuron process branching, it is somewhat surprising that we did not observe DAF-16 nuclear foci formation nor a requirement for DAF-16 in lifespan extension upon treatment with chaga. None of the differentially regulated transcripts in treatment versus control comparisons are known to be directly regulated by the aging-central transcription factors we previously explored, DAF-16/FOXO or HSF-1, supporting the robust nature of techniques that allow of the visualization of such transcription factors with GFP (Morton and Lamitina, 2013; Henderson and Johnson, 2001). Also, chaga treatment caused an additional phenotype among posterior neurons not observed with lowbush cranberry treatments – process loops. The mechanisms driving posterior touch receptor branching events versus posterior branch *and* loop

events may be distinct. We believe that the lack of detection of DAF-16 involvement in chaga treatments may also be due to the following: (1) chaga treatments specifically activate neuronal DAF-16, causing branching while escaping detection in the aging DAF-16::GFP model and whole organism RNAseq; (2) DAF-16 is activated at a time point other than the two we tested (day 3 and day 9); or (3) an additional, as of yet undescribed pathway exists to regulate PLM process branching (and loops).

By comparing the transcriptomes of young adult (day 3) blueberry- and chaga-treated populations to control and to each other, we unveiled and screened candidate aging touch receptor neuron modulators. This approach uncovered 8 previously undescribed aging touch receptor neuron modulators: *max-1*, *pck*-1, *stn*-1, ttx-*1*, *tub-1*, unc-*115*, *unc-44*, ZK418.3 (Figure 4.8; Table 4.4). When knocked down with neuronal RNAi, all of these modulators differentially impacted mechanosensory neuron morphology while increasing motility and/or touch response late in life (Figure 4.8). While all of these genes have functions related to metabolism or neuron differentiation and morphogenesis and are expressed in neurons, most have not been extensively studied in the context of aging. We only identified previous aging-related work on two modulators: *pck-1* and *tub-1*, both of which fall into our "metabolism" general function classification (Figure 4.8). *pck-1* (phosphoenolpyruvate carboxykinase, an enzyme in gluconeogenesis) exhibits decreased function with age in *C. elegans* (Yuan et al., 2016), supporting a model of altered cellular metabolism as a factor in aging (Feng et al., 2016). *tub-1* (a homolog of the vertebrate *tubby* gene) was shown to regulate two biological processes through different signaling processes: lifespan via DAF-16/FOXO signaling and fat storage via RGB-3 signaling in ciliated neurons (Mukhopadhyay et al., 2005). Many of these modulators have known or predicted interactions with the neuronal cytoskeleton (*max-1; stn-1; tub-1; unc-115; unc-44;* ZK418.3; Table 4.5) and are involved in developmental processes (*max-1; unc-115; unc-44;* ZK418.3; *ttx-1;* Table 4.5). The known interactions of these gene products with the

cytoskeleton and axonal transport suggest that these genes may be involved in the underlying structural mechanisms of touch receptor neuron phenotype development.

ZK418.3 was the only aging touch receptor neuron modulator uncovered in this study that had decreased expression in the treatment (i.e. blueberry) versus control transcriptome comparison. Interestingly, its experimental knockdown in neurons resulted in somewhat different effects when compared to blueberry treatment alone: occurrence of extended soma outgrowths was not impacted (as it was in Chapter 3 with blueberry treatment alone), occurrence of posterior process branching and ratio of Class A/B animals was increased over blueberry alone, and occurrence of posterior process loops was increased (which was not impacted by blueberry alone; Figure 4.5). These findings suggest that ZK418.3 is not the only gene modified by blueberry treatment effects and suggest an intricate relationship between networks of genes for the maintenance mechanosensory neuron morphology and function.

Somewhat surprisingly, we found relatively small early (day 3) whole animal transcriptome-level changes when comparing controls with either Alaskan blueberry (17 transcripts differentially regulated) or chaga treatments (118 transcripts; Figure 4.3), despite their striking effects on wildtype lifespan, healthspan, and touch receptor neuron aging. Other research groups have observed both very large and relatively small gene expression effects in whole *C. elegans*: developmental stage impacts 8606 transcripts on average (Spencer et al., 2011), bacterial and fungal infection impacted ~2000-3000 transcripts (Engelmann et al., 2011), and mutations in the xenobiotic-responsive transcription factor aryl hydrocarbon receptor (AHR-1) impacted ~120 genes (Aarnio et al., 2014). However, while the number of genes impacted by blueberry and chaga treatment was small, the genes' impact on aging touch receptor neurons is striking (Figures 4.5-4.6, Figure 4.8). Other, non-genetic factors (i.e. microRNA translational regulation, pH-induced functional changes) may also impact the blueberry- and chaga-mediated aging of whole animals and touch receptor neurons.

We have shown here that the increased incidence of age-related mechanosensory neuron morphologies is not directly correlated with poorer health: both decreased incidence of ALM aberrations (i.e. soma outgrowths, abnormal soma shape) and increased incidence of PLM aberrations (i.e. process branching and loops) correlate with increased lifespan, improved motility, and improved touch response. This lack of direct association between increased morphological changes and function is also described in Chapters 2 and 3. To further complicate an understanding of the damaging versus protective roles of neuronal aberrations with respect to aging, our findings provided evidence that *increased* incidence of ALM aberrations can be correlated with improved motility and/or touch response (i.e. *ttx-1*(RNAi), *unc-44*(RNAi), and *stn-1*(RNAi)). The ALM and PLM pairs of touch receptor neurons consistently respond to the aging process different manners; thus, age-related changes in neuron morphology cannot be interpreted wholesale as biomarkers of detrimental effects of aging.

The cellular and molecular mechanisms behind the health benefits of nutritional interventions can be complex and challenging to uncover. Here, we described a requirement for DAF-16/FOXO in Alaskan lowbush cranberry-mediated lifespan extension and altered touch receptor neuron aging (i.e. posterior process branching development), but not in Alaskan blueberry and chaga treatment effects. Early transcriptome changes (day 3) revealed modest numerical genetic changes with blueberry and chaga treatment, but did reveal novel candidate touch receptor neuron morphology modulators. Many of these candidate modulators do indeed impact aged (day 11) touch receptor neuron morphology and function, and their interactions with the cytoskeleton suggest a direct mechanism for development of morphological changes. These results demonstrate the different molecular mechanisms of the Alaskan nutraceuticals' effects and support a model in which specific changes in touch receptor neuron morphology correspond to specific changes in intra- and intercellular signaling pathways.

4.6 Acknowledgements

The authors would like to thank Dr. Marton Toth for the ZB154 strain and members of the Taylor/Harris laboratory for their support. Some *C. elegans* strains were provided by the CGC, which is funded by NIH Office of Research Infrastructure Programs (P40 OD010440). Work reported in this publication was supported by the National Institute of General Medical Sciences of the National Institutes of Health (1) under an Institutional Development Award (IDeA; grant number P20GM103395) and (2) under three linked awards numbered RL5GM118990, TL4 GM 118992 and 1UL1GM118991. The work is solely the responsibility of the authors and does not necessarily represent the official view of the National Institutes of Health.

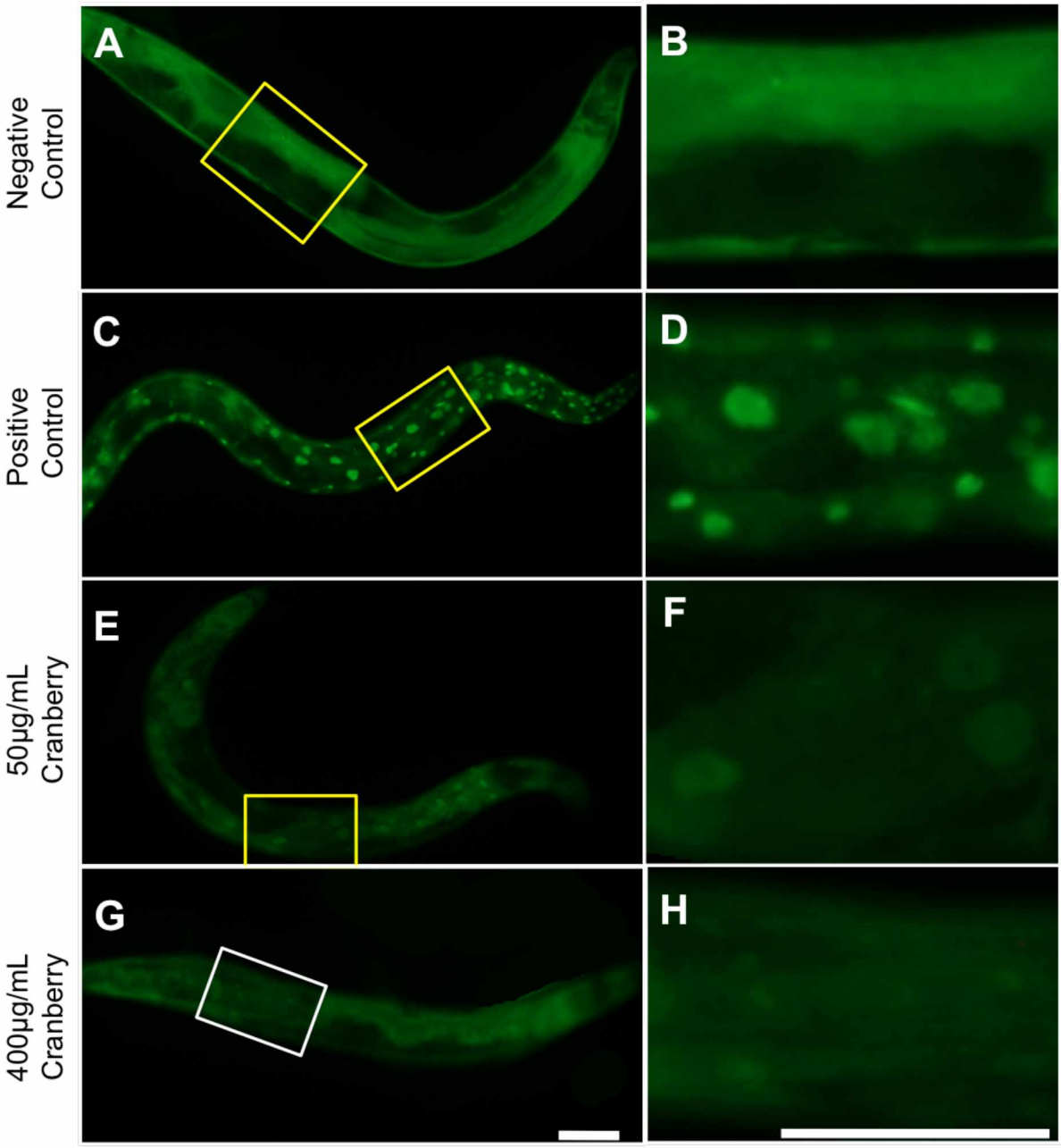

Figure 4.1 Alaskan lowbush cranberry activates DAF-16/FOXO nuclear translocation later in life.

Representative images of GFP-labeled DAF-16 (strain TJ356) day 9 adult untreated negative (A-B) and positive (C-D) controls and treatment with lifespan-extending Alaskan lowbush cranberry treatments (E-H) are shown. Notice the presence of foci or punctae in the positive controls and both lowbush cranberry treatment groups. Yellow boxes on images to the left mark the magnified area in corresponding panels on the right. All images were collected at constant image exposure and 10x magnification. Positive control effects were induced by 30min at 37°C. Scale bars represent 60µm for all images in each column.

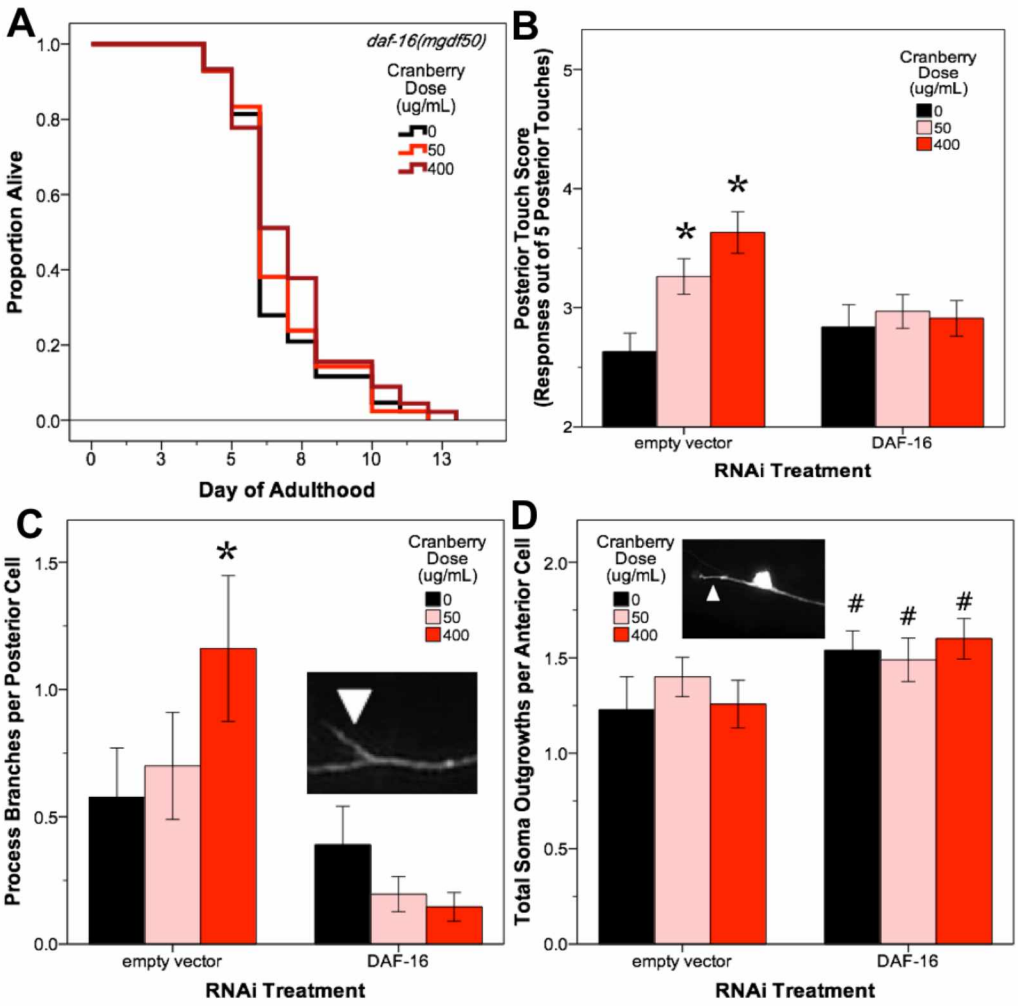

Figure 4.2 Alaskan lowbush cranberry requires DAF-16 for lifespan extension and posterior neuron branching events late in life.

(A) Lowbush cranberry treatments that extend wildtype *C. elegans* lifespan (50 and 400µg/mL) do not extend the lifespan of DAF-16 mutant animals (*daf-16)mgdf50)*). Representative Kaplan Meier curve is shown (N=50 per treatment group) and results were replicated in 3 independent trials. DAF-16 RNAi treatment blocks lowbush cranberry treatment-mediated improvement in posterior touch response (B) and increased posterior process branching (C). Asterisks denote significant difference ($p<0.05$; Poisson log linear model) from untreated control in each RNAi treatment group. (D) DAF-16 impacts anterior cell soma outgrowth development in all lowbush cranberry treatment groups somewhat significantly. Hashtags denote slight significance ($0.09<p<0.06$; Poisson log linear model) compared to treatment matched empty vector control. Insets in C and D are representative images of touch receptor neurons with the appropriate neuron morphology marker (anterior of each individual oriented to the left). Bars represent mean ± standard error of the mean. N_{worms}=17-31, $N_{anterior\ cells}$=22-40 cells, $N_{posterior\ cells}$= 26-51 per bar.

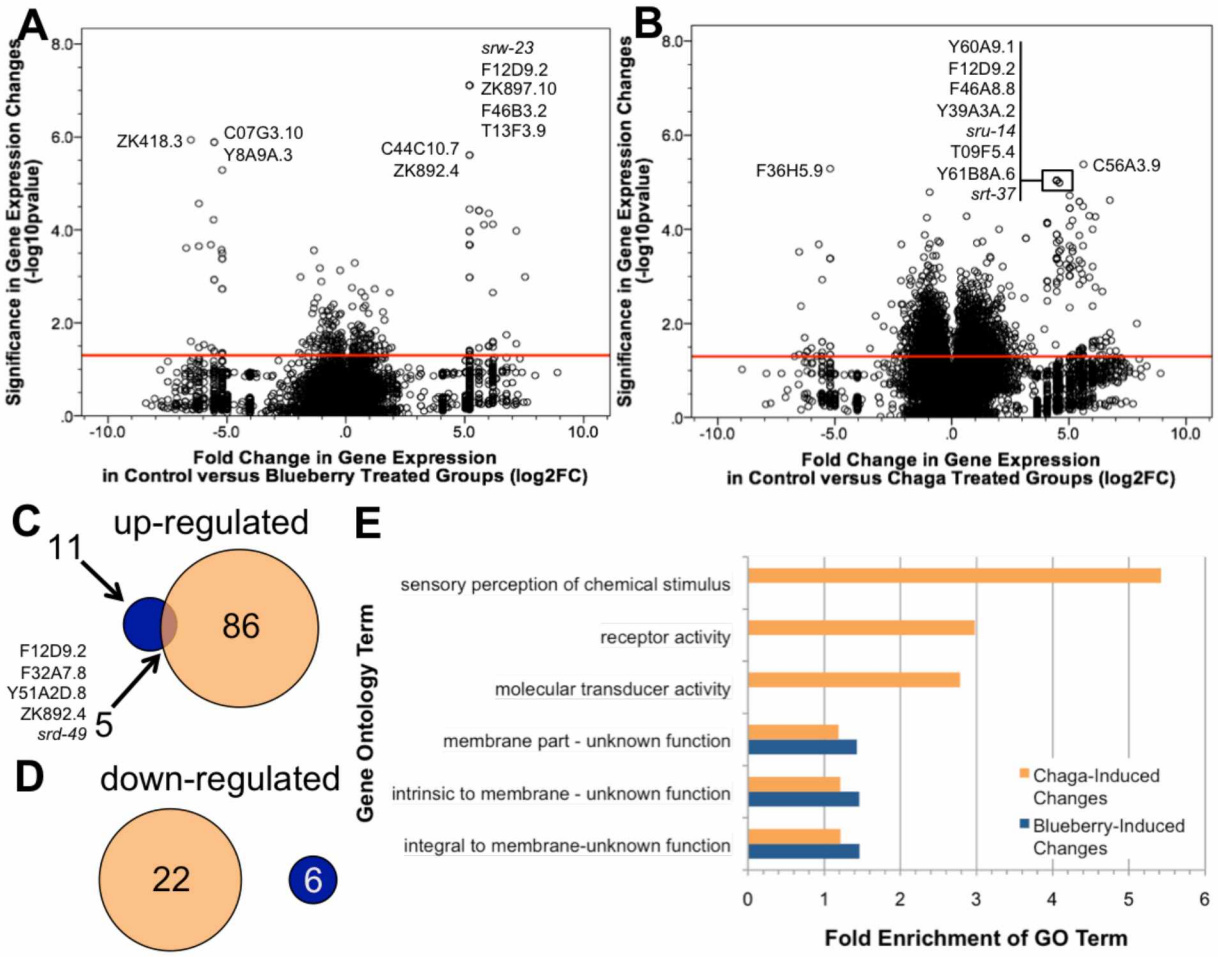

Figure 4.3 Gene expression is differentially regulated following treatment with Alaskan blueberry and chaga extracts.

Volcano scatter plots of mean fold change in transcript expression levels ($\log_2$(fold change)) versus significance in gene expression change (-$\log_{10}$(*p* value)) in control relative to blueberry treatment (A) or chaga treatment (B) calculated from *N*=3 transcriptomes from each group are shown. The red line represents –$\log_{10}$(0.05), to aid in determining significance (false discovery rate was also considered in the analysis). The 10 transcripts with the lowest false discovery rate (FDR) are listed for each group and identified on the volcano scatter plot. Venn diagrams of up-regulated (C) and down-regulated (D) by blueberry (blue circles) and chaga (orange circles) treatments are also shown. Note that neither treatment down-regulated the same genes. (E) Gene ontology terms with significant overrepresentation in treatment-induced transcriptome changes (fold enrichment; DAVID analysis) following blueberry (blue bars) and chaga (orange bars) treatments is shown.

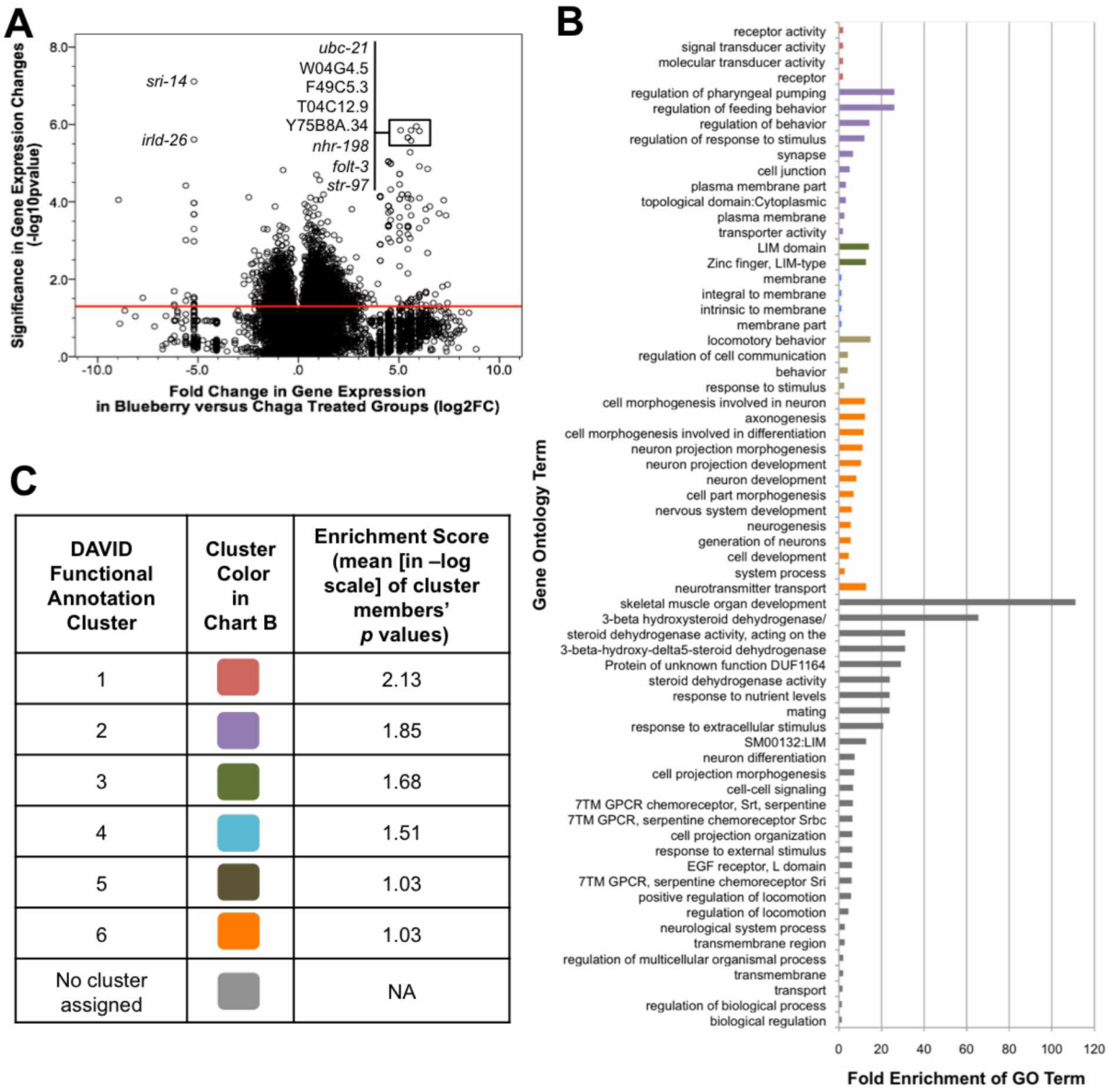

C

DAVID Functional Annotation Cluster	Cluster Color in Chart B	Enrichment Score (mean [in –log scale] of cluster members' *p* values)
1		2.13
2		1.85
3		1.68
4		1.51
5		1.03
6		1.03
No cluster assigned		NA

Figure 4.4 Transcriptome comparison between blueberry and chaga treatment yields more effects.

(A) Volcano scatter plot of fold change in transcript expression levels ($\log_2$(fold change)) versus significance in gene expression change (-$\log_{10}$(*p* value)) in blueberry relative to chaga groups. The red line represents –$\log_{10}$(0.05), to aid in determining significance (false discovery rate was also considered in the analysis). The 10 transcripts with the lowest false discovery rate (FDR) are listed for each group and identified on the volcano scatter plot. (B) Gene ontology terms with significant overrepresentation in chaga- versus blueberry-treated transcriptomes (fold enrichment; DAVID analysis). Bar colors in chart B denote DAVID functional annotation cluster, described in C. (C) Functional annotation clustering results of chaga- versus blueberry-treated transcriptome changes (DAVID analysis). Enrichment score (-log scale) ranks cluster groups by overrepresentation, highlighting important GO annotation groups.

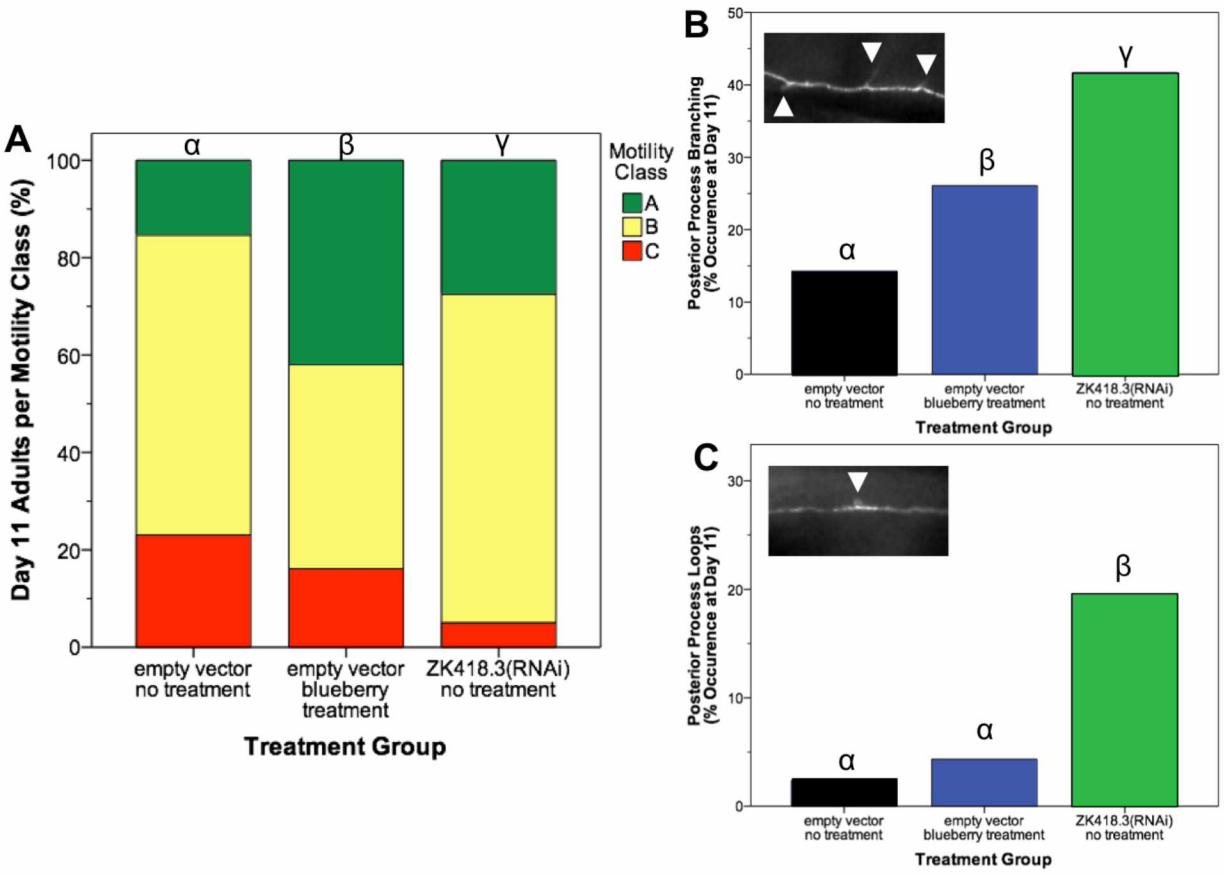

Figure 4.5 The impacts of Alaskan blueberry-mediated candidate gene on aging neuron morphology.

Proportion of adults per motility class (A; detailed description in Methods section) and exhibiting posterior touch receptor neuron morphologies (B, branching; C, loops) in control (black bars), blueberry treatment (blue bars), and neuronal RNAi knockdown of ZK418.3 (green bars) are shown. Greek letters above bars designate statistically homogenous subsets (p<0.05; ordinal logistic model [A] or binary logistic model [B-C]). Insets show representative image of affected neuron morphology. N=31-40 animals from at least 3 separate biological replicates per treatment group.

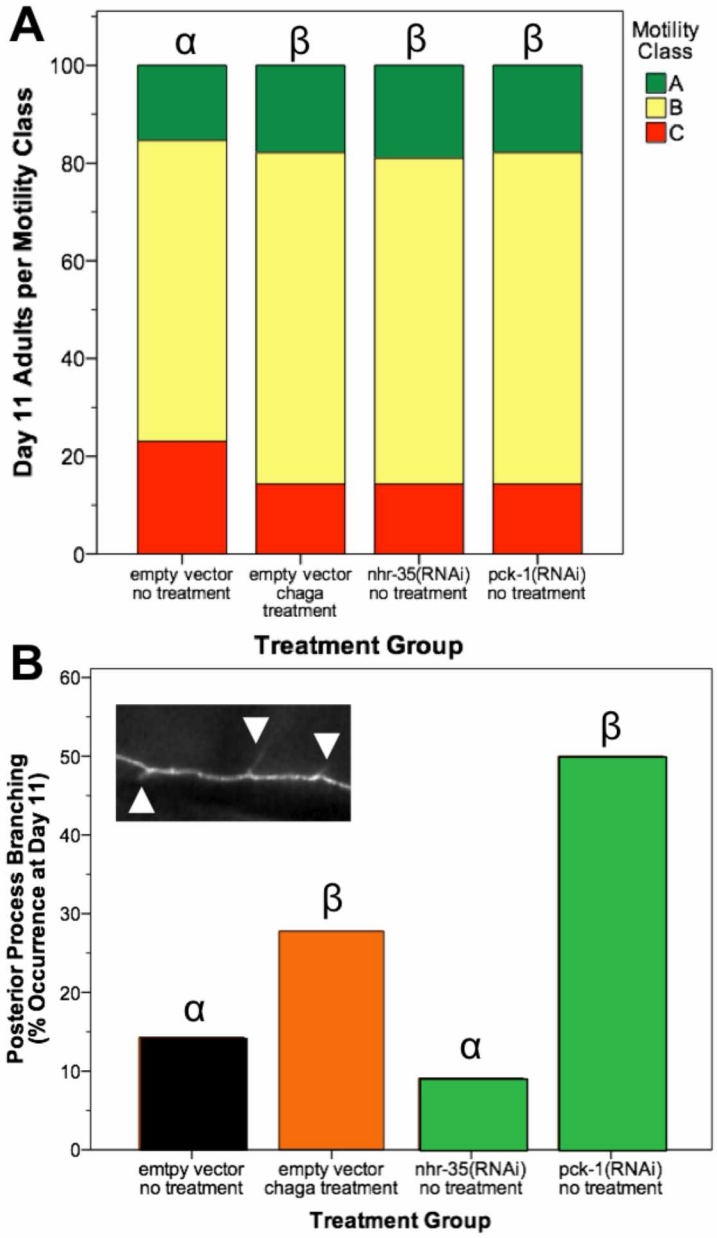

Figure 4.6 The impacts of Alaskan chaga-mediated candidate gene on aging neuron morphology.

Proportion of adults per motility class (A) and exhibiting posterior neuron process branching (B) in control (black bar), chaga treatment (orange bar), and neuronal RNAi knockdown of candidate genes (green bars) are shown. Greek letters above bars designate statistically homogenous subsets (p<0.05; ordinal logistic model [A] or binary logistic model [B]). Inset shows representative image of affected neuron morphology. N=28-39 animals from at least 3 separate biological replicates per treatment group.

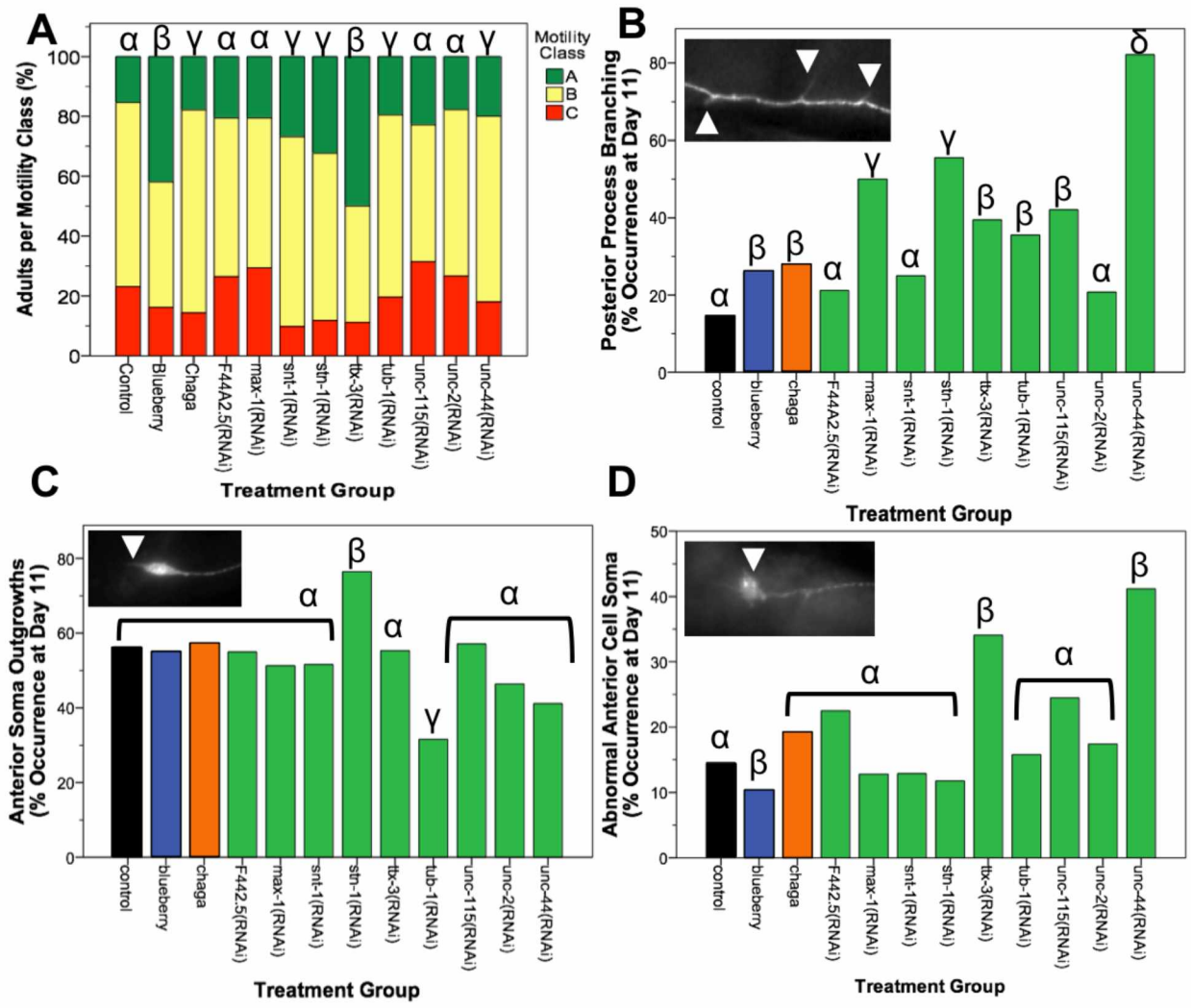

Figure 4.7 The impacts of candidate neuron morphology modulators on aging neuron morphology.

Proportion of adults per motility class (A), exhibiting posterior process branching (B), and exhibiting anterior neuron morphologies (outgrowths from the soma; C and abnormal cell somas; D) in control (black bars), chaga-treated (orange bars), blueberry treated (blue bars), and neuronal RNAi treatment of candidate genes (green bars) groups are shown. Greek letters above bars designate statistically homogenous subsets ($p<0.05$; ordinal logistic model [A] or binary logistic model [B-D]). Insets show representative image of affected neuron morphology. N=28-50 animals from at least 3 separate biological replicates per treatment group.

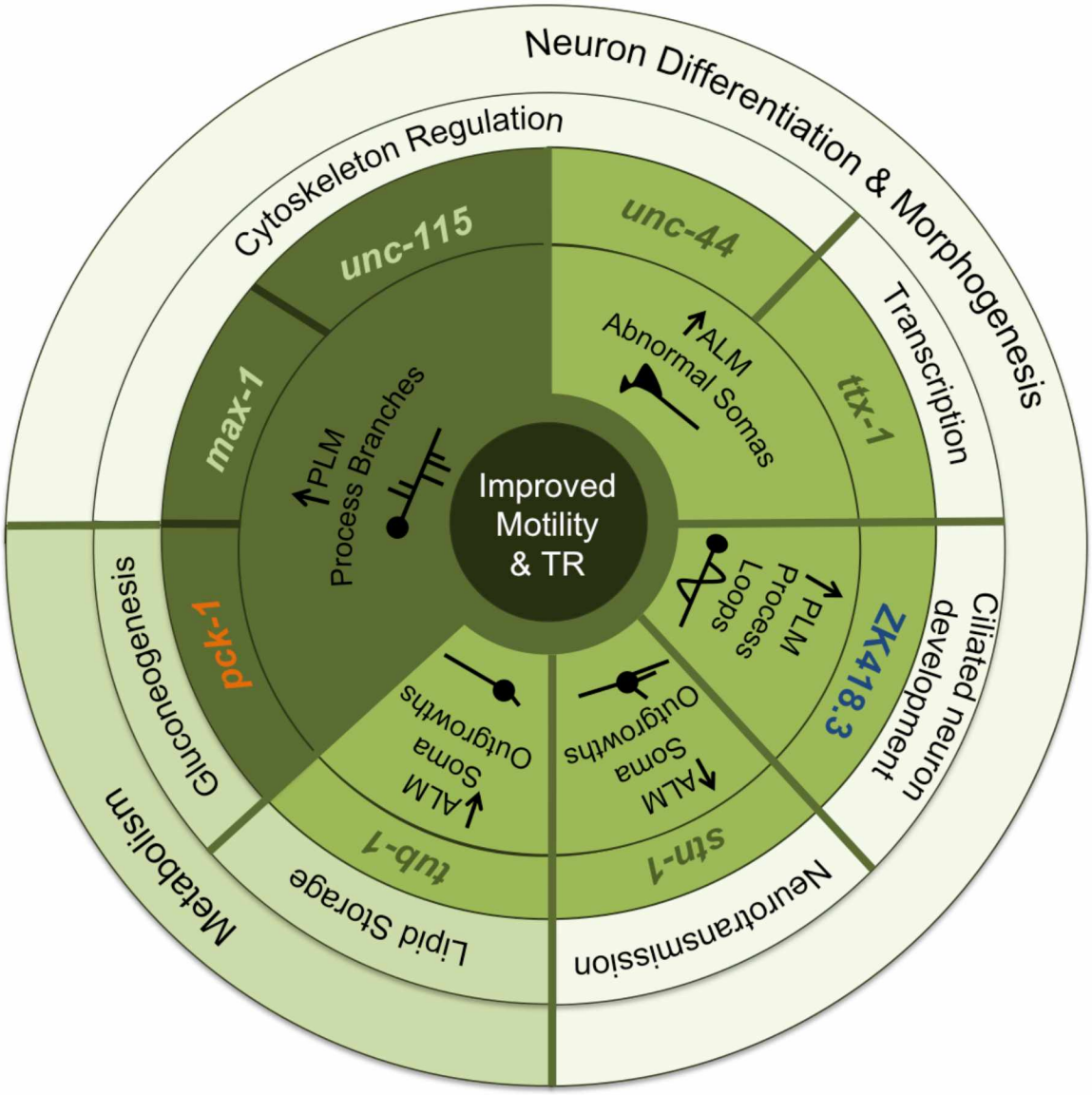

Figure 4.8 Summary of touch receptor neuron aging modulators detected with Alaskan nutraceutical treatment.

A diverse group of *C. elegans* neuronal genes impacted by Alaskan blueberry and chaga treatments modulate touch receptor neuron aging. From outer circle inwards: general gene function; specific gene function; gene name; touch receptor neuron morphology impacted at day 11 following RNAi (with cartoon of impacted morphology); posterior neuron branching impacted by all genes at day 11 following neuronal RNAi; all neuronal phenotype modifications result in improved motility and touch response (i.e. improved touch response and/or motility). More detailed results for each gene found in Figure 5 (blue gene name), Figure 6 (orange gene name), and Figure 7 (green gene names). Abbreviations: PLM - posterior lateral touch receptor neuron; ALM - anterior lateral touch receptor neuron; TR – touch response.

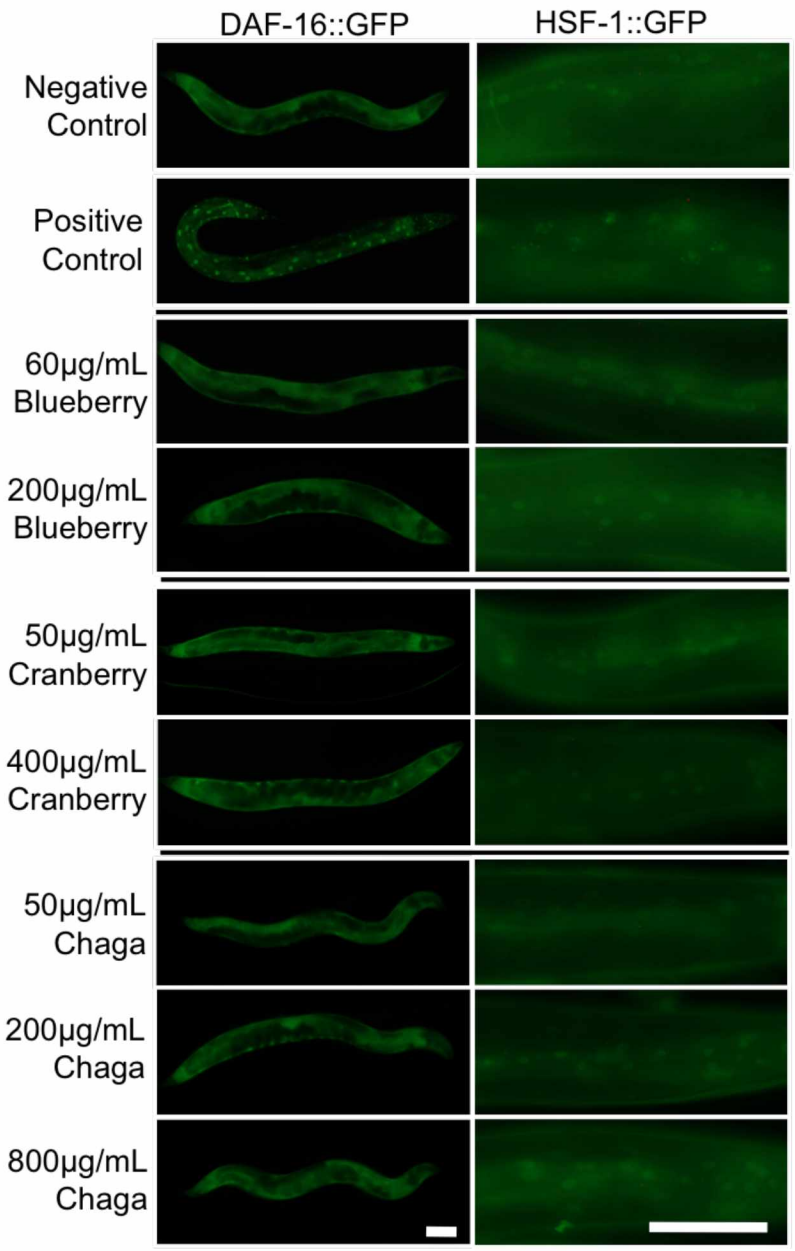

Supplemental Figure 4.1 DAF-16 and HSF-1 nuclear translocation are not induced after 48h treatment with Alaskan berry or fungus.

Representative images of age-matched, GFP-labeled DAF-16 (strain TJ356) or HSF-1 (strain OG497) day 3 adult untreated positive and negative controls and 48-h treatment with lifespan-extending Alaskan berry and fungus treatments are shown. Notice the striking appearance of the positive controls for each strain when compared with other treatment groups. DAF-16::GFP images (left panels) were collected at 10x and HSF-1::GFP images (right panels) were collected at 40x magnification. Positive control effects were induced by 30min at 37°C (DAF-16) or 35°C (HSF-1). Scale bars represent 60µm for the images in each column.

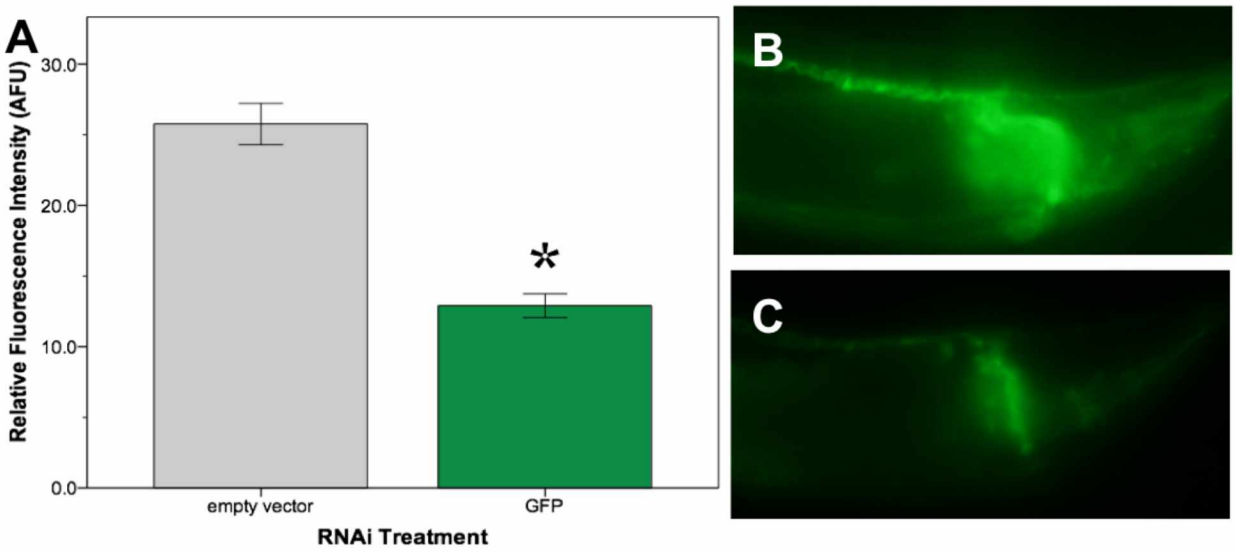

Supplemental Figure 4.2 GFP RNAi treatment blocks GFP expression.

(A) Mean fluorescence (arbitrary fluorescent units; AFU) of the pharynx region following treatment with empty vector and GFP RNAi at day 11 of adulthood using a strain previously genetically modified to be susceptible to neuronal RNAi (ZB064 (*zdIs5* [P_{mec-4}*GFP, lin-15*(+)]; *uIs57* [$P_{unc-119}$*SID-1*, $P_{unc-119}$*yfp*, P_{mec-6}*mec-6*])). Representative images of a pharynx region from a day 11 adult treated with empty vector (B) and GFP (C) RNAi are also shown. Asterisks denote significance from empty vector control (p<0.05; unpaired t-test). N=8 animals per bar. All images analyzed and shown were collected using the same fluorescent imaging parameters (i.e. 20x magnification, 1/20s exposure, no additional image processing). This experiment was repeated with similar significant results for each experimental replicate involving RNAi (Figure 2; Figures 5-7).

Table 4.1 Alaskan lowbush cranberry treatments cause DAF-16::GFP nuclear foci formation later in life.

Animals were classified based on the presence of DAF-16::GFP nuclear foci at day 9 of adulthood following treatment. Animals with cytosolic DAF-16 had diffuse GFP expression throughout the animal (example in Figure 1A), nuclear DAF-16 foci seen throughout the animal with very little diffuse fluorescence (example in Figure 1C), and intermediate DAF-16 had at least three distinct DAF-16::GFP foci with mostly diffuse fluorescence (examples in Figures 1E and 1G). Treatments were grouped into statistically homogenous subsets ($p<0.05$, ordinal logistic model). Data and sample size represent all individuals examined from 3 independent trials, each with a significant effect.

Treatment (ug/ml)	Percent (%) Animals Tested			Total Sample Size	Statistical Group
	Cytosolic	Intermediate	Nuclear		
0 Positive Control (Heat Shock)	0	0	100	20	a
0 Negative Control	72.7	27.3	0	33	b
50 Lowbush cranberry	38.7	61.3	0	31	c
400 Lowbush cranberry	19.3	80.6	0	31	c

Table 4.2 The effect of Alaskan berry and fungus treatments on *daf-16(mgdf50)* mutant lifespan.

Mean lifespan for Alaskan blueberry-, lowbush cranberry-, and chaga-treated mutant DAF-16 *C. elegans* (*daf-16(mgdf50)*) from representative trials are shown. Untreated mutants had significantly decreased mean lifespan compared to untreated wildtype control, as expected. Significance from appropriate control (*p* value) calculated using Kaplan-Meier log-rank test.

Treatment	**Dose (µg/mL)**	**Lifespan (mean days ± S.E.M.)**	**N**	***p* value**
Blueberry	0	9.85±0.50	50	
	60	13.4±0.49	48	<0.001
	200	15.8±0.83	41	<0.001
Lowbush cranberry	0	7.17±0.33	50	
	50	6.97±0.31	50	0.608
	400	7.65±0.44	50	0.560
Chaga	0	8.36±0.68	50	
	50	7.43±0.39	50	0.131
	200	8.27±0.48	50	0.674

Table 4.3 Summary of alignments from RNA library.

	Control			Blueberry Treatment			Chaga Treatment		
	Sample 1	Sample 2	Sample 3	Sample 1	Sample 2	Sample 3	Sample 1	Sample 2	Sample 3
Total Number of Reads (millions)	18.25	29.05	17.44	18.75	28.84	25.65	19.25	25.79	26.56
Number of Reads Filtered on Quality	230254	277897	210010	245506	476239	492313	252872	355482	382463
Percent Reads Filtered on Quality	1.26	0.96	1.20	1.31	1.65	1.92	1.31	1.38	1.44
Number of Genes Detected Above Threshold	15658	17373	14980	15464	17408	15424	16834	17328	17727
Percent of Genes Detected based on Current Transcriptome Definition	33.49	37.16	32.04	33.08	37.24	32.99	36.01	37.07	37.92
Percent of Reads Mapped Either to the Transcriptome or the Genome	99.08	99.15	99.04	99.07	99.22	99.32	99.16	99.03	98.98

Table 4.4 Candidate touch receptor neuron morphology regulators selected for follow-up.

Table lists the candidate genes selected selected for neuron morphology follow-up from the three transcriptome comparisons: control versus blueberry treatment, control versus chaga treatment, or blueberry versus chaga treatments. The fold change in gene expression relative to the indicated treatment (log2FC & FC), false discovery rate (FDR), relevant biological process and cellular component gene ontology terms (GO), and human homolog for each candidate gene are also listed.

Candidate Gene	log2FC	FDR	GO	Human Homolog
Candidate Gene Impacted in Blueberry Treatment versus Control Comparison				
ZK418.3	-6.5	0.01	vulval development; neurons	TMEM17; cillia membrane transport
Candidate Genes Impacted in Chaga Treatment versus Control Comparison				
nhr-35	-0.59	0.14	DNA binding; transcription	Hepatocyte nuclear factor 4A/4G; transcription
pck-1	1.1	0.14	gluconeogenesis	Phosphoenolpyruvate carboxykinase
Candidate Genes Impacted in Blueberry versus Chaga Comparison				
F44A2.5	0.51	0.18	RNA binding, sarcoplasmic reticulum	CTIF; CPB80/20-dependent translation initiation factor
max-1	0.52	0.29	cytoskeleton	PLEKHH1; cytoskeleton
snt-1	1.23	0.21	synaptic vesicle exocytosis	synaptotagmin; pre-synaptic Ca^{2+} sensor
stn-1	0.5	0.28	neurotransmitter (acetylcholine) transport	α- and β-syntrophins; neuromuscular junction
ttx-3	1.45	0.16	axon guidance; associative learning	LIM/homeobox protein Lhx2; transcriptional activator in cell differentiation
tub-1	0.97	0.22	lipid storage; chemotaxis; axon	TUBBY; transcription/signaling factor
unc-115	0.39	0.108	neuron projection morphogenesis	ABLIM1; actin binding
unc-2	0.81	0.21	regulation of neurotransmitter levels	CACNA1A; P/Q-type calcium channel
unc-44	0.21	0.26	axon guidance & extension	Ankyrin-1 isoform Br21; integral adapter protein

Table 4.5 Known interactions of the aging *C. elegans* touch receptor neuron aging modulators detected with Alaskan nutraceutical treatment with the cytoskeleton, axon transport, and developmental processes.

Table lists each of the 8 aging touch receptor neuron morphology modulators (gene), its level of interaction with the cytoskeleton (yes/no/predicted/unknown), and previous neuron-related functional studies of the gene and its homolog in *C. elegans* and vertebrates.

Gene	Interacts with Cytoskeleton?	Functional studies in C. elegans	Functional studies in Vertebrates
max-1	Yes	GABA motor neurons developmental cell guidance (Huang et al., 2002)	Zebrafish motor neurons and epithelial cells developmental cell guidance (Zhong et al., 2006) Mediates endocytosis in lysosomes (PLEKHM1; McEwan et al., 2015)
pck-1	No (kinase)	Energy metabolism (gluconeogenesis)	Energy metabolism (gluconeogenesis)
stn-1	Indirectly (predicted)	Linked to dystrophin function (Kim et al., 2004) Interacts with the SNF-6 acetylcholine receptor at neuromuscular junctions (Kim et al., 2004)	Scaffolding proteins in neuromuscular synapses (α- and β-syntrophins; Grisoni et al., 2003; Albrecht and Froehner, 2002)
ttx-1	No (transcription factor)	Differentiation of AFD thermosensory neurons (Satterlee et al., 2001)	Brain embryogenesis (otd/Otx homeodomain transcription factors; Acampora et al., 2001)
tub-1	Predicted	Fat deposition and chemosensation through signaling in ciliated neurons (via RBG-3; Mukhopadhyay et al., 2005) Regulates lifespan (via DAF-16/FOXO; Mukhopadhyay et al., 2005)	neuron function during and after development (Ikeda et al., 2002) Associated with retinal dystrophy and obesity (Borman et al., 2014)
unc-115	Yes	Neuron class (e.g. VD and DD motor neurons) developmental cell guidance (Lundquist et al., 1998)	Binds action in many cell types (including neurons) and predicted to regulate cell morphology (ABLIM1; Roof et al., 1997)
unc-44	Yes	Axon guidance (Otsuka et al, 1995)	Adapter protein with a variety of structural applications (Ankryin-1)
ZK418.3	Unknown	Expressed in amphid and labial head neurons (Phirke et al., 2011) Involved in the development of ciliated neurons and vuval development (Phirke et al., 2011)	Part of a complex required for normal primary cilia development and function (TMEM17; Chih et al., 2012) Implicated in trafficking regulation to and from the cilia (TMEM17; Chih et al., 2012)

Supplemental Table 4.1 Comparison of control versus blueberry treatment transcriptomes.

Supplemental Table 4.2 Comparison of control versus chaga treatment transcriptomes.

Supplemental Table 4.3 Comparison of blueberry versus chaga treatment transcriptomes.

Supplemental Tables 4.1-4.3 show expression level (log_2mean) for each group and fold change (log_2mean), unadjusted *p* value, and false discovery rate (FDR) for all transcripts detected during sequencing (≥5). Transcripts with an FDR of ≤0.30 and unadjusted *p* value ≤0.01 were considered significantly impacted by treatment.

Supplemental Table 4.4 Selection of candidate touch receptor neuron morphology regulators.

Supplemental table 4.4 lists genes chosen through each round of selection: (1) all genes significantly impacted (FDR<0.3 and p value <0.05) in any of the three described comparisons with duplicates (N=92) removed for clarity; (2) genes from 1 with known functions relevant to the current study (i.e. neuron function and development, known connection to the aging process); (3) genes from 2 with known human homologs.

Tables are oversized and included in supplementary CD/archive.

4.7 References cited

Aarnio, V., Heikkinen, L., Peltonen, J., Goldsteins, G., Lakso, M., and Wong, G. (2014). Transcriptional profiling reveals differential expression of a neuropeptide-like protein and pseudogenes in aryl hydrocarbon receptor-1 mutant *Caenorhabditis elegans*. *Comp Biochem Physiol* 9, 40-48.

Acampora, D., Gullisano, M., Broccoli, V., and Simeone, A. (2001). Otx genes in brain morphogenesis. *Prog Neurobiol* 64(1), 69-95.

Albrecht, D.E. and Froehner, S.C. (2002). Syntrophins and dystrobrevins: defining the dystrophin scaffold at synapses. *Neurosignals* 11(3), 123-129.

Bersamin, A., Luick, B.R., King, I.B., Stern, J.S., and Zindenberg-Cherr, S. (2008). Westernizing diets influence fat intake, red lood cell fatty acid composition, and health in remote Alaskan Native communities in the Center for Alaska Native Health Study. *J American Dietetic Ass*, 266-273.

Borman, A.D., Pearce, L.R., Mackay, D.S., Nagel-Wolfrum, K., Davidson, A.E., Henderson, R., Garg, S., Waseem, N.H., Webster, A.R., Plagnol, V., Wolfrum, U., Farooqi, I.S., and Moore, A.T. (2014). A homozygous mutation in the TUB gene associated with retinal dystrophy and obesity. *Hum Mutat* 35, 289-293.

Brenner, S. (1974). The genetics of *Caenorhabditis elegans*. *Genetics* 77, 71–94.

Calixto, A., Chelur, D., Topalidou, I., Chen, X., and Chalfie, M. (2010). Enhanced neuronal RNAi in C. elegans using SID-1. *Nat Methods* 7, 554–559.

Chih, B., Liu, P., Chinn, Y., Chalouni, C., Komuves, L.G., Hass, P.E., Sandoval, W. and Peterson, A.S. (2012). A ciliopathy complex at the transition zone protects the cilia as a privileged membrane domain. *Nat Cell Biol* 14, 61-72.

Elks, C.M., Francis, J., Stull, A.J., Cefalu, W.T., Shukitt-Hale, B., and Ingram, D.K. (2013). "Overview of the health properties of blueberries," in *Bioactives in fruit: Health benefits and functional foods*, eds. M. Skinner and D. Hunter (John Wiley & Sons), 251–271.

Engelmann, I., Griffon, A., Tichit, L., Montanana-Sanchis, F., Wang, G., Reinke, V., Waterson, R.H., Hiller, L.W., and Ewbank, J.J. (2011). A comprehensive analysis of gene expression changes provoked by bacterial and fungal infection in *C. elegans.* PLoS One 6(5), 1-13.

Feng, Z., Hanson, R.W., Berger, N.A., and Trubitsyn, A. (2016). Reprogramming of energy metabolism as a driver of aging. *Oncotarget*, *Epub ahead of print.*

Fleming, J.A., Holigan, S., and Kris-Etherton, P.M. (2013). Dietary patterns that decrease cardiovascular disease and increase longevity. *J Clin Exp Cardiolog* S6(6), 1-7.

Garabaldi, A. (1999). *Medicinal flora of the Alaska Natives.* Anchorage, Alaska: Environment and Natural Resources Institute, Alaska Natural Heritage Program.

Grisoni, K., Gieseler, K., Mariol, M.C., Martin, E., Carre-Pierrat, M., Moulder, G., Barstead, R., and Segalat, L. (2003) The stn-1 syntrophin gene of C. elegans is functionally related to dystrophin and dystrobrevin. *J Mol Biol* 332(5), 1037-46.

Guha, S., Cao, M., Kane, R., Savino, A., Zou, S., and Dong, Y. (2012). The longevity effect of cranberry extract in Caenorhabditis elegans is modulated by daf-16 and osr-1. *AGE* 35(5), 1559-1574.

Henderson, S., and Johnson, T. (2001). daf-16 integrates developmental and environmental inputs to mediate aging in the nematode *Caenorhabditis elegans. Current Biol* 11(24), 1975-1980.

Herndon, L., Schmeissner, P., Dudaronek, J., Brown, P., Listner, K., Sakano, Y., Paupard, M., Hall, D., and Driscoll, M. (2002). Stochastic and genetic factors influence tissue-specific decline in ageing C. elegans. *Nature* 419, 808–814.

Huaiyu, M., Muruganujan, A., Casagrande, J.T., and Thomas, P.D. (2013). Large-scale gene function analysis with the PANTHER classification system. *Nat Protocols* 8(8), 1551-1566.

Huang, X., Cheng, H.J., Tessier-Lavigne, M., and Jin, Y. (2002). MAX-1, a novel PH/MyTH4/FERM domain cytoplasmic protein implicated in netrin-mediated axon repulsion. *Neuron* 34(4), 563-576.

Huang, D.W., Sherman, B.T., and Lempicki, R.A. (2009). Systematic and integrative analysis of large gene lists using DAVID bioinformatics resources. *Nat Protocols* 4(1), 44-57.

Hsu, A.L., Murphy, C., and Kenyon, C. (2003). Regulation of aging and age-related disease by DAF-16 and heat-shock factor. *Science* 300, 1142–1145.

Ikeda, A., Nishina, P.M., and Naggert, J.K. (2002). The tubby-like proteins, a family with roles in neuronal development and function. *J Cell Science* 115, 9-14.

Kaletsky, R., Lakhina, V., Arey, R., Williams, A., Landis, J., Ashraf, J., and Murphy, C.T. (2016). The *C. elegans* adult neuronal IIS/FOXO transcriptome reveals adult phenotype regulators. *Nature* 529, 92-96.

Kari, P.R. (1995). *Tanaina plantlore, Dena'ina k'et'una*. 4th ed. Fairbanks, Alaska : Alaska Native Language Center, Alaska Natural History.

Kim, H., Rogers, M.J., Richmond, J.E., and McIntire, S.L. (2004) SNF-6 is an acetylcholine transporter interacting with the dystrophin complex in *Caenorhabditis elegans*. *Nature* 430, 891-896.

Li, J.J., Huang, H., Bickel, P.J., and Brenner, S.E. (2014). Comparison of *D. melanogaster* and *C. elegans* developmental stages, tissues, and cells by modENCODE RNA-seq data. *Genome Res* 24, 1086-1101.

Liu, R.H. (2004). Potential synergy of phytochemicals in cancer prevention: mechanism of action. *J Nutrition* 134, 3479S-3485S.

Lundquist, E.A., Herman, R.K., Shaw, J.E., and Bargmann, C.I. (1998). UNC-115, a conserved protein with predicted LIM and actin-binding domains, mediates axon guidance in *C. elegans. Neuron* 21, 385-392.

McEwan, D.G., Popovic, D., Gubas, A., Terawaki, S., Suzuki, H., Stadel, D., Coxon, F.P., de Stegmann, M.D., Bhogaraju, S., Maddi, K., Kirchof, A., Gatti, E., Helfrich, M.H., Wakatsuki, S., Behrends, C., Pierre, P., and Dikic, I. (2015) PLEKHM1 regulates autophagosome-lysosome fusion through HOPS complex and LC3/GABARAP proteins. *Mol Cell* 57(1) 39-54.

Morton, E., and Lamitina, T. (2013). Caenorhabditis elegans HSF‐1 is an essential nuclear protein that forms stress granule‐like structures following heat shock. *Aging Cell 12*, 112–120.

Mukhopadhyay, A., Oh, S., and Tissenbaum, H. (2006). Worming pathways to and from DAF-16/FOXO. *Exp Geron* 41(10), 928-934.

Mukhopadhyay, A., Deplancke, B., Walhout, A.J.M., and Tissenbaum, H.A. (2005). *C. elegans tubby* regulates life span and fat storage by two independent mechanisms. *Cell Met* 2, 35-42.

Neri, C. (2012). Role and therapeutic potential of the pro-longevity factor FOXO and Its regulators in neurodegenerative disease. *Front Pharmacol 3*, 1-8.

Ogg, S., Paradis, S., Gottlieb, S., Patterson, G., Lee, L., Tissenbaum, H., and Ruvkun, G. (1997). The Fork head transcription factor DAF-16 transduces insulin-like metabolic and longevity signals in C. elegans. *Nature* 389, 994–999.

Oh, S., Mukhopadhyay, A., Svrzikapa, N., Jiang, F., Davis, R., and Tissenbaum, H. (2005). JNK regulates lifespan in Caenorhabditis elegans by modulating nuclear translocation of forkhead transcription factor/DAF-16. *PNAS* 102, 4494–4499.

Otsuka, A.J., Franco, R., Yang, B., Shim, K.H., Tang, L.Z., Zhang, Y.Y., Boontrakulpoontawee, P., Jeyaprakash, A., Hedgecock, E., Wheaton, V.I., and Sobery, A. (1995). An ankyrin-related gene (*unc-44*) is necessary for proper axonal guidance in *Caenorhabditis elegans*. *J Cell Biol* 129(4), 1081-1092.

Pan, C.L., Peng, C.Y., Chen, C.H., and McIntire, S. (2011). Genetic analysis of age-dependent defects of the *Caenorhabditis elegans* touch receptor neurons. *PNAS* 108, 9274–9279.

Patel, A.P., Tirosh, I., Trombetta, J.J., Shalek, A.K., Gilespie, S.M., Wakimoto, H., Cahill, D.P., Nahed, B.V., Curry, W.T., Martuza, R.L., Louis, D.N., Rozenblatt-Rosen, O., Suva, M.L., Regev, A., and Berstein, B.E. (2014). Single-cell RNA-seq highlights intratumoral heterogeneity in primary glioblastoma. *Science* 344, 1396-1401.

Phirke, P., Efimenko, E., Mohan, S., Burghoorn, J., Crona, F., Bakhourn, M.W., Trieb, M., Schuske, K., Jorgensen, E.M., Piasecki, B.P., Leroux, M.R., and Swoboda, P. (2011). Transcriptional profiling of *C. elegans* DAF-19 uncovers a ciliary base-associated protein and a CDK/CCRK/LF2p-related kinase required for intraflagellar transport. *Develop Biol* 357(1), 235-247.

Rea, S.L., Wu, D., Cypser, J.R., Vaupel, J.W., and Johnson, T.E. (2005). A stress-sensitive reporter predicts longevity in isogenic populations of Caenorhabditis elegans. *Nature Genetics 37*, 894–898.

Roof, D.J., Hayes, A., Adamian, M., Chishti, A.H., and Li, T. (1997). Molecular characterization of abLIM, a novel acint-binding and double zinc funger protein. *JCB* 138(3), 575-588.

Satterlee, J.S., Sasakura, H., Kuhara, A., Berkeley, M., Mori, I., and Sengupta, P. (2001) Specification of thermosensory neuron fate in C. elegans requires ttx-1, a homolog of otd.Otx. *Neuron* 31(6), 943-956.

Scerbak, C., Vayndorf, E., Parker, A., Neri, C., Driscoll, M., and Taylor, B. (2014). Insulin signaling in the aging of healthy and proteotoxically stressed mechanosensory neurons. *Front Genetics* 5(212), 1-14.

Spencer, J. (2008). Food for thought: the role of dietary flavonoids in enhancing human memory, learning and neuro-cognitive performance. *Pro Nutrition Soc* 67, 238–252.

Spencer, W.C., Zeller, G., Watson, J.D., Henz, S.R., Watkins, K.L., McWhirter, R.D., Peterson, S., Sreedharan, V.T., Widmer, C., Jo, J., Reinke, V., Petrella, L., Strome, S., Von Stetina, S.E., Katz, M., Shaham, S., Raetsch, G., and Miller, D.M. (2011). A spatial and temporal map of *C. elegans* gene expression. *Genome Research* 21, 325-341.

Tank, E., Rodgers, K., and Kenyon, C. (2011). Spontaneous age-related neurite branching in *Caenorhabditis elegans*. *J Neurosci* 31, 9279–9288.

Toth, M., Melentijevic, I., Shah, L., Bhatia, A., Lu, K., Talwar, A., Naji, H., Ibanez-Ventoso, C., Ghose, P., Jevince, A., Xue, J., Herndon, L.A., Bhanot, G. Rongo, C., Hall, D.H., and Driscoll, M. (2012). Neurite sprouting and synapse deterioration in the aging *Caenorhabditis elegans* nervous system. *J Neurosci* 32, 8778–8790.

Vayndorf, E.M., Lee, S., and Liu, R. (2013). Whole apple extracts increase lifespan healthspan and resistance to stress in Caenohabditis elegans. *J Funct Foods* 5(3), 1235-1243.

Wilson, M.A., Shukitt-Hale, B., Kalt, W., Ingram, D.K., Joseph, J.A., and Wolkow, C.A. (2006). Blueberry polyphenols increase lifespan and thermotolerance in *Caenorhabditis elegans*. *Aging Cell* 5, 59-68.

Yuan, Y., Hakimi, P., Kao, C., Kao, A., Liu, R., Janocha, A., Boyd-Tressler, A., Hang, X., Alhoraibi, H., Slater, E., Xia, K., Cao, P., Shue, Q., Ching, T.T., Hsu, A.L., Erzurum, S.C., Dubyak, G.R., Berger, N.A., Hanson, R.W., and Feng, Z. (2016). Reciprocal changes in phosphoenolpyruvate carboxykinase and pyruvate kinase with age are determinant of aging in *C. elegans*. *J Biol Chem* 291, 1307-1319.

Zafra-Stone, S., Yasmin, T., Bagchi, M., Chatterjee, A., Vinson, J., and Bagchi, D. (2007). Berry anthocyanins as novel antioxidants in human health and disease prevention. *Mol Nutrition Food Res* 51, 675–683.

Zhong, H., Wu, X., Huang, H., Gan, Q., Zhu, Z., and Lin, S. (2006). Vertebrate MAX-1 is required for vascular patterning in zebrafish. *PNAS* 103(45), 16800-16805.

Chapter 5

General Conclusions

5.1 Summary of findings

Aging is a ubiquitous process affecting the health of increasing numbers of individuals throughout the world. Here, we studied the molecular mechanisms driving touch receptor neuron aging in the model nematode, *Caenorhabditis elegans*, with the goal of further describing the intricate relationship between genetics and diet in the aging process. In the experiments described in Chapter 2, we tested the effects of components of the insulin signaling pathway on aging mechanosensory neurons expressing a neurotoxic expanded polyglutamine transgene (polyQ128; model of Huntington's disease) or lacking this proteotoxicity stressor (polyQ0). We found that genetic manipulations that mimic decreased insulin signaling (i.e. DAF-2/insulin receptor knockdown with RNA interference (RNAi)) improved biomarkers of aging (e.g. lifespan, touch response) when compared to those that mimic insulin availability (DAF-16/FOXO transcription factor knockdown) in both the neurodegenerative and natural aging models. As reported in Chapter 3, we also evaluated the *in vivo* anti-aging characteristics of four medicinal Alaskan berry and fungal species (*Vaccinium uliginosum,* blueberry; *Vaccinium vitis-idaea,* lowbush cranberry; *Empetrum nigrum,* crowberry; and *Innonotus obliquus*, chaga). Blueberry, lowbush cranberry, and chaga treatments increased wildtype *Caenorhabditis elegans* lifespan and improved markers of healthspan (e.g. motility) while crowberry treatment did not affect wildtype lifespan. We then tested the hypothesis that the lifespan-extending treatments influence touch receptor neuron aging by modulating age-related morphological changes and functional decline. Interestingly, each of these treatments improved the age-related decline in touch response and motility but differentially impacted touch receptor neuron aging trajectories: the development of aberrant neuron morphologies was either slowed (blueberry; decreased

anterior neuron soma outgrowths at day 11), amplified (lowbush cranberry; increased posterior neuron process branching at day 11), or both (chaga; decreased anterior soma outgrowths and increased posterior process branching). Lastly, as reported in Chapter 4, we tested the hypothesis that lifespan-extending Alaskan berry and fungal treatments modify the aging process via specific, distinct cellular and molecular mechanisms. Only lowbush cranberry treatment effects were specifically modulated by DAF-16/FOXO activity, a well-studied, aging-related component of the insulin signaling pathway. Interestingly, we observed the same morphological phenotype (i.e. posterior neuron process branching) with *daf-2*(RNAi) (see Chapter 2) and lowbush cranberry treatment, both of which appear to increase the activity of DAF-16/FOXO. RNA sequencing revealed modest genetic changes early in life with blueberry and chaga treatments, but allowed us to uncover a novel role for a group of neuronal morphogenesis and metabolism genes that interact with the cytoskeleton in the development of touch receptor neuron morphologies. These results demonstrate for the first time that culturally valued Alaskan nutraceuticals exhibit *in vivo* anti-aging properties. Importantly, the results herein demonstrate that although an accumulation of abnormal neuron morphologies is associated with aging and decreased health, not all of these morphologies are detrimental to neuronal and organismal health and may in fact be defense or protective mechanisms. These results also support the large body of knowledge positing that there are multiple cellular strategies (e.g. cellular signaling, gene expression) and interventions (e.g. nutrition) for promoting health with age.

5.2 Proteostasis in aging neurons

In healthy cells, proteins are monitored for proper folding and misfolded proteins are corrected or degraded in order to maintain protein homeostasis ("proteostasis") within the cell. Dysregulation of proteostasis is a hallmark of neurodegenerative diseases. One such disease, Huntington's disease, is characterized by polyglutamine (polyQ)-expanded huntingtin protein

that aggregates within neurons. Introduction of mutated huntingtin (polyQ128) into *C. elegans* neurons results in deficient mechanosensation and development of neuronal aberrations (e.g. process bumps; Parker et al., 2001). Insulin signaling is implicated in the progression of neurodegenerative diseases, in part because of its regulation of stress response genes (e.g. protein chaperones, which regulate protein folding; reviewed in Dillin and Cohen, 2011). The study reported in Chapter 2 aimed to explore the link between healthy and diseased insulin signaling processes in touch receptor neurons. Indeed, insulin signaling regulation of touch receptor neuron form and function are somewhat distinct between the healthy and polyQ128 models: insulin receptor knockdown (*daf-2*(RNAi)) increases morphological aberrations in healthy animals and decreases aberrations in polyQ128 animals. However, the central aging transcription factor, DAF-16/FOXO, is neuroprotective in both models. The addition of a proteostatic imbalance (polyQ128 transgene) altered the response of touch receptor neurons to insulin signaling disruption, highlighting the importance of protein balance in cellular function and the aging process.

Our research group recently demonstrated that maintaining neuron proteostasis is a critical step in the touch receptor neuron aging process (Vayndorf et al., 2016). Both toxic polygluatamine-expanded huntingtin and neuronal RNAi of proteostatsis pathway components (e.g. proteosome, ubiquitin pathway) modified the age-related morphological aging trajectory of touch receptor neurons. These specific genetic interventions did not result in specific morphological changes, unlike the Alaskan nutraceutical interventions employed in the studies described in Chapters 3 and 4, suggesting that (1) proteostasis has wide-ranging cellular impacts on the aging process and (2) proteostasis dysregulation is not a mechanism of our Alaskan nutraceutical treatment effects (which is also supported in our RNAseq results).

Loss of proteostasis within cells is also an accepted marker of the normal, non-diseased aging process (reviewed in Lopez-Otin et al., 2013). For example, wildtype aged *C. elegans* have lower protein expression of proteins involved in proteostasis processes (e.g. translation,

proteosomal function; Copes et al., 2015) and accumulate widespread, insoluble protein aggregates (David et al., 2010). Maintenance of proteostasis within neurons (and other cells) is critical to the health of the cell and the organism. Future work will continue to describe strategies to maintaining proteostasis with age, but must consider the source of proteostasis dysregulation (i.e. aging versus neurodegeneration).

5.3 Nutritional impacts on insulin signaling and DAF-16/FOXO activity

Changes in nutrient sensing at the organismal (e.g. olfaction) and cellular level (e.g. insulin signaling) are known to be associated with aging (reviewed in Lopez-Otin et al., 2013). In *C. elegans,* various mutations in components of the insulin signaling pathway (e.g. DAF-2 receptor, AGE-1/P13K kinase, DAF-16/FOXO transcription factor), a key nutrient sensing pathway, consistently regulate lifespan, response to stress, and neuron aging (reviewed in Fontana et al., 2010; Broughton and Partridge, 2009). Similarly, decreasing insulin signaling in rodents increases lifespan and improves neurodegenerative phenotypes (reviewed in Broughton and Partridge, 2009). Several epidemiological studies have indicated that genetic variation in the FOXO transcription factor (homolog to *C. elegans* DAF-16 and central to the insulin signaling pathway) is involved in human lifespan (Deelen et al., 2014; Beekman et al., 2013; Newman and Murabito, 2013). Interestingly, levels of human growth hormone and IGF-1 (that bind to and activate human insulin receptors) decrease with age, which is thought to represent a defensive response to the damage associated with aging (reviewed in Lopez-Otin et al., 2013). The idea that food intake and nutrition influences the activity of this central signaling pathway and transcription factor is a very interesting one. Given the known genetic differences in human FOXO, the potential for individual variation in the response (e.g. inactivate/activate, speed and duration of response) of this transcription factor in response to nutrients and/or bioactive compounds should be investigated.

Due to its known interactions with the aging process, we chose to screen for DAF-16/FOXO activation upon treatment with Alaskan nutraceuticals (Chapter 4). We found that DAF-16/FOXO was activated in aged (day 9) animals treated with Alaskan lowbush cranberry (but not treatment with blueberry or chaga), mimicking low insulin receptor (DAF-2) activation and, thus, low nutrient availability. Although the *C. elegans* insulin signaling pathway is well known to regulate development, metabolism, and stress response, the regulation of *C. elegans* insulin peptide levels (of which there are 40) and their interactions with the DAF-2 receptor is not completely described (reviewed in Gami and Wolkow, 2006). To further describe the relationship of DAF-16/FOXO with other broadly acting cellular signaling pathways, it would be interesting to test the involvement of Alaskan lowbush cranberry treatment on insulin peptide availability and the activity of other conserved upstream regulators of DAF-16/FOXO (e.g. heat shock factor [HSF-1] and JNK signaling).

5.4 Aging phenotypes of anterior versus posterior touch receptor neurons

The anterior (ALM) and posterior (PLM) mechanosensory (or touch receptor) neurons respond to aging and aging manipulations with different morphological changes: ALM neurons exhibit increased soma outgrowths and abnormal soma shapes while PLM neurons exhibit increased process outgrowths (i.e. branching, loops; Vayndorf et al., 2016; Toth et al., 2012; Pan et al., 2011; Tank et al., 2011). Additionally, we have shown here that the increased incidence of these age-related morphologies is not directly correlated with poorer health: both decreased incidence of ALM aberrations (i.e. soma outgrowths, abnormal soma shape) and increased incidence of PLM aberrations (i.e. process branching and loops) correlate with increased lifespan, improved motility, and improved touch response. To further complicate an understanding of the damaging versus protective roles of neuronal aberrations with respect to aging, our findings provided evidence that *increased* incidence of ALM aberrations can be correlated with improved motility and/or touch response (i.e. *ttx-1*(RNAi), *unc-44*(RNAi), and *stn-*

1(RNAi)). What remains to be determined is whether increased incidence of morphological aberrations (e.g. PLM process branching) is a stimulatory response that *actively promotes* healthy aging or whether this phenotype occurs as a *consequence* of good health and aging. The ALM and PLM pairs of touch receptor neurons consistently respond to the aging process different manners; thus, age-related changes in neuron morphology cannot be interpreted wholesale as biomarkers of detrimental effects of aging.

The heterogeneity in morphological responses to aging between ALM and PLM neurons may be due to their particular neural networks and, thus, activity levels. In general terms, the touch receptor neurons (including the pairs of ALM and PLM neurons) synapse on interneurons, which then synapse on motor neurons, resulting in forward or backward movement (reviewed in Goodman, 2006). Specifically, the PLM neurons have stimulatory gap junctions with the AVB/PVC interneurons (which regulate forward movement) and inhibitory chemical synapses on the AVA/AVD interneurons (which regulate backward movement). Thus, PLM activation by posterior touch stimulates forward movement. ALM neurons are involved in opposing neuronal interactions (inhibitory chemical synapses on AVB/PVC and stimulatory gap junctions with AVA/AVD), stimulating backward movement upon anterior touch (reviewed in Goodman, 2006). As they age, the three anterior touch receptor neurons (ALML, ALMR, AVM) form their own neural network via gap junctions, a characteristic not shared with the posterior touch receptor neurons (Chalfie et al., 1985). Additionally, only ALM neurons (not PLM) sensitize to high salt, hypoxia, dauer, and prolonged vibration, which prevents the animal from repeatedly changing direction in response to non-localized stressors (Chen and Chalfie, 2014). Toth et al. (2012) proposed that the age-related morphological differences between neurons of the same class (e.g. PLM and ALM neurons) and between classes of neurons (e.g. touch receptor versus dopamine neurons) may also be due to neuronal position (i.e. space to grow) or cell-specific gene expression. Taken together, the functional differences in the ALM and PLM neurons likely

have consequences for their age-related morphological changes and, thus, their responses to the aging process.

5.5 Environmental factors in medicinal food efficacy

The relationship between plant and fungal species' biochemical composition, *in vivo* medicinal action, and ecology is an area of research that warrants further study. Plant and fungus species adapt to extreme environments (such as Alaska's extreme photoperiods) by producing a wide variety of secondary metabolites (Elks et al., 2013), chemicals known to interact with health- and aging-related cellular processes (e.g. quercitin impacts insulin signaling; Youl et al., 2010), perhaps via xenohormesis. It is well accepted in agricultural chemistry that the biochemical composition of food sources may be detected (i.e. by flavor), and even preferred, upon consumption by consumers. For example, grape ripening is regulated by environmentally-responsive hormones, and the particular molecular basis of ripening directly influences secondary metabolite production and, thus, aroma and taste (reviewed in Kuhn et al., 2013). One study found that blueberry tasters discern flavor biochemical profiles (which were determined by genetics and environment), validating approaches to breed for flavor (Gilbert et al., 2015). However, studying the effects of environment-induced (e.g. variations in temperature, precipitation, and/or soil composition) intraspecies variation in biochemical composition and on subsequent *in vivo* health metrics (e.g. neuronal aging in *C. elegans*) would offer an interdisciplinary approach to understanding the basic biology of aging and to promoting healthy aging.

5.6 Final conclusions

C. elegans touch receptor neurons exhibit changes in morphology and a decline in function with age (Toth et al., 2012; Pan et al., 2011; Tank et al., 2011). Here, we demonstrate that these age-related changes can be modulated by both genetic (e.g. insulin signaling) and

nutritional (e.g. Alaskan nutraceuticals) interventions. We also uncovered a novel role for a group of genes in touch receptor neuron aging by studying Alaskan nutraceutical treatment-induced transcriptome changes. The cellular and molecular aging processes (e.g. insulin signaling, cytoskeletal regulations) are impacted by both intrinsic (e.g. genetic determinants of aging) and extrinsic (e.g. nutrition) factors. This supports the large body of knowledge positing that there are multiple, interrelated cellular strategies and mechanisms promoting health with age. Finally, studying the impact of culturally valued foods, such as Alaskan berries and fungi, not only supports the traditional ecological knowledge that these foods are healthy, but provides novel insights into the mechanisms of neuronal aging and aging in general.

5.7 References cited

Beekman, M., Blanche, H., Perola, M., Hervonen, A., Bezrukov, V., Sikora, E., Flachsbart, F., Christiansen, L., De Craen, A.J.M., Kirkwood, T.B.L., Rea, I.A., Poulain, M., Robine, J.M., Valensin, S., Stazi, M.A., Passarino, G., Deiana, L., Gonos, E.S., Paternoster, L., Sørensen, T.I.A., Tan, Q., Helmer, Q., van den Akker, E.B., Deelen, J., Martella, F., Cordell, H.J., Ayers, K.L., Vaupel, J.W., Teornwall, O., Johnson, T.E., Schreiber, S., Lathrop, M., Skytthe A., Westendorp, R.G.J., Christensen, K., Gampe, J., Nebel, A., Houwing-Duistermaat, J.J., Slagboom, P.E., and Franceschi, C. (2013). Genome-wide linkage analysis for human longevity: Genetics of healthy aging study. *Aging Cell* 12, 184-193.

Broughton, S. and Partridge, L. (2009). Insulin/IGF-like signaling, the central nervous system and aging. *Biochem J* 418, 1-12.

Chalfie, M., Sulston, J.E., White, J.G., Southgate, E., Thomson, N., and Brenner, S. (1985). The neural circuit for touch sensitivity in *Caenorhabditis elegans. J Neurosci* 5(4), 956-964.

Chen, X. and Chalfie, M. (2014). Modulation of *C. elegans* touch sensitivity is integrated at multiple levels. *J Neurosci* 34(19), 6522-6536.

Copes, N., Edwards, C., Chaput, D., Saifee, M., Barjuca, I., Nelson, D., Paraggio A., Saad, P., Lipps, D., Stevens, S.M. Jr., and Bradshaw, P.C. (2015) Metabolome and proteosome changes with aging in *Caenorhabditis elegans. Exp Geron* 72, 67-84.

David, D.C., Ollikainen, N., Trinidad, J.C., Cary, M.P., Bulingame, A.L., and Kenyon, C. (2010). Protein aggregation as an inherent part of aging in *C. elegans. PLoS Biol* 8(8), e1000450.

Deelen, J., Beekman, M., Uh, H.W., Broer, L., Ayers, K.L., Tan, Q., Kamatani, Y., Bennet, A.M., Tamm, R., Trompet, S., Guõbjartsson, D.F., Flachsbart, F., Rose, G.,Viktorin, A., Fischer, K., Nygaard, M., Cordell, H.J., Crocco, P., van den Akker, E.B., Böhringer, S., Helmer, Q., Nelson, C.P., Saunders, G.I., Alver, M., Andersen-Ranberg, K., Breen, M.E., van der Breggen, R., Caliebe, A., Capri, M., Cevenini, E.,Collerton, J.C., Dato, S., Davies, K., Ford, I., Gampe, J., Garagnani, P., de Geus, E.J., Harrowo, J., van Heemst, D., Heijmans, B.T., Heinsen, F.A., Hottenga, J.J.,Hofman, A., Jeune, B., Jonsson, P.V., Lathrop, M., Lechner, D., Martin-Ruiz, C.,McNerlan, S.E., Mihailov, E., Montesanto, A., Mooijaart, S.P., Murphy, A., Nohr, E.A., Patemoster, L., Postmus, I., Rivadeneira, F., Ross, O.A., Salvioli, S., Sattar, N.,Schreiber, S., Stefansson, H., Stott, D.J., Tiemeier, H., Uitterlinden, A.G., Westen-dorp, R.G., Willemsen, G., Samani, N.J., Galan, P., Sørensen, T.I., Boomsma, D.I.,Jukema, J.W., Rea, I.M., Passarino, G., de Graen, A.J., Christensen, K., Nebel, A., Stefánsson, K., Metspalu, A., Magnusson, P., Blanché, H., Christiansen, L., Kirkwood,T.B., van Duijn, C.M., Franceschi, C., Houwing-Duistermaat, J.J., Slagboom, P.E., 2014. Genome-wide association meta-analysis of human longevity identifies a novel locus conferring survival beyond 90 years of age. *Hum Mol Genet* 23, 4420–4432.

Dillin, A., and Cohen, E. (2011). Ageing and protein aggregation-mediate disorders: from invertebrates to mammals. *Philos Trans R Soc Lond B Biol Sci* 366, 94-98.

Elks, C. M., Francis, J., Stull, A. J., Cefalu, W. T., Shukitt-Hale, B., & Ingram, D. K. (2013). Overview of the health properties of blueberries. In M. Skinner & D. Hunter (Eds.), *Bioactives in fruit: Health benefits and functional foods* (1st ed., pp. 251–271). John Wiley & Sons.

Fontana, L., Partridge, L., and Longo, V.D. (2010). Extending healthy lifespan—from yeast to humans. *Science* 328, 321–326.

Gami, M.S. and Wolkow, C.A. (2006). Studies of *Caenorhabditis elegans* DAF-2/insulin signaling reveal targets for pharmacological manipulation of lifespan. *Aging Cell* 5(1), 31-37.

Gilbert, J.L., Guthart, M.J., Gezan, S.A., de Carvalho, M.P., Schwieterman, M.L., Colquhoun, T.A., Bartoshuk, L.M., Sims, C.A., Clark, D.G., and Olmstead, J.W. (2015). Identifying breeding priorities for blueberry flavor using biochemical, sensory, and genotype by environment analyses. *PLoS ONE* 10(9): e0138494.

Goodman, M.B. Mechanosensation (2006), *WormBook*, ed. The *C. elegans* Research Community, WormBook,

Kuhn, N., Guan, L., Dai, Z.W., Wu, B.H., Lauvergeat, V., Gomes, E., Li, S.H., Godoy, F., Arce-Johnson, P., and Deirot, S. (2013). Berry ripening: recently heard through the grapevine. *J Exp Botany,* 65(15), 4543-4559.

Lopez-Otin, C., Blasco, M.A., Partridge, L., Serrano, M., and Kroemer, G. (2013). The hallmarks of aging. *Cell* 153, 1194-1217

Newman, A.B. and Murabito, J.M. (2013). The epidemiology of longevity and exceptional survival. *Epidemiology Rev* 35, 181-197.

Pan, C.L., Peng, C.Y., Chen, C.H., and McIntire, S. (2011). Genetic analysis of age-dependent defects of the Caenorhabditis elegans touch receptor neurons. *PNAS* 108, 9274–9279.

Parker, J.A., Connolly, J.B., Wellington, C., Hayden, M., Dausset, J., and Neri, C. (2001) Expanded polyglutamines in *Caenorhabditis elegans* cause axonal abnormalities and severe dysfunction of PLM mechanosensory neurons without cell death. *PNAS* 98(23):13318-13323.

Tank, E., Rodgers, K., and Kenyon, C. (2011). Spontaneous Age-Related Neurite Branching in Caenorhabditis elegans. *J Neurosci* 31, 9279–9288.

Toth, M., Melentijevic, I., Shah, L., Bhatia, A., Lu, K., Talwar, A., Naji, H., Ibanez-Ventoso, C., Ghose, P., Jevince, A., Xue, J., Herndon, L.A., Bhanot, G. Rongo, C., Hall, D.H., and Driscoll, M. (2012). Neurite sprouting and synapse deterioration in the aging *Caenorhabditis elegans* nervous system. *J Neurosci* 32, 8778–8790.

Vayndorf, E.M., Scerbak, C., Hunter, S., Neuswanger, J.R., Toth, M., Parker, A.J., Neri, C., Driscoll, M., and Taylor, B.E. (2016). Morphological remodeling of *C. elegans* neurons during aging is modified by compromised protein homeostasis. *NPJ Aging Mech Dis* 2, e16001.

Youl, E., Bardy, G., Magous, R., Cros, G., Sejalon, F., Virsolvy, A., Richard, S., Quignard, J.F., Gross, R., Petit, P., Bataille, D., and Oiry, C. (2010). Quercetin potentiates insulin secretion and protects INS-1 pancreatic β-cells against oxidative damage via the ERK1/2 pathway. *Br J Pharmacol.* 161, 799–814.